Supporting information

Lan Enzyme-Free Construction of Lanthionine-Bridged Macrocyclic Phage Libraries

Fan Yang, Jiaxi Xiao, Weihang Huang and Jianmin Gao*

Department of Chemistry, Merkert Chemistry Center, Boston College, 2609 Beacon Street,
Chestnut Hill, MA 02467

*Correspondence should be sent to: Jianmin.Gao@bc.edu

Table of Contents

1. General Information

1.1 General Information for Reagents and Methods

2-Formylphenylboronic acid (2-FPBA), salicylaldehyde and benzaldehyde were purchased from SigmaAldrich (St. Louis, MO). Methyl-2,5-dibromopentanoate (MDBP) was purchased from Ambeed (Buffalo Grove, IL). 2,5-Dibromohexanediamide (DBHDA) was purchased from ChemScene (Monmouth Junction, NJ). Commercially purchased chemicals were used without further purification. Mesitylenesulfonylhydroxylamine (MSH) was synthesized following the literature.[1] All Fmoc-protected amino acids, HBTU, amino acids were purchased from Chem-Impex International (Wood Dale, IL). Piperidine was purchased from Thermofisher (Waltham, MA). N-Methylmorpholine (NMM) was purchased from SigmaAldrich (St. Louis, MO). N, N-Dimethylformamide (DMF) was purchased from Fisher Chemical (Waltham, MA). Fmoc-Rink Amide MBHA resin was purchased from ChemScene (Monmouth Junction, NJ). 5(6)-Carboxyfluorescein was purchased from SigmaAldrich (Rockville, MD). Peptide synthesis was carried out on a CSBio II Peptide Synthesizer (CSBio, CA). Peptides were purified on a Waters PrepLC System with a Phenomenex Jupiter C18 column (Torrance, CA). LC-MS data were collected using an Agilent 6230 LC TOF mass spectrometer and processed using the Agilent MassHunter Qualitative Analysis software package. NMR spectra were collected using a VNMRS 500 MHz, or 600 MHz NMR spectrometer (Varian NMR Inc, CA). NMR data were processed using MestReNova 14.2.1. Chemical shifts were referenced to internal solvent resonances and reported relative to $SiMe_4$; multiplicities are indicated by s (singlet), d (doublet), t (triplet), q (quartet), m (multiplet) and br (broad). Coupling constants, *J*, are reported in Hz (Hertz). Mass-spec data of synthetic molecules were collected using an AccuTOF DART (JEOL, MA). Fluorescence polarization experiments were carried out using a SpectraMax M5 Microplate Reader (Molecular Devices, San Jose, CA).

1.2 LC-MS Methods

Solvent compositions:

Solvent A: 0.1% formic acid, 5% acetonitrile in H_2O

Solvent B: 0.1% formic acid, 5% H_2O in acetonitrile

Method A:
Column: Agilent Poroshell 120 EC-C18 column: 3.0 x 50 mm, 2.7 µm

Table S1. Gradient for LC-MS Method A

Time (min)	Solvent A (%)	Solvent B (%)	Flow (mL/min)
0.00	100.0	0.0	0.200
1.00	100.0	0.0	0.200
9.00	0.0	100.0	0.200
9.00	0.0	100.0	0.200
9.01	100.0	0.0	0.200

16.00	100.0	0.0	0.200

MS conditions: positive electrospray ionization (ESI) extended dynamic mode in mass range 100 – 2000 m/z, temperature of drying gas = 325 °C, flow rate of drying gas = 8 L/min, pressure of nebulizer gas = 35 psi, the capillary = 4.286 uA, fragmentor = 175 V, octupole rf voltages = 750.

Method B:
Column: AerisTM 3.6 µm WIDEPORE XB-C8 200 Å, LC Column 100 x 4.6 mm

Table S2. Gradient for LC-MS Method B

Time (min)	**Solvent A (%)**	**Solvent B (%)**	**Flow (mL/min)**
0.00	95.0	5.0	0.200
1.00	1.0	99.0	0.200
8.00	1.0	99.0	0.200
9.00	99.0	1.0	0.200
10.00	95.0	5.0	0.200
14.00	95.0	5.0	0.200

MS conditions: positive electrospray ionization (ESI) extended dynamic mode in mass range 100 – 2000 m/z, temperature of drying gas = 325 °C, flow rate of drying gas = 8 L/min, pressure of nebulizer gas = 35 psi, the capillary = 0.059 uA, fragmentor = 175 V, octupole rf voltages = 750 V.

1.3 General Protocol for Solid Phase Peptide Synthesis

All peptides were synthesized using the standard Fmoc solid-phase peptide synthesis (SPPS) protocol on Rink Amide MBHA resin (0.2 mmol scale). Commercially available Fmoc-protected amino acid building blocks were employed. For each coupling step, the resin was treated with Fmoc-amino acid (5.0 equiv) and HBTU (5.0 equiv) in 0.40 M NMM in DMF. Following coupling, Fmoc groups were removed with 20% piperidine in DMF. To enable site-specific fluorophore conjugation, Fmoc-Dap(Alloc)-OH was incorporated at the C-terminus, preceded by a Gly-Gly-Gly spacer that separates the fluorophore and the peptide of interest. The Alloc protecting group was selectively removed on resin using tetrakis(triphenylphosphine)palladium(0) (160 mg) and phenylsilane (1.6 mL) in DCM (3 mL). The resin was then washed thoroughly and coupled with 5(6)-carboxyfluorescein (5(6)-FAM) in presence of HBTU and NMM. Peptides were cleaved from the resin and globally deprotected using either Reagent K (82.5% TFA, 5% H2O, 5% phenol, 5% thioanisole, 2.5% 1,2-ethanedithiol) or Reagent B (90% TFA, 2.5% H_2O, 2.5% TIPS, 5% phenol) at room temperature for 4 h. The crude peptides were obtained by filtration of the cleavage mixture, precipitation with cold diethyl ether, and centrifugation. The resulting solids were dissolved in aqueous acetonitrile containing 0.1% TFA and purified by reverse-phase HPLC (Waters Prep LC, Jupiter C18 column) using a linear acetonitrile/water gradient. The purified peptides were characterized by LC-MS to confirm purity (>95%) before lyophilization to yield the final products.

1.4 Synthesis of O-(mesitylsulfonyl)hydroxylamine (MSH)

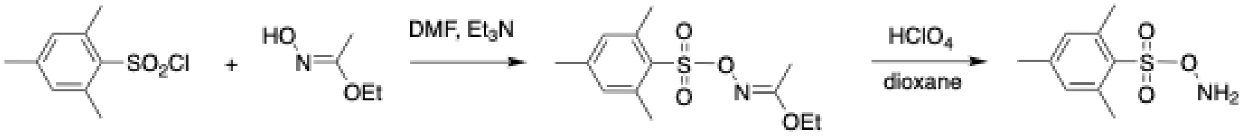

Scheme S1. Synthesis route of MSH. MSH was synthesized following the reference.[1]

1.4.1 Synthesis of MSH precursor ethyl (E)-N-((mesitylsulfonyl)oxy)acetimidate

Ethyl *N*-hydroxyacetimidate (2.36 g, 22.9 mmol) was added to a 50 mL round bottom flask and dissolved in 15 mL of DMF, then the solution was cooled to 0 ºC for 30min. Et_3N (6.4 mL, 46 mmol) and 2-Mesitylenesulfonyl chloride (5.00 g, 22.9 mmol) was added in to the cooled reaction solution as a solid in several portions sequentially. The reaction was stirred vigorously at 0 ºC for 30 minutes. The formation of white solid was observed over the course of the reaction. Upon completion, the reaction was diluted with 150 mL of EtOAc and then washed with 100 mL of H_2O for three times and 100 mL of brine one time. The organic layer was dried over MgSO4, filtered, and concentrated under reduced pressure to give a light yellow oil (6.45 g, 88.3%), then stored at -20 ºC for the further use. ^{1}H NMR (600 MHz, $CDCl_3$) δ 6.96 (s, 2H), 3.90 (q, *J* = 7.1 Hz, 2H), 2.64 (s, 6H), 2.31 (s, 3H), 2.03 (s, 3H), 1.18 (t, *J* = 7.1 Hz, 3H). HRMS (TOF-ESI$^+$) *m/z* calc. for $C_{13}H_{20}NO_4S$, $[M+H]^+$ 286.11076, found 286.11043.

1.4.2 Synthesis of O-(mesitylsulfonyl)hydroxylamine (MSH)

The MSH precursor (1747.8 mg, 6.12 mmol) was dissolved in 3 mL of dioxane at room temperature and then cooled to 0 ºC for 30min. 2mL of perchloric acid (70% solution) was added into the reaction solution dropwise over 2 minutes. The reaction was stirred vigorously at 0 ºC and thickens and solidifies over the course of reaction. After the observation of solid formation, the reaction was incubated for an additional 5 minutes to ensure complete hydrolysis. Then the reaction solution was poured onto 50 g of ice. 100mL of Et_2O and 100mL of H_2O were added to the ice mixture to quench the reaction. The mixture was then transferred to a separatory funnel. The organic layer was separated and collected, then dried over K_2CO_3. The organic layer was recovered by filtration. The filtrate was concentrated under reduced pressure to a volume of about 50 mL. The solution was poured into a beaker with 150 mL of ice-cold hexane. MSH crystals formed immediately. The beaker was incubated at 0 ºC for 30 minutes to complete the crystallization. The product crystals were then isolated by filtration and dried under vacuum. The white needles (502.8 mg, 38.24%) were transferred into a plastic vial, sealed with parafilm and stored at -20 ºC for the further use. ^{1}H NMR (600 MHz, $CDCl_3$) δ 7.00 (s, 2H), 5.17 (s, 2H), 2.65

(s, 6H), 2.33 (s, 2H). HRMS (TOF-ESI$^+$) *m/z* calc. for $C_9H_{14}NO_3S$, $[M+H]^+$ 216.06889, found 216.06873.

1.5 Synthesis of Lanthionine Building Block for Solid-Phase Peptide Synthesis

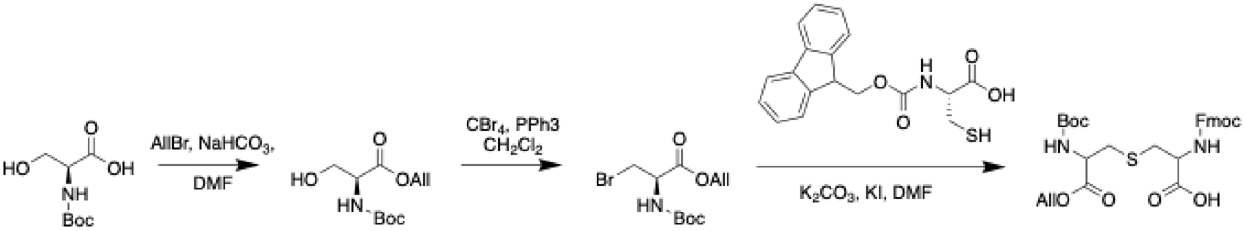

Scheme S2. Synthesis route of Boc-protected lanthionine building block for SPPS following the reference.[2,3]

1.5.1 Synthesis of allyl (tert-butoxycarbonyl)-L-serinate

(tert-butoxycarbonyl)-L-serine (1025.5 mg, 5.0 mmol) was disolved in 30 mL of DMF, and potassium bicarbonate (420.0 mg, 25 mmol) was added into the solution, allyl bromide (2.3mL, 26.6mmol) was added dropwise. The reaction mixture was monitored by TLC, and vigorously stirred at room temperature for overnight. Upon completion, the reaction was diluted with 100 mL of ethyl acetate, then 100 mL of water was added, product was extracted into the organic layer by separatory funnel, then washed with 150 mL of water for three times, continued with the washing with 150 mL of saturated sodium bicarbonate solution for one time, brine for one time. The organic layer was collected and dried over magnesium sulfate, then concentrated under reduced pressure and purified by chromatography (n-hexane/ethyl acetate = 1/1) to give the product as colorless oil (1087 mg, 88.7%), then stored at 20 ºC for the further use. 1H NMR (600 MHz, $CDCl_3$) δ 5.92 (s, 1H), 5.53 (s, 1H), 5.34 (s, 1H), 5.24 (s, 1H), 4.65 (s, 2H), 4.37 (s, 1H), 3.91 (d, J = 39.3 Hz, 2H), 1.43 (s, 9H). HRMS (TOF-ESI+) *m/z* calc. for $C_{11}H_{19}NO_5$, [M+H]+246.13360, found 246.13389.

1.5.2 Synthesis of allyl (R)-3-bromo-2-((tert-butoxycarbonyl)amino)propanoate

Allyl (*tert*-butoxycarbonyl)-*L*-serinate (1.00 g, 4.07 mmol) and carbon tetrabromide (1395 mg, 4.47 mmol) were added to a 250 mL round bottom flask and dissolved in 100 mL of DCM, then the solution was cooled to 0 ºC for 30 min. Triphenylphosphine (1172 mg, 4.47 mmol) were added in to the cooled reaction solution in several portions sequentially. After adding, bring the reaction back to room temperature and stired for 2 hours. Upon completion, the reaction was washed with 200 mL of H_2O for three times and 200 mL of brine one time. The organic layer was dried over $MgSO_4$, filtered, concentrated under reduced pressure and purified by flash column chromatography (*n*-hexane/ethyl acetate = 4/1) to give a colorless oil (1657 mg, 66.1%), then stored at -20 ºC for the further use. ^1H NMR (600 MHz, $CDCl_3$) δ 5.87 (ddt, *J* = 16.3, 10.5, 5.8

Hz, 1H), 5.44 (d, *J* = 7.7 Hz, 1H), 5.31 (dd, *J* = 17.2, 1.3 Hz, 1H), 5.26 – 5.19 (m, 1H), 4.71 (dt, *J* = 7.2, 3.1 Hz, 1H), 4.63 (qd, *J* = 13.1, 5.8 Hz, 2H), 3.78 (dd, *J* = 10.5, 3.2 Hz, 1H), 3.67 (dd, *J* = 10.5, 3.5 Hz, 1H), 1.40 (s, 9H). ^{13}C NMR (151 MHz, $CDCl_3$) δ 168.91, 154.97, 131.31, 119.14, 80.39, 66.57, 54.01, 34.01, 28.27. HRMS (TOF-ESI$^+$) *m/z* calc. for $C_{11}H_{19}BrNO_4$, $[M+H]^+$ 308.04920, found 308.04861.

1.5.3 Synthesis of (E)-N-(((9H-fluoren-9-yl)methoxy)carbonyl)-S-(2-((tert-butoxycarbonyl)amino)-3-oxo-3-(prop-1-en-1-yloxy)propyl)cysteine

(((9H-fluoren-9-yl)methoxy)carbonyl)-*L*-cysteine (1416 mg, 4.12 mmol) was added to a 250 mL round bottom flask and dissolved in 50 mL of DMF, then potassium carbonate (1139 mg, 8.24 mmol) as a solid in several portions sequentially at room temperature. Then sodium iodide (185 mg, 1.24 mmol) was added into the reaction solution. The reaction was stirred vigorously at room temperature for 10 minutes. After that, allyl (*R*)-3-bromo-2-((tert-butoxycarbonyl)amino)-propanoate (1525 mg, 4.95 mmol) was added into the reaction solution dropwise. The reaction was stirred vigorously at room temperature for 12 hours. Upon completion, the reaction was diluted with 150 mL of EtOAc and 500 mL of H_2O. Adjust the pH of the aqueous phase to be 2 by adding 1 M HCl. Collect the organic phase and washed with acidic water similarly for another two times and 100 mL of brine one time. The organic layer was dried over $MgSO_4$, filtered, concentrated under reduced pressure and purified by flash column chromatography (MeOH/dichloromethane/acetic acid = 1/20/0.02) to give a colorless oil (801 mg, 34.1%), then stored at -20 ºC for the further use. ^{1}H NMR (600 MHz, DMSO-*d*$_6$) δ 7.89 (d, *J* = 7.5 Hz, 2H), 7.73 (d, *J* = 7.6 Hz, 2H), 7.42 (t, *J* = 7.5 Hz, 2H), 7.33 (t, *J* = 7.4 Hz, 3H), 5.88 (td, *J* = 10.9, 5.3 Hz, 1H), 5.32 (d, *J* = 18.4 Hz, 1H), 5.19 (d, *J* = 10.5 Hz, 1H), 4.58 (s, 2H), 4.29 (m, 2H), 4.26 – 4.12 (m, 3H), 3.00 – 2.90 (m, 2H), 2.85 – 2.78 (m, 2H), 1.38 (s, 9H). ^{13}C NMR (126 MHz, DMSO-*d*$_6$) δ 172.29, 170.77, 156.09, 155.39, 143.81, 140.75, 132.30, 127.70, 127.14, 125.33, 120.18, 117.65, 78.53, 65.81, 65.01, 53.97, 53.85, 46.62, 32.95, 32.64, 28.16. HRMS (TOF-ESI$^+$) *m/z* calc. for $C_{29}H_{35}N_2O_8S$, $[M+H]^+$ 571.21086, found 571.21115.

2. Protein Expression

2.1 Expression of Sortase A Double Mutant (C153A, K159C)

The expression vectors for Sortase A_C153A, K159C protein were generated from a parental Sortase A plasmid (pET28a-SrtAdelta59 from Addgene) using the Q5 site-directed mutagenesis kit (NEB #E0554). The primers used were:

Primers for inserting TEV site after His tag:
Forward: 5’-TCATCATCACGAAAACCTGTACTTCCAGTCCTCCAGCAGCGGCC-3’
Reverse: 5’-GGCCGCTGCTGGAGGACTGGAAGTACAGGTTTTCGTGATGATGA-3’

Primers for C153A, K159C two sites mutation

Forward: 5’-ACATTAATTACTGCCGATGATTACAATGAATGCACAGGCGTTTGG-3’
Revers: 5’-CCAAACGCCTGTGCATTCATTGTAATCATCGGCAGTAATTAATGT-3’

Sequence:

MRGSSHHHHHHENLYFQSSGLVPRGSHMQAKPQIPKDKSKVAGYIEIPDADIKEPVYPG
PATPEQLNRGVSFAEENESLDDQNISIAGHTFIDRPNYQFTNLKAAKKGSMVYFKVGNE
TRKYKMTSIRDVKPTDVGVLDEQKGKDKQLTLIT**A**DDYNE**C**TGVWEKRKIFVATEVK*

The resulting plasmid construct was verified by Sanger sequencing (Genewiz, NJ) and transformed into *E. coli* BL21(DE3) competent cells. For protein expression, transformed cells were cultured in 1 L of LB medium supplemented with kanamycin (50 µg/mL) at 37 °C with vigorous shaking until the optical density at 600 nm (OD600) reached 0.5-0.8. Protein production was induced by addition of IPTG (1 mM), and the culture was incubated for ~16 h at room temperature with vigorous shaking. Cells were harvested by centrifugation (5000 rpm, 20 min, 4 °C), and the resulting pellet was resuspended in 15 mL lysis buffer (20 mM Tris, 300 mM NaCl, 10 mM imidazole). Cell lysis was performed by sonication on ice, and the lysate was clarified by centrifugation (8730 rpm, 20 min, 4 °C). The supernatant was filtered through a 0.25 µm filter to remove residual debris prior to purification on Ni-NTA resin. The resin was washed three times with one column volume of wash buffer (20 mM Tris, 300 mM NaCl, 25 mM imidazole), and Sortase A was eluted with 2.5 column volumes of elution buffer (20 mM Tris, 300 mM NaCl, 250 mM imidazole). The eluate was desalted using a PD-10 desalting column (Cytiva, Marlborough, MA) and stored in PBS buffer (pH 7.4) at -80 °C. Protein purity was confirmed by LC-MS analysis (Method B, as described in the LC-MS Methods).

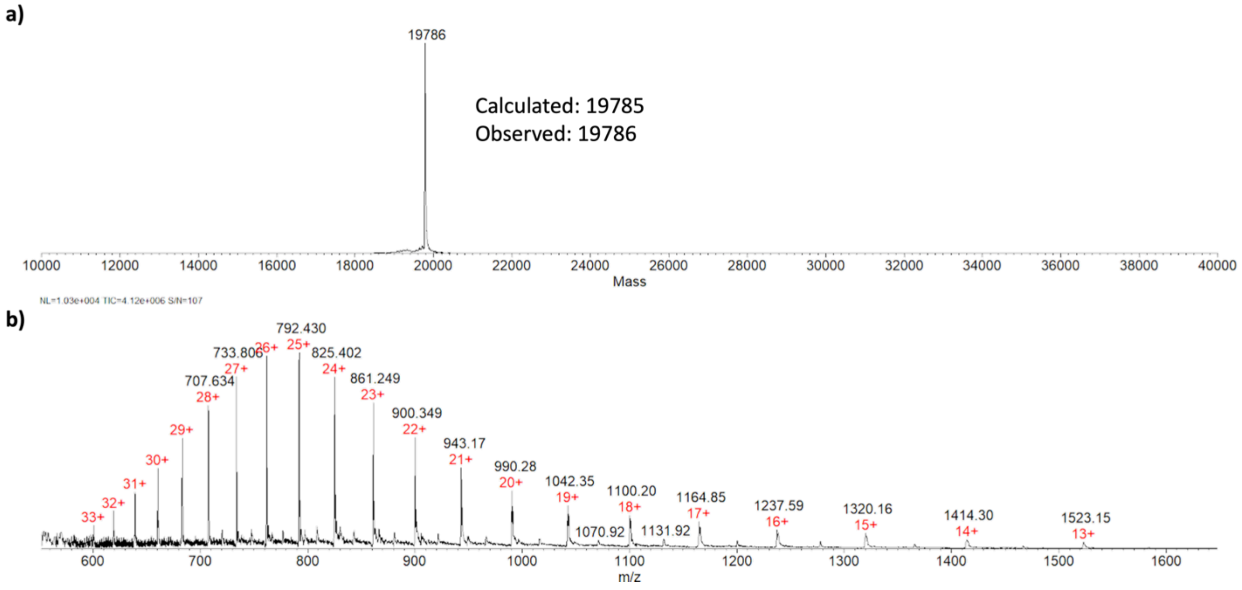

Figure S1. a) Deconvoluted mass and b) crude mass envelope of Sortase A_C153A/K159C protein.

2.2 Expression of pIII protein with MIEGRCX$_9$C Peptide Fused on N-terminus

The expression vectors for CX$_9$C-pIII protein were generated from a parental pIII plasmid using the Q5 site-directed mutagenesis kit (NEB). The primers used were:

Forward: 5′-TTCCCTGATGCCTACGTGGGGCATGCATTGCGGTGGAGGT-3′
Revers: 5′-CCCGCACACCGGCCCTCAATCATAGAGTGAGAATAGAAAGGTACCAC-3′

The resulting plasmid sequence was verified by Sanger sequencing and subsequently transformed into *E. coli* BL21(DE3) competent cells. A 10 mL overnight preculture in LB medium supplemented with 50 µg/mL ampicillin was used to inoculate 1 L of LB medium. Cells were grown at 37 °C with shaking at 250 rpm until the optical density at 600 nm (OD$_{600}$) reached 0.4–0.6. Protein expression was induced by adding IPTG to a final concentration of 1 mM, followed by incubation at room temperature with shaking for 16 h. Cells were harvested by centrifugation at 5,000 × g for 15 min and lysed in buffer (20 mM Tris, 300 mM NaCl, 10 mM imidazole) using sonication on ice. The lysate was clarified by centrifugation at 10,000 × g for 15 min, and the supernatant was subjected to affinity purification using Ni-NTA agarose resin. The purified protein was desalted using a NAP-10 column (GE Healthcare) and stored in PBS at −80 °C until use. Protein purity was confirmed by LC-MS analysis (Method B, as described in the LC-MS Analysis Methods).

Sequence:

MIEGR**CAGSLMPTWGC**ENLYFQSAETVESCLAKSHTENSFTNVWKDDKTLDRYANYE
GCLWNATGVVVCTGDETQCYGTWVPIGLAIPENEGGGSEGGGSEGGGSEGGGTKPPEY
GDTPIPGYTYINPLDGTYPPGTEQNPANPNPSLEESQPLNTFMFQNNRFRNRQGALTVYT
GTVTQGTDPVKTYYQYTPVSSKAMYDAYWNGKFRDCAFHSGFNEDLFVCEYQGQSSD
LPQPPVNAAAALEHHHHHH

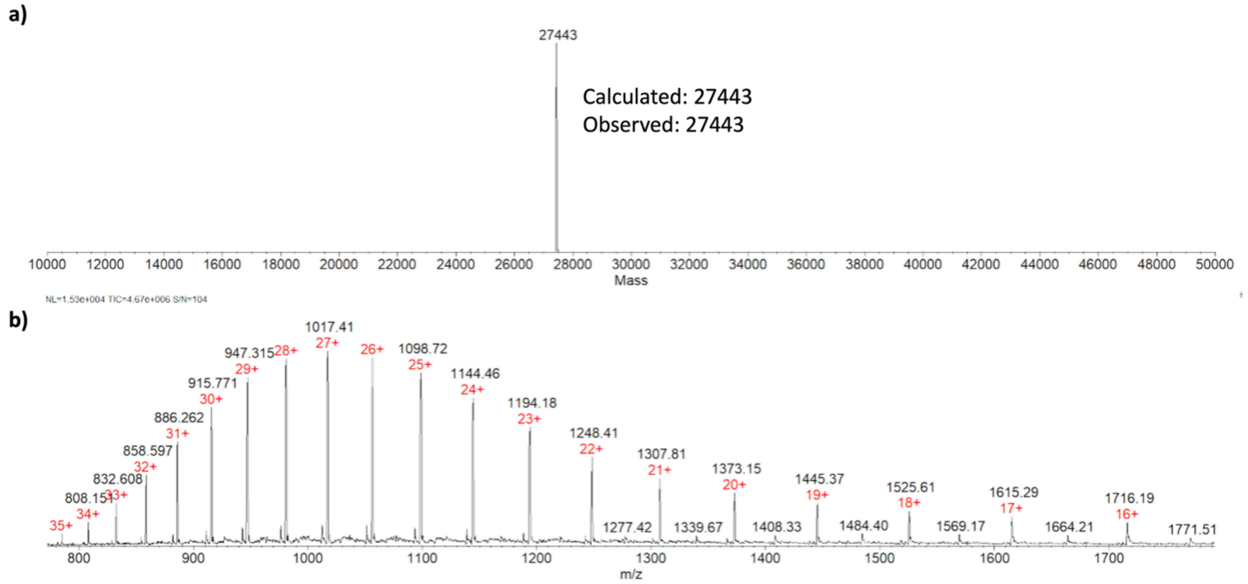

Figure S2. a) Deconvoluted mass and b) crude mass envelope of MIEGRCX$_9$C_pIII protein. Factor Xa cleavage site IEGR is for the generation of an NCys.

2.3 Expression of Keap1 Protein

A truncated Keap1 construct (residues 321–624) was generated by deleting the N-terminal region (residues 1–320) from plasmid pET28a-His$_6$-Keap1 (Addgene plasmid #62454) using a Q5 mutagenesis kit (New England Biolabs). The following primers were used:

Forward: 5′-CATCCCTGAGCCCTGGAAATACAAGTTTTCTCCG-3′
Reverse: 5′-GCGCCCAAGGTGGGCCGC-3′

The sequence of the modified plasmid was verified by Sanger sequencing and subsequently transformed into *E. coli* BL21(DE3) competent cells for protein expression.

For expression, a single colony was inoculated into 10 mL LB media with 50 µg/mL kanamycin and grown 16h at 37 °C with shaking at 250 rpm. The overnight culture was transferred into 1 L LB media (50 µg/mL kanamycin) in a 4 L flask and incubated at 37 °C with shaking at 250 rpm until the optical density (OD$_{600}$) of 0.4–0.6 was reached. Protein over expression was induced by the addition of 1 mM IPTG, followed by incubation at room temperature for 16 h with shaking at 250 rpm. Cells were harvested by centrifugation (4°C, 5,000 g, 20 min), resuspended in lysis buffer (20 mM Tris, 300 mM NaCl, 10 mM imidazole), and lysed by sonication on ice. The lysate was separated by centrifugation (4°C, 10,000 g, 20 min), and the supernatant was filtered by 0.45 µm filter (Macherey-Nagel), then purified using Ni-NTA agarose resin. The eluted protein was desalted on a NAP-10 column (GE Healthcare) and stored in PBS buffer at -80 °C until further use. Protein purity was confirmed by LC-MS analysis (Method B, as described in the LC-MS Analysis Methods).

Sequence:

MGSSHHHHHHSSSGSGENLYFQGSGMAPKVGRLIYTAGGYFRQSLSYLEAYNPSDGTW
LRLADLQVPRSGLAGCVVGGLLYAVGGRNNSPDGNTDSSALDCYNPMTNQWSPCAPM
SVPRNRIGVGVIDGHIYAVGGSHGCIHHNSVERYEPERDEWHLVAPMLTRRIGVGVAVL
NRLLYAVGGFDGTNRLNSAECYYPERNEWRMITAMNTIRSGAGVCVLHNCIYAAGGY
DGQDQLNSVERYDVETETWTFVAPMKHRRSALGITVHQGRIYVLGGYDGHTFLDSVEC
YDPDTDTWSEVTRMTSGRSGVGVAVTMEPCRKQIDQQNCTC

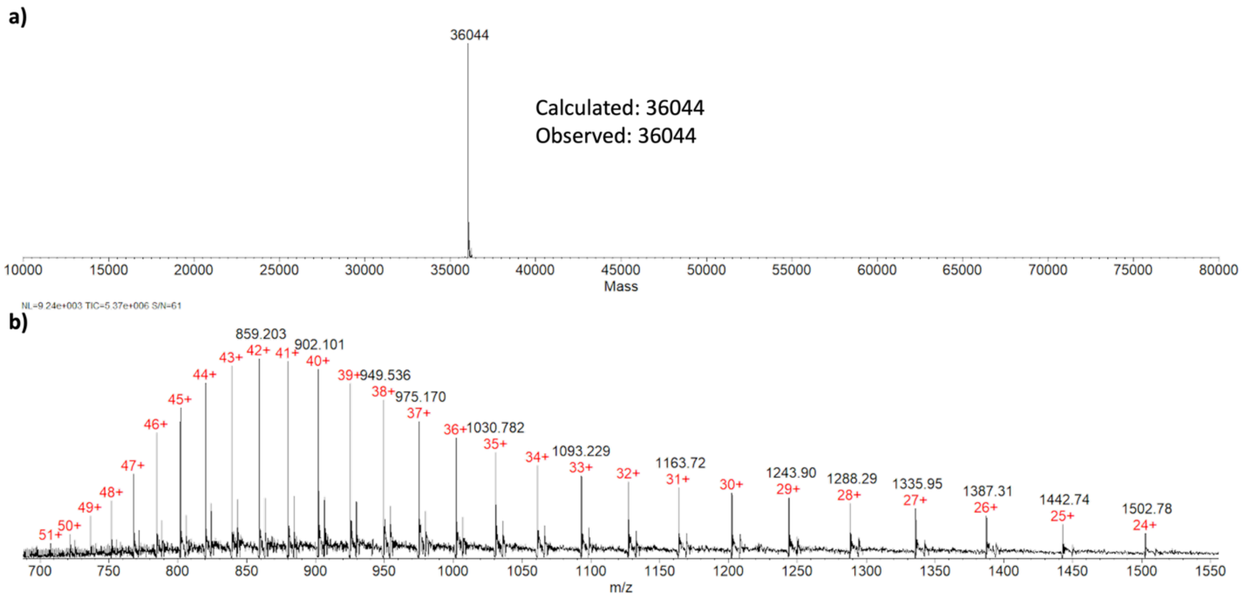
Calculated: 36044
Observed: 36044

Figure S3. a) Deconvoluted mass and b) crude mass envelope of Keap1(321–624) protein.

For biotinylation, Keap1 (5 µM) was incubated with Sulfo-NHS-Biotin (1eq, ThermoFisher, #21217) in PBS buffer (pH 7.4) at 4 °C overnight. Biotinylation was confirmed by LC-MS (Figure S4). Excess unreacted Sulfo-NHS-Biotin was removed using a NAP-5 column (GE Healthcare).

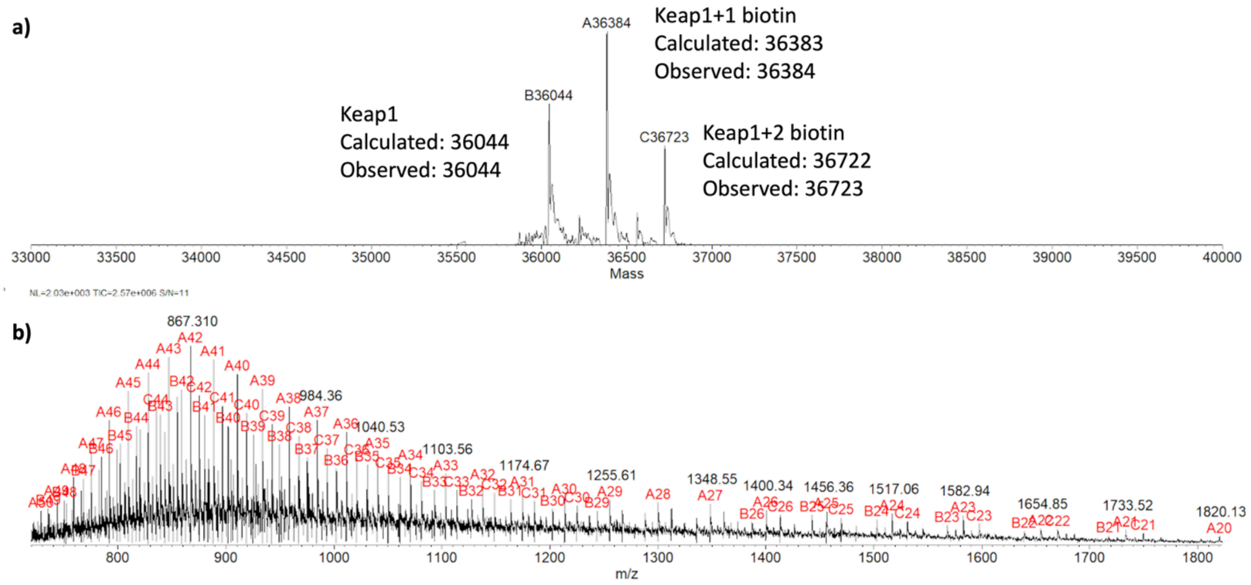
Keap1+1 biotin
Calculated: 36383
Observed: 36384

Keap1
Calculated: 36044
Observed: 36044

Keap1+2 biotin
Calculated: 36722
Observed: 36723

Figure S4. a) Deconvoluted mass and b) crude mass envelope of biotinylated Keap1 protein.

3. Cys-to-Dha Conversion

3.1 Cys-to-Dha Conversion on Model Peptide

To evaluate efficient chemical strategies for the installation of dehydroalanine (Dha), a model peptide was synthesized bearing an N-terminal acylated sequence, Ac-AAAACW. The cysteine residue within this peptide was subjected to chemical conversion into dehydroalanine using three different reagents: methylsulfonyl hydroxyimidazole (MSH), 2,5-dibromohexanediamide (DBHDA), and methyl 2,5-dibromopentanoate (MDBP).

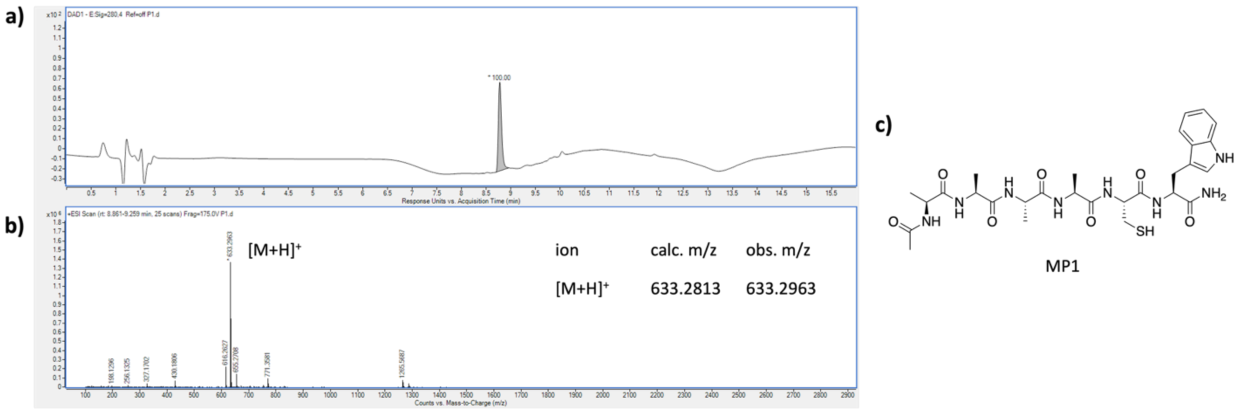

Figure S5. a) LC-MS UV (280 nm) trace of **MP1,** b) mass spec readout of **MP1**, c) chemical structure of **MP1**.

3.1.1 Cys-to-Dha Conversion on Model Peptide by MSH

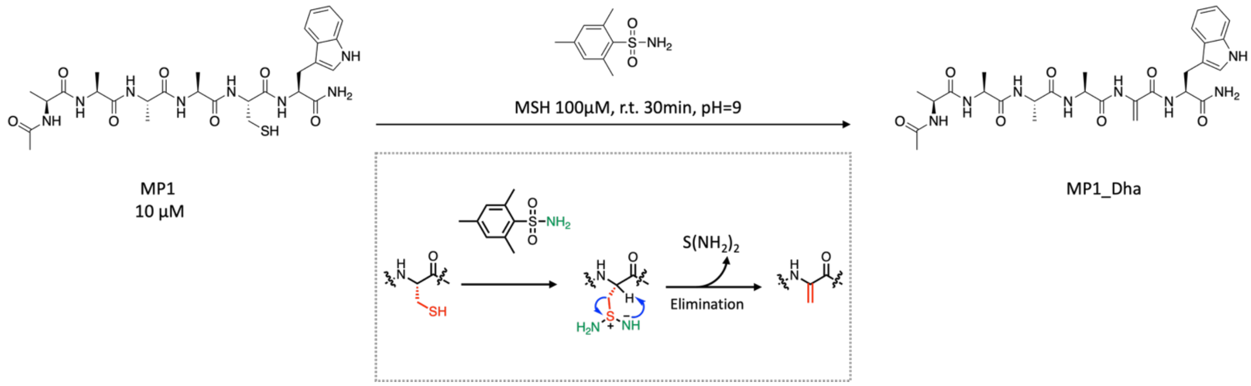

Scheme S3. Cys-to-Dha conversion by MSH on model peptide **MP1**.

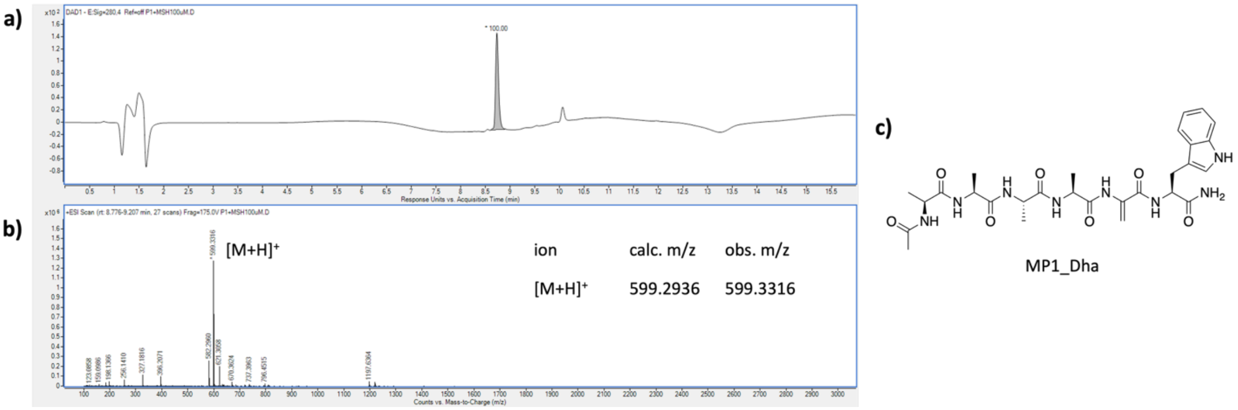

Figure S6. a) LC-MS UV (280 nm) trace of **MP1_Dha** generated using MSH**,** b) mass spec readout of **MP1_Dha**, c) chemical structure of **MP1_Dha**.

3.1.2 Cys-to-Dha Conversion on Model Peptide by DBHDA

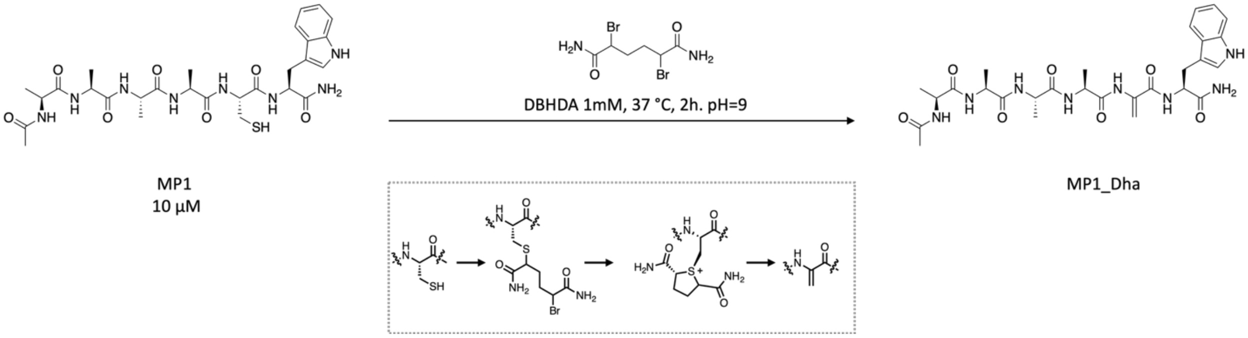

Scheme S4. Cys-to-Dha conversion by DBHDA on model peptide **MP1**.

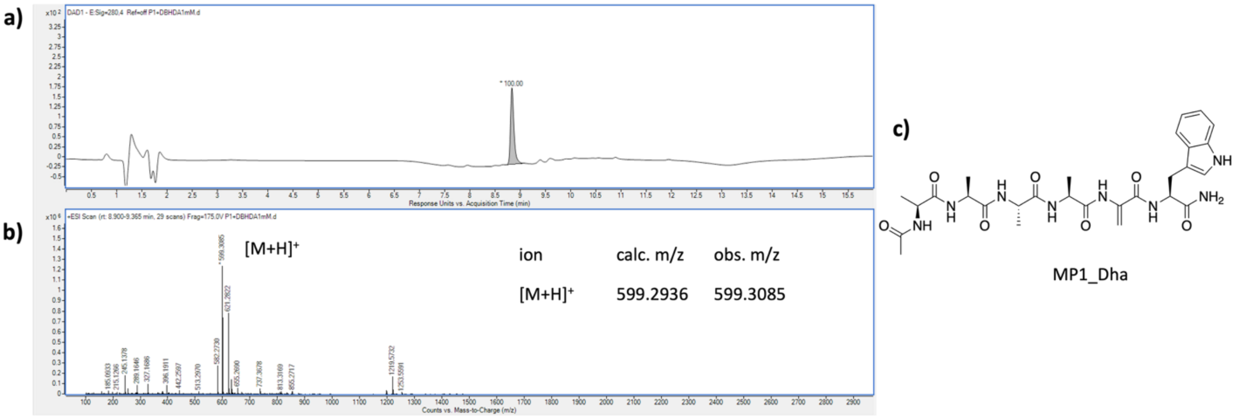

Figure S7. a) LC-MS UV (280 nm) trace of **MP1_Dha** generated using DBHDA**,** b) mass spec readout of **MP1_Dha**, c) chemical structure of **MP1_Dha**.

3.1.3 Cys-to-Dha Conversion on Model Peptide by MDBP

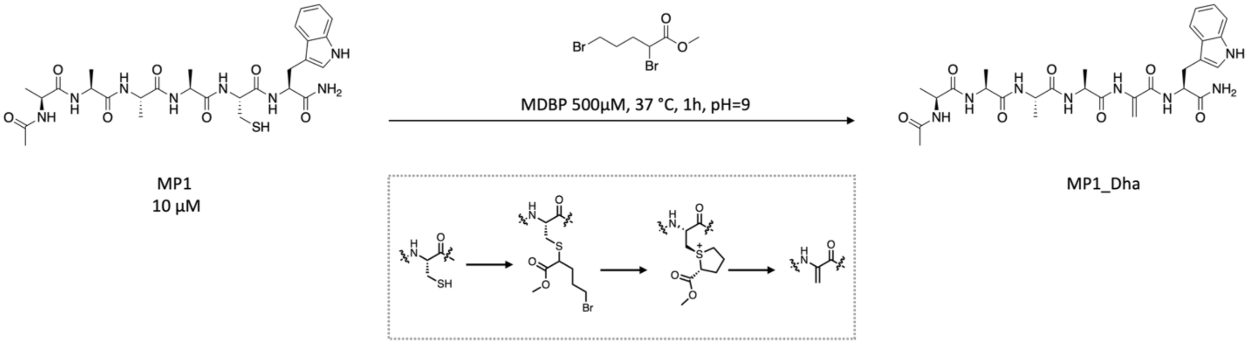

Scheme S5. Cys-to-Dha conversion by MDBP on model peptide **MP1**.

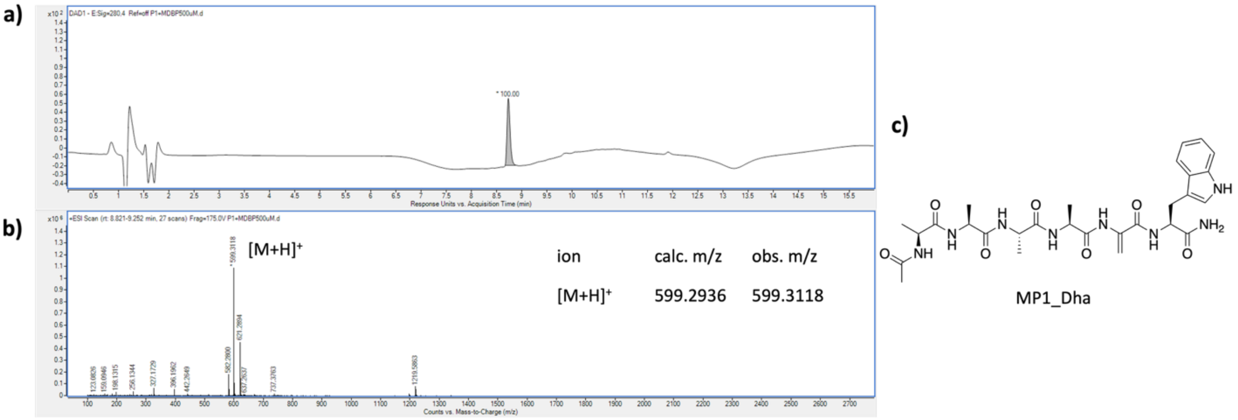

Figure S8. a) LC-MS UV (280 nm) trace of **MP1_Dha** generated using MDBP**,** b) mass spec readout of **MP1_Dha**, c) chemical structure of **MP1_Dha**.

3.2 Cys-to-Dha Conversion Toxicity Evaluation on Phage

20 μL of the prepared phage library (10^{13} pfu/mL) was reduced with 1 mM TCEP in 80 μL of buffer R (20 mM ammonium bicarbonate, pH= 8.0). The reducing reaction was carried out at room temperature for 1 h with shaking at 100 rpm. The reduced phage particles were precipitated with 1/5 volume of 20% PEG/2.5 M NaCl on ice for 1 h, then the precipitated phage was pelleted at 4°C by centrifugation at 14000 rpm for 20 min. For dehydroalanine conversion phage viability evaluation, the supernatant was discarded and the phage pellet was re-suspended in 400 μL of NaPi (100 mM, pH = 9), and aliquoted into four portions of 100 μL of phage. For the control group, 1 μL of DMF was added. For MSH conversion test group, 1 μL of MSH (1-10 mM stock in DMF) was added, then the reaction was mixed and incubated at room temperature for 30min. For DBHDA conversion test group, 1 μL of DBHDA (1-100 mM stock in DMF) was added, then the reaction was mixed and incubated at 37 °C for 2h. For MDBP conversion test group, 1 μL of MDBP (1-100 mM stock in DMF) was added. The reaction was mixed and incubated at 37 °C for

60 min. After the reaction completion, the phage particles were precipitated with 1/5 volume of 20% PEG/2.5 M NaCl on ice for 1 h, then the precipitated phage was pelleted at 4°C by centrifugation at 14000 rpm for 20 min. After removal of supernatant, the phage pellet were resuspended in 100 µL of PBS (pH=7.4) and subjected for titering to count the phage particles.

3.3 Cys-to-Dha Conversion on Model Protein Sortase A

To investigate dehydroalanine (Dha) formation in a protein context, a Sortase A variant was engineered as a model system. The catalytic cysteine at position 153 was mutated to alanine (C153A), and a solvent-accessible cysteine was introduced at position 159 (K159C). The resulting Sortase A_C153A/K159C mutant was expressed and purified as described in the previous section, and its identity was confirmed by LC-MS. For Dha installation, the mutant protein was incubated with the conversion reagents 2,5-dibromohexanediamide (DBHDA) and methyl 2,5-dibromopentanoate (MDBP). Reaction kinetics and conversion efficiency were monitored over time by LC-MS analysis.

3.3.1 Cys-to-Dha Conversion on Model Protein Sortase A by DBHDA

Sortase A_C153A K159C (100 µM) was reduced by with 1mM TCEP in PBS buffer (pH 7.4) at room temperature for 1h. 10 µL of reduced Sortase A_C153A K159C protein was diluted with 89 µL of NaPi buffer (100mM, pH 9), 1 µL of DBHDA stock solution (100mM, DMF) was added in to the reaction, resulting 10 µM of protein and 1 mM of DBHDA in NaPi buffer with 1% DMF. The mixture was pipetted several times, incubated at 37 ºC with 250 rpm shaking. The reaction conversion was monitored at 0min, 15min, 30min, 45min, 60min, 90min, 120min time point by LC-MS.

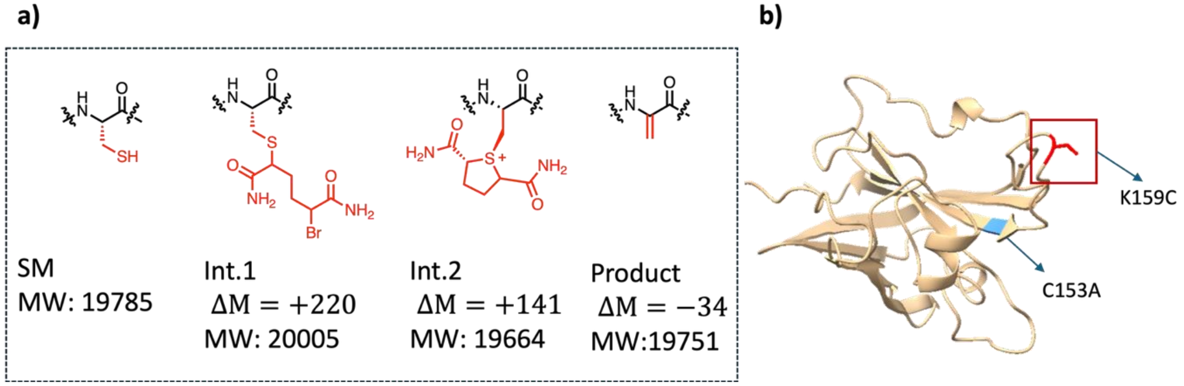

Figure S9. a) Cys-to-Dha conversion of Sortase A_C153A/K159C by DBHDA**,** b) predicted three-dimensional (3D) structures structure of Sortase A_C153A/K159C (Protein structure prediction was processed by Alphafold2).

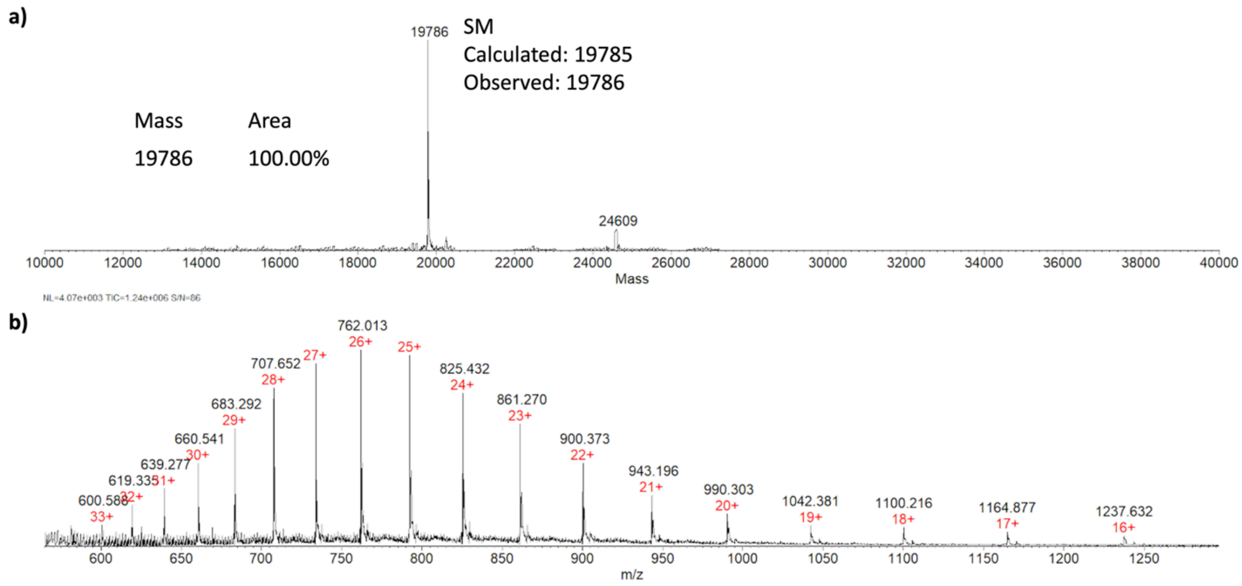

Figure S10. a) Deconvoluted mass and b) crude mass envelope of Sortase A_C153A/K159C after 1mM of DBHDA treatment at the time point of 0 min.

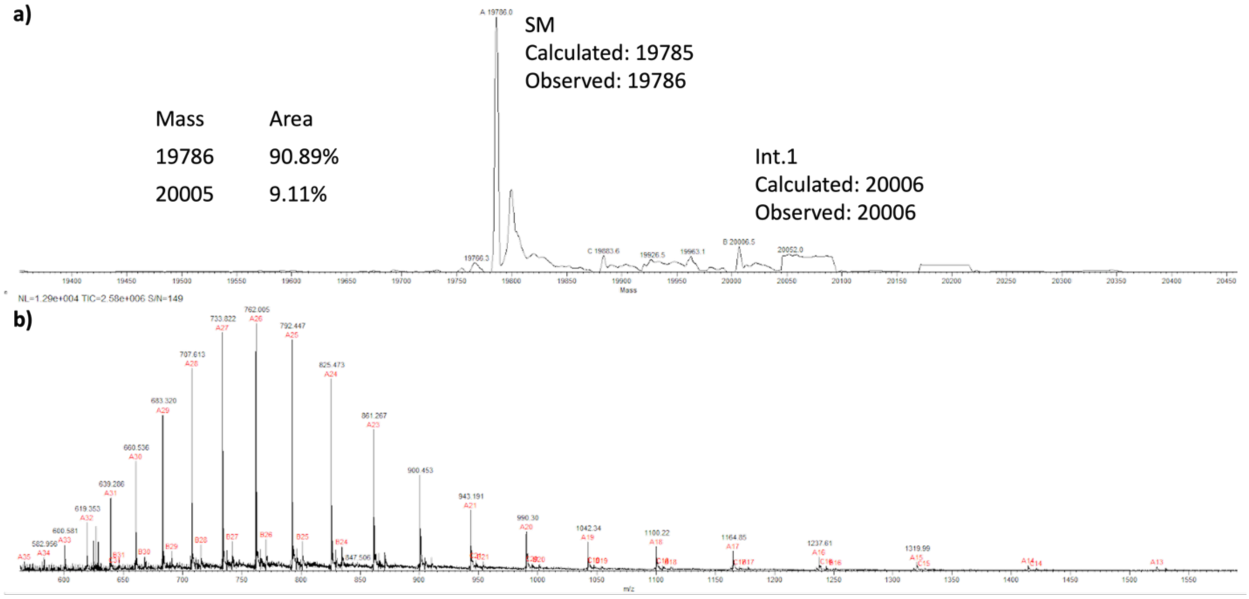

Figure S11. a) Deconvoluted mass and b) crude mass envelope of Sortase A_C153A/K159C after 1mM of DBHDA treatment at the time point of 15 min.

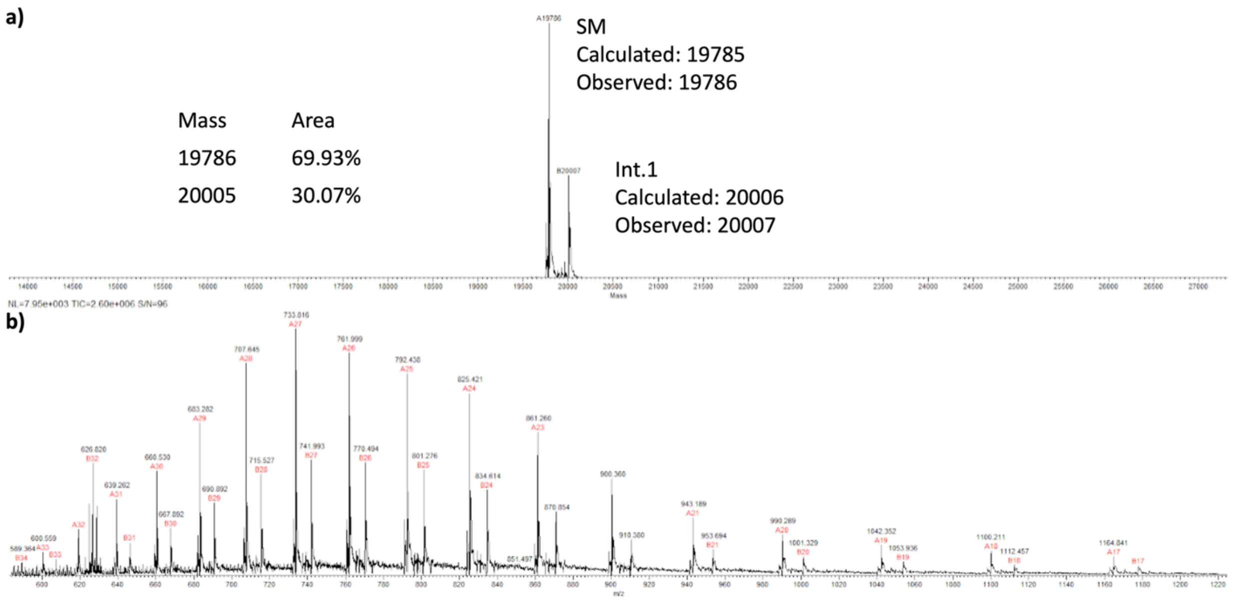

SM
Calculated: 19785
Observed: 19786

Int.1
Calculated: 20006
Observed: 20007

Mass	Area
19786	69.93%
20005	30.07%

Figure S12. a) Deconvoluted mass and b) crude mass envelope of Sortase A_C153A/K159C after 1mM of DBHDA treatment at the time point of 30 min.

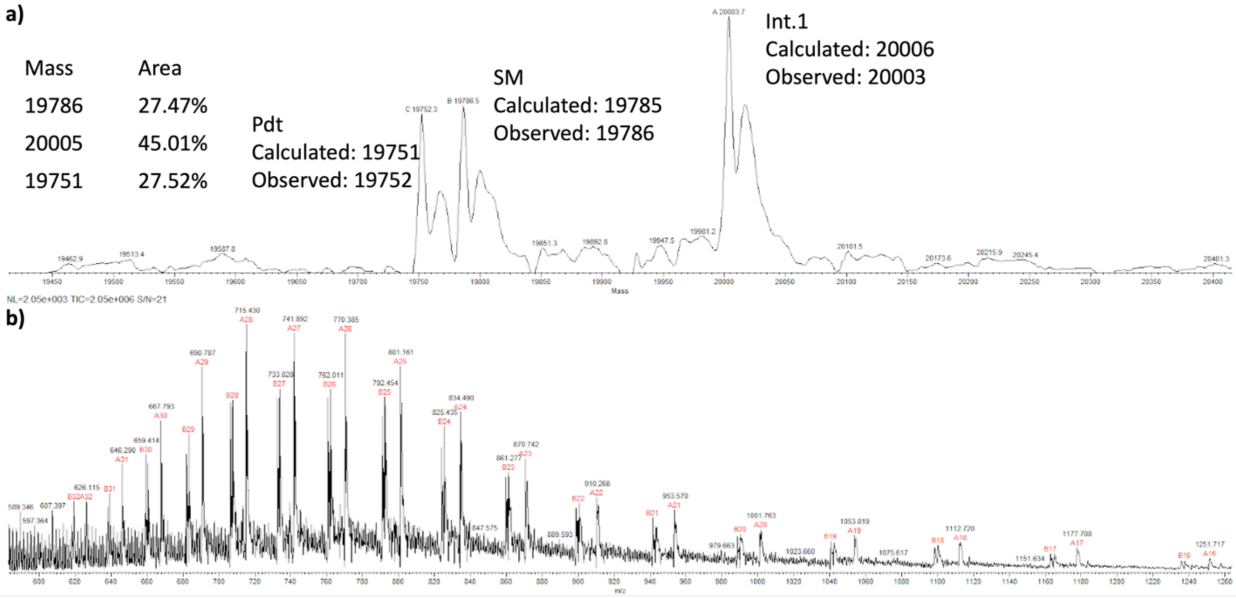

Int.1
Calculated: 20006
Observed: 20003

SM
Calculated: 19785
Observed: 19786

Pdt
Calculated: 19751
Observed: 19752

Mass	Area
19786	27.47%
20005	45.01%
19751	27.52%

Figure S13. a) Deconvoluted mass and b) crude mass envelope of Sortase A_C153A/K159C after 1mM of DBHDA treatment at the time point of 45 min.

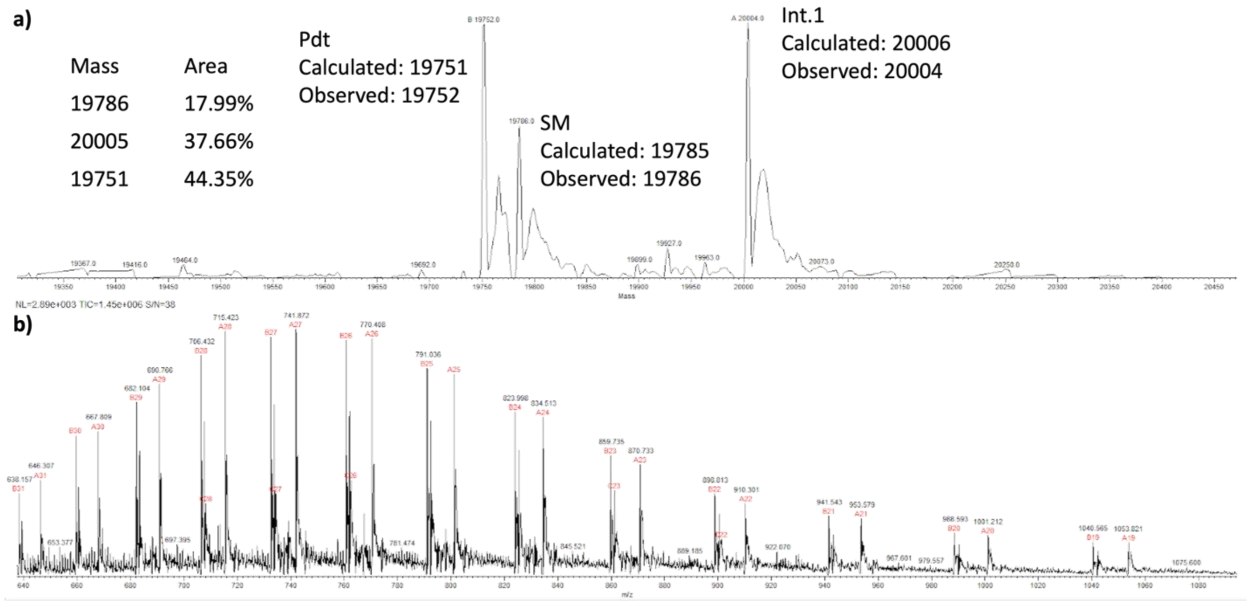

Figure S14. a) Deconvoluted mass and b) crude mass envelope of Sortase A_C153A/K159C after 1mM of DBHDA treatment at the time point of 60 min.

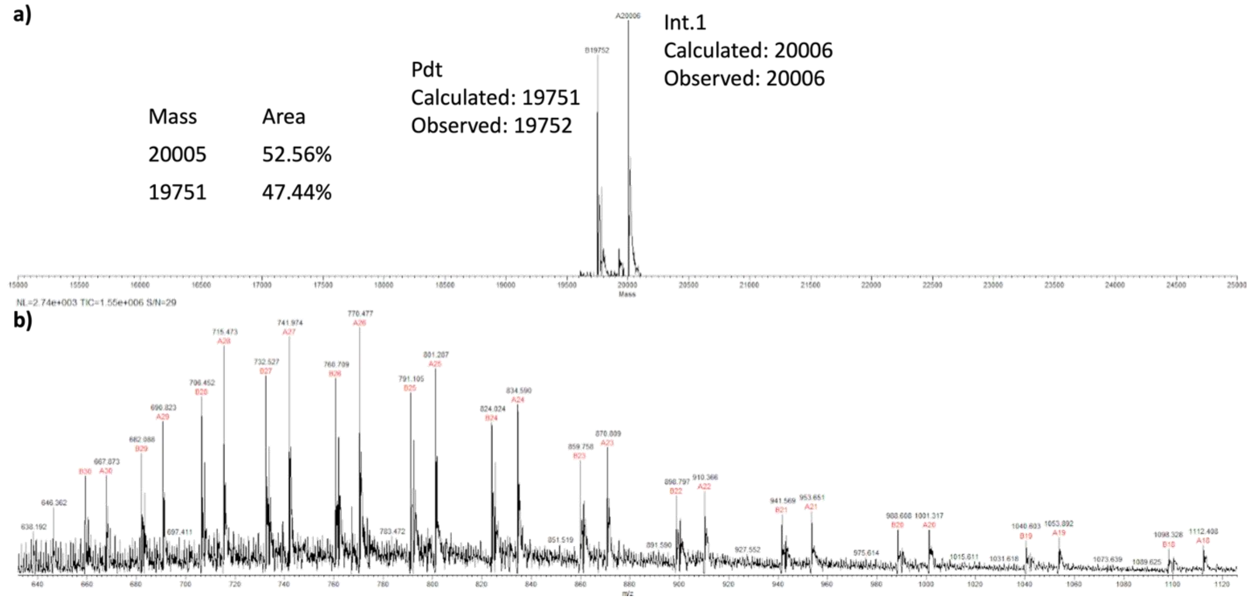

Figure S15. a) Deconvoluted mass and b) crude mass envelope of Sortase A_C153A/K159C after 1mM of DBHDA treatment at the time point of 75 min.

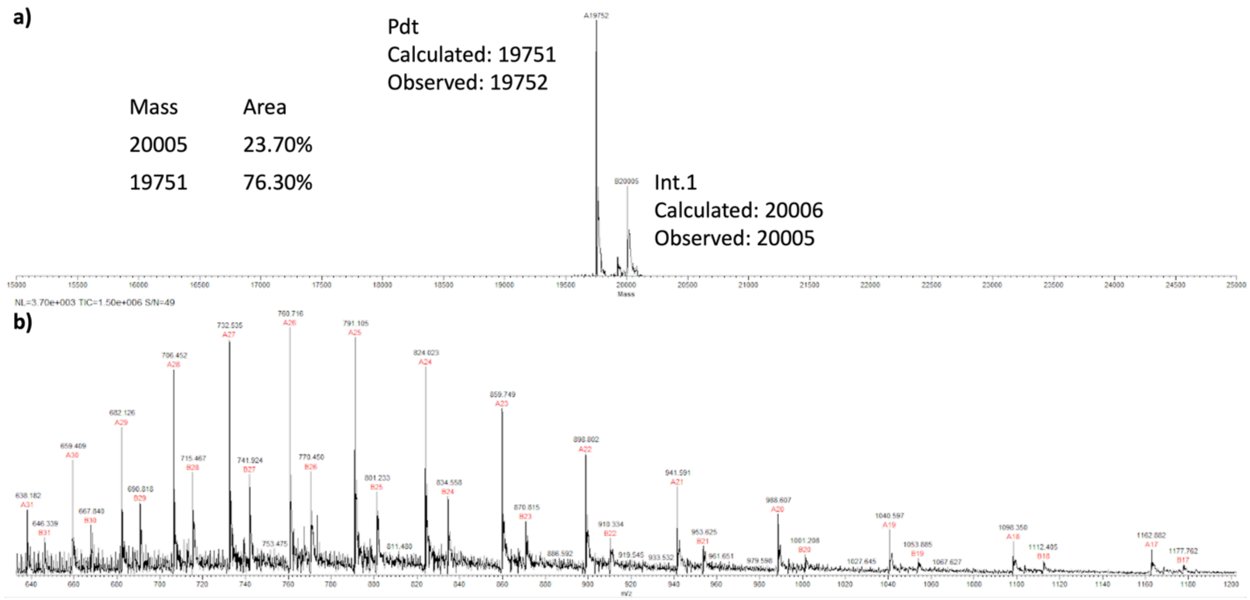

Pdt
Calculated: 19751
Observed: 19752

Mass	Area
20005	23.70%
19751	76.30%

Int.1
Calculated: 20006
Observed: 20005

Figure S16. a) Deconvoluted mass and b) crude mass envelope of Sortase A_C153A/K159C after 1mM of DBHDA treatment at the time point of 90 min.

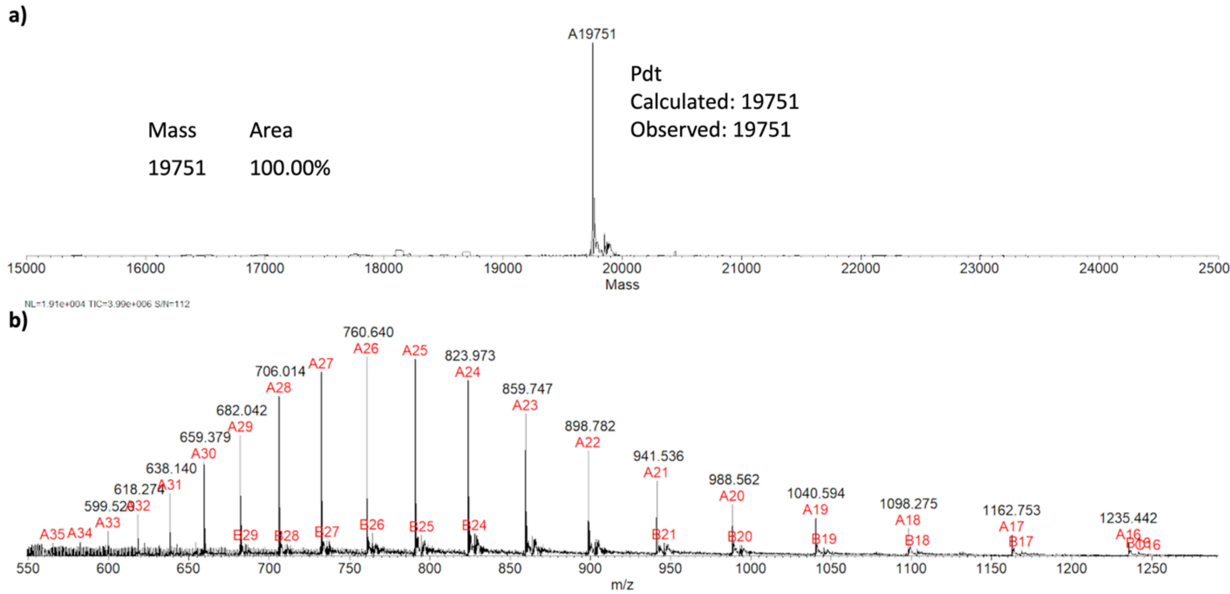

Pdt
Calculated: 19751
Observed: 19751

Mass	Area
19751	100.00%

Figure S17. a) Deconvoluted mass and b) crude mass envelope of Sortase A_C153A/K159C after 1mM of DBHDA treatment at the time point of 120 min.

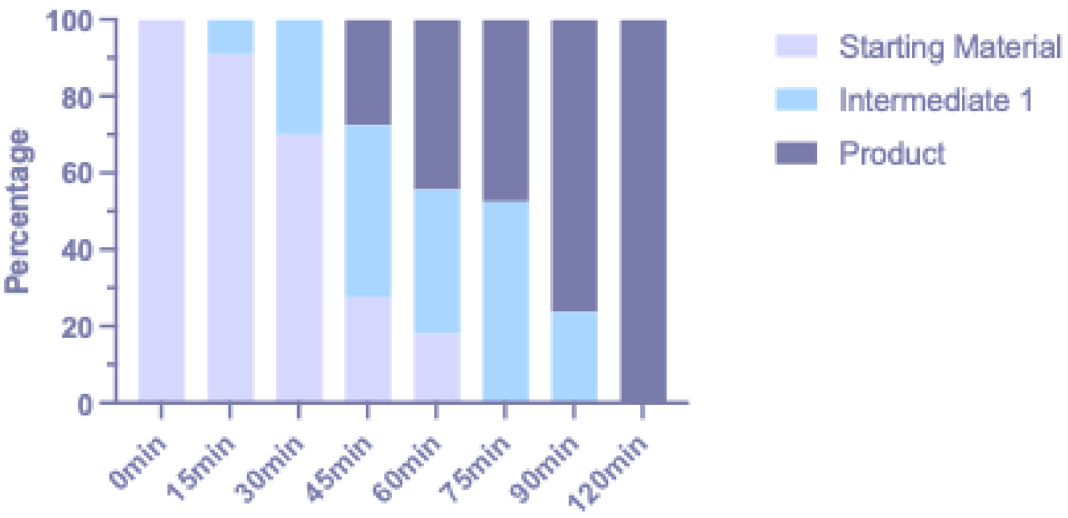

Figure S18. Reaction kinetics of Cys-to-Dha conversion on Sortase A_C153A/K159C by 1mM of DBHDA.

3.3.2 Cys-to-Dha Conversion on Model Protein Sortase A by MDBP

Sortase A_C153A K159C (100 µM) was reduced by with 1mM TCEP in PBS buffer (pH 7.4) at room temperature for 1h. 10 µL of reduced Sortase A_C153A K159C protein was diluted with 89 µL of NaPi buffer (100mM, pH 9), 1 µL of MDBP stock solution (50mM, DMF) was added in to the reaction, resulting 10 µM of protein and 500 µM of MDBP in NaPi buffer with 1% DMF. The mixture was pipetted several times, incubated at 37 ºC with 250 rpm shaking. The reaction conversion was monitored at 0min, 5min, 10min, 15min, 20min, 30min, 50min time point by LC-MS.

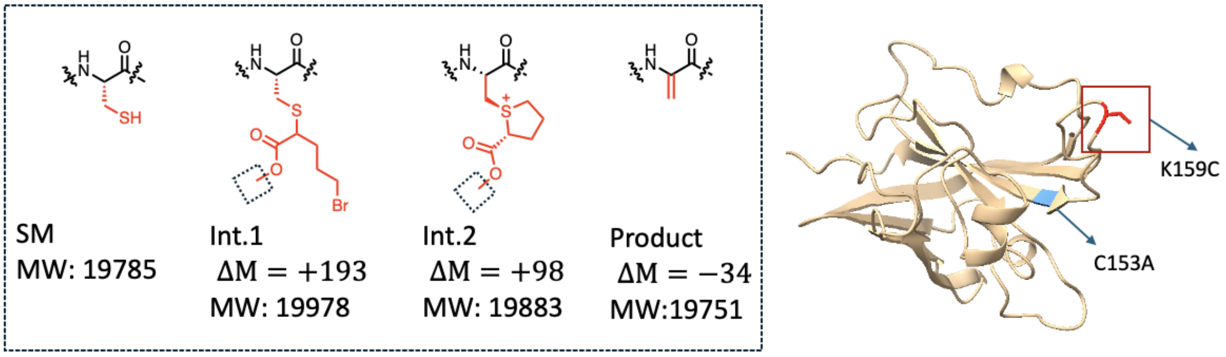

Figure S19. a) Cys-to-Dha conversion of the model protein Sortase A_C153A/K159C by MDBP**,** b) predicted three-dimensional (3D) structures structure of Sortase A_C153A/K159C (Protein structure prediction was processed by Alphafold2).

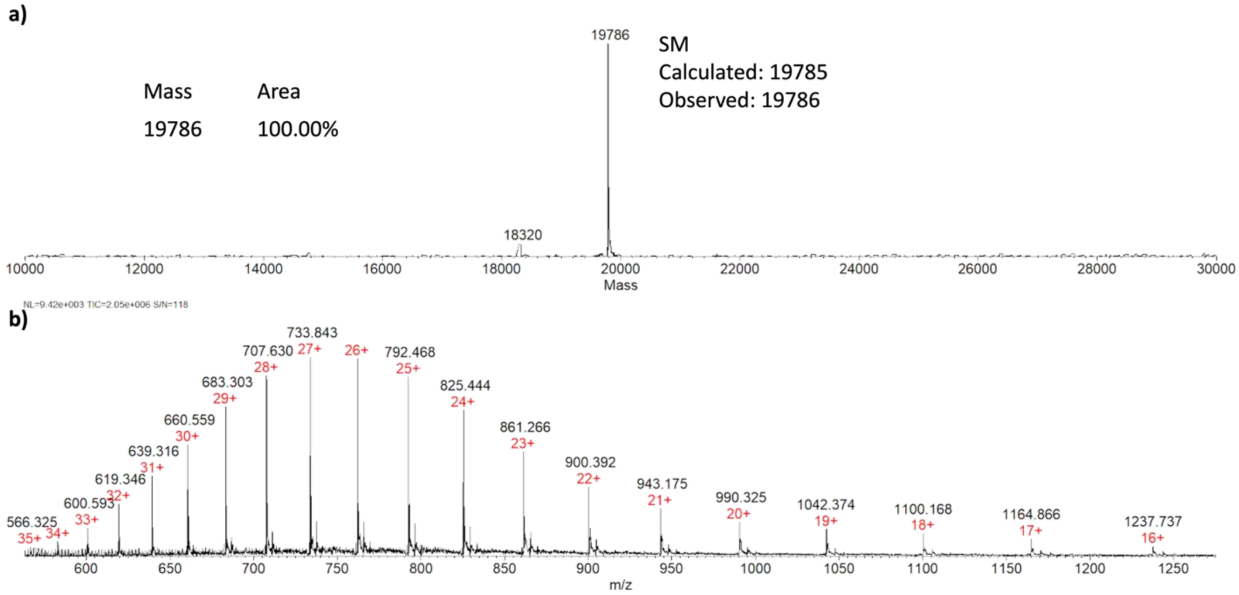

Figure S20. a) Deconvoluted mass and b) crude mass envelope of Sortase A_C153A/K159C after 500 µM of MDBP treatment at the time point of 0 min.

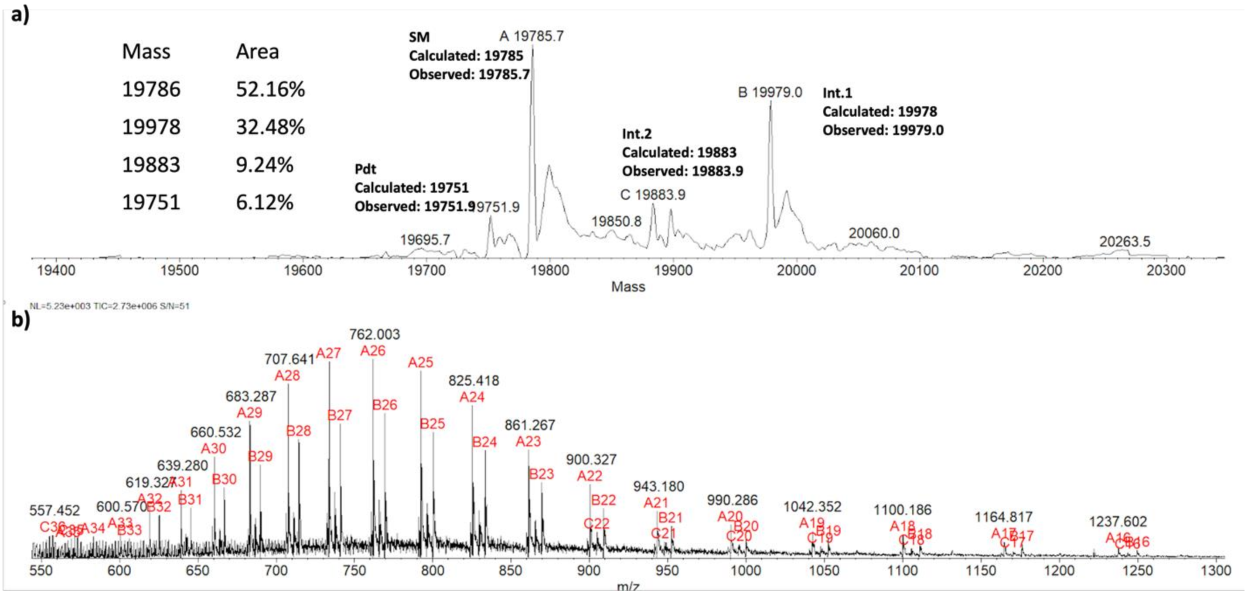

Figure S21. a) Deconvoluted mass and b) crude mass envelope of Sortase A_C153A/K159C after 500 µM of MDBP treatment at the time point of 5 min.

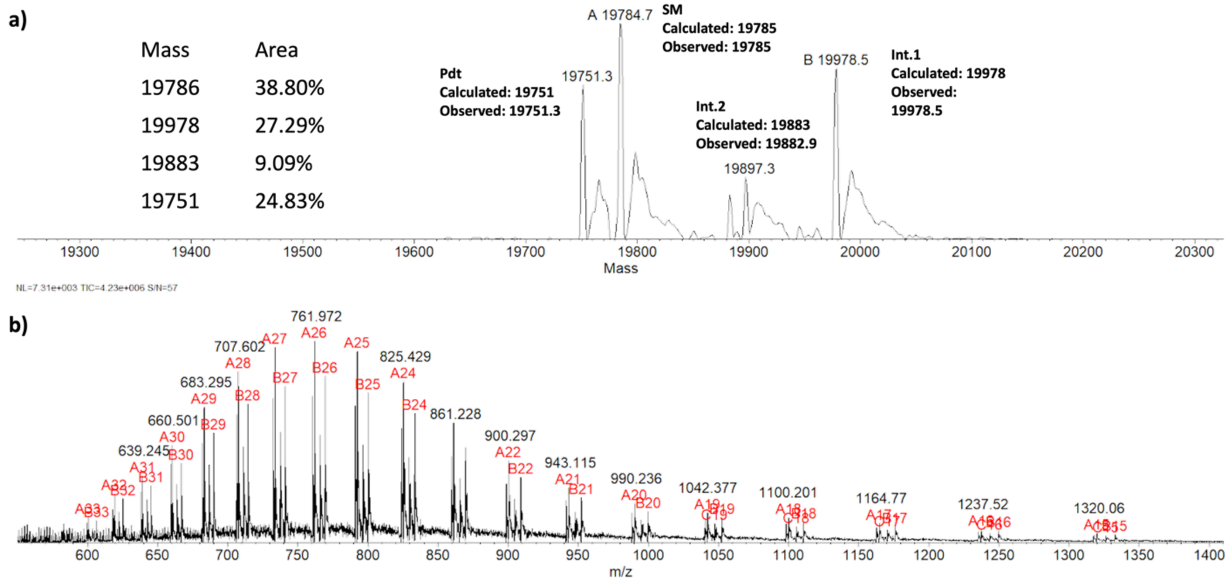

Mass	Area
19786	38.80%
19978	27.29%
19883	9.09%
19751	24.83%

Figure S22. a) Deconvoluted mass and b) crude mass envelope of Sortase A_C153A/K159C after 500 µM of MDBP treatment at the time point of 10 min.

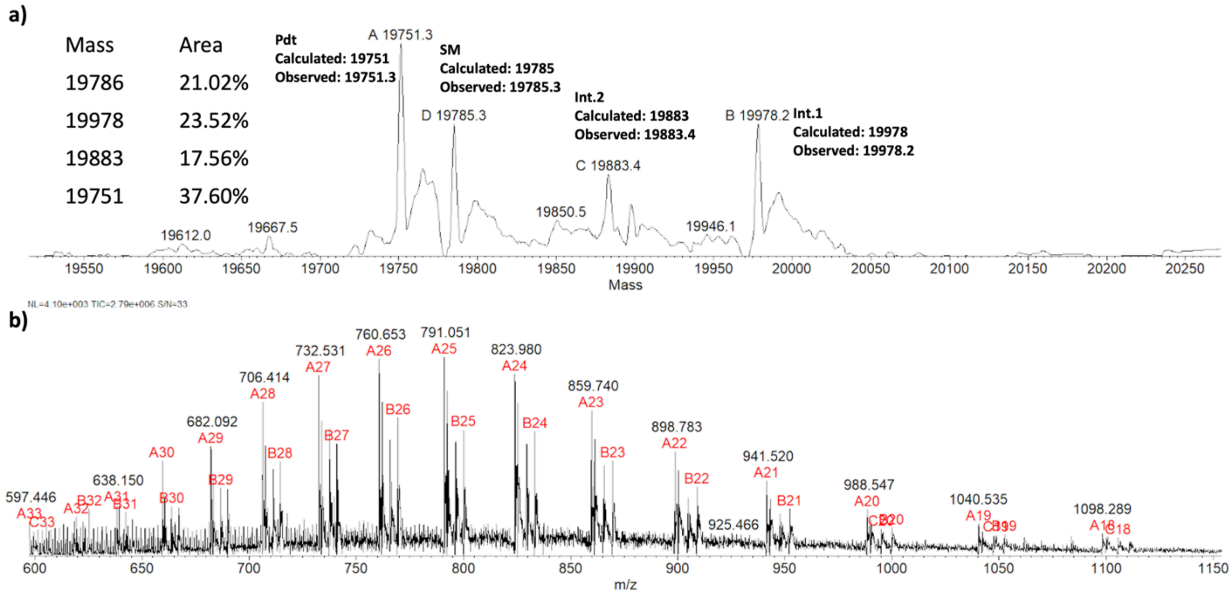

Mass	Area
19786	21.02%
19978	23.52%
19883	17.56%
19751	37.60%

Figure S23. a) Deconvoluted mass and b) crude mass envelope of Sortase A_C153A/K159C after 500 µM of MDBP treatment at the time point of 15 min.

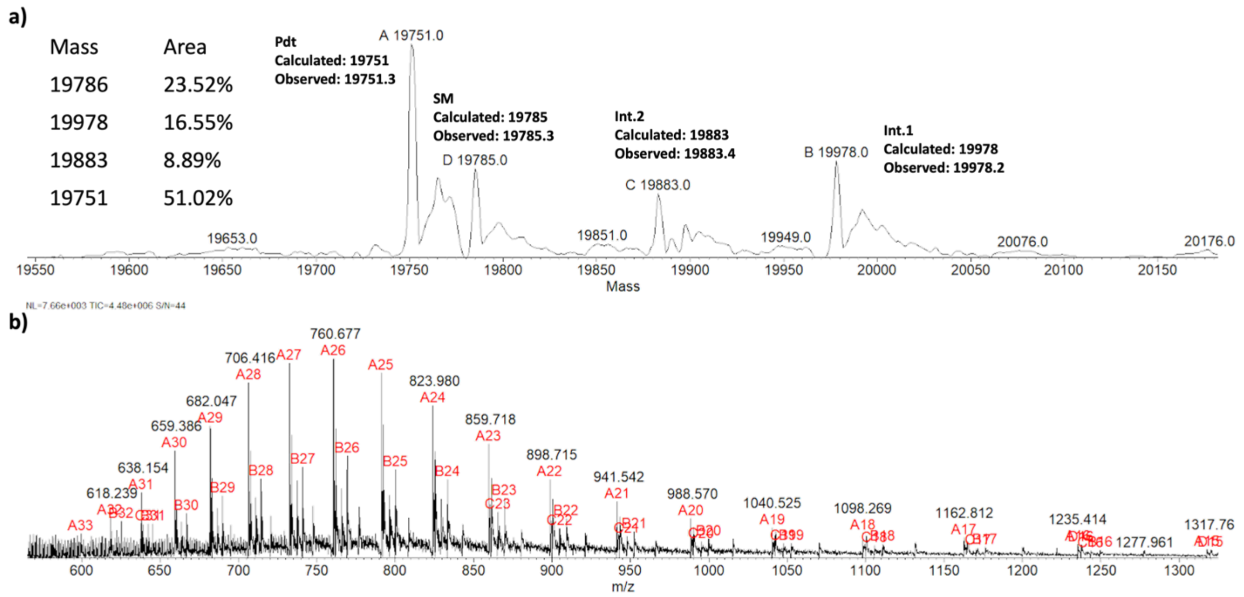

Figure S24. a) Deconvoluted mass and b) crude mass envelope of Sortase A_C153A/K159C after 500 µM of MDBP treatment at the time point of 20 min.

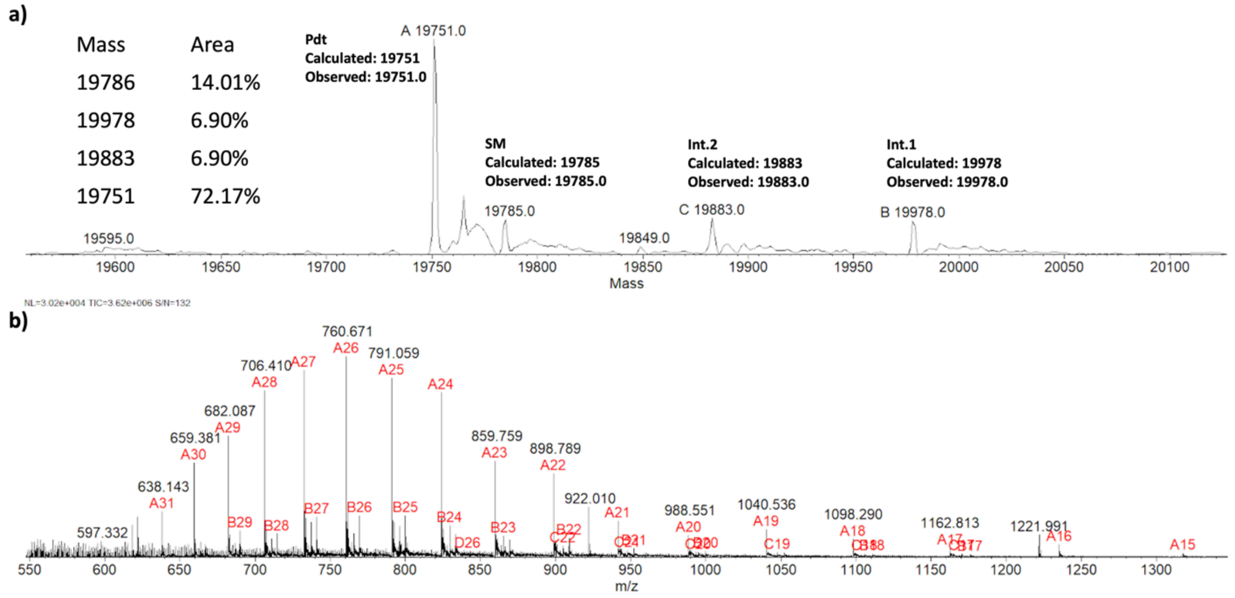

Figure S25. a) Deconvoluted mass and b) crude mass envelope of Sortase A_C153A/K159C after 500 µM of MDBP treatment at the time point of 30 min.

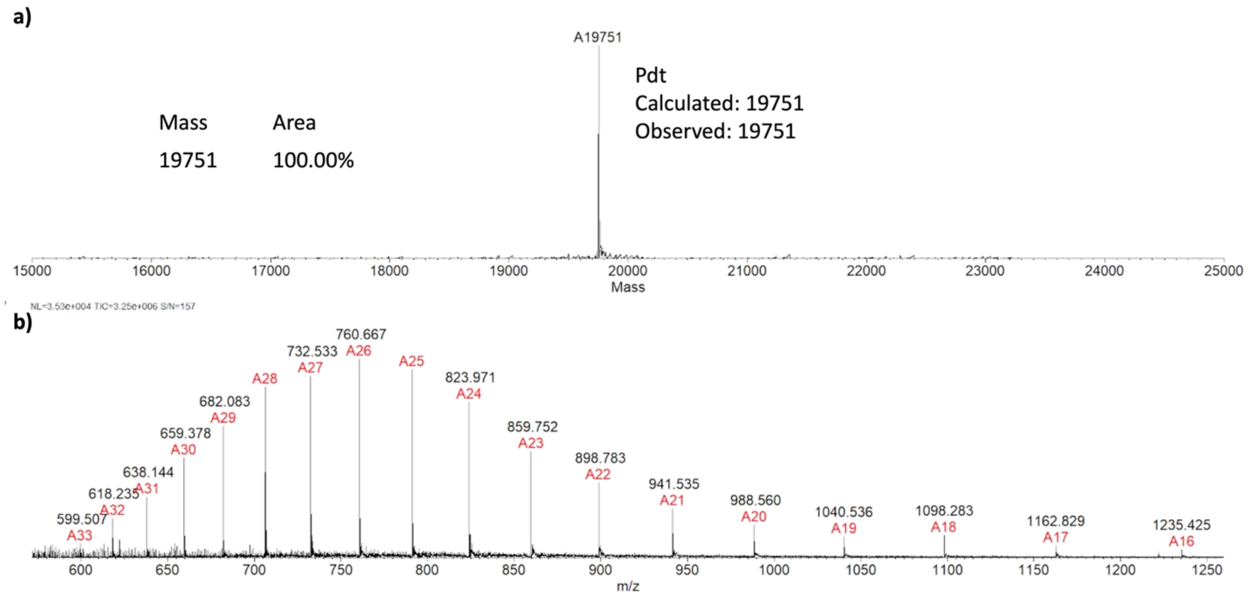

Figure S26. a) Deconvoluted mass and b) crude mass envelope of Sortase A_C153A/K159C after 500 µM of MDBP treatment at the time point of 50 min.

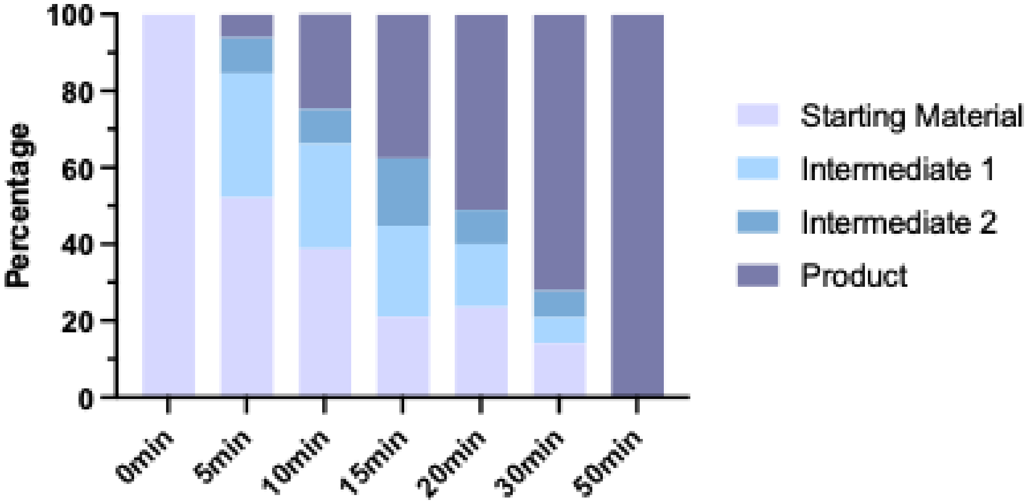

Figure S27. Reaction kinetics of Cys-to-Dha conversion on Model protein Sortase A_C153A/K159C by 500 µM of MDBP.

4. Cyclization of Model Peptides

4.1 Cyclization of Model Peptide S1 (CLIPSWGC)

4.1.1 Cyclization of S1 (CLIPSWGC) through benzaldehyde protection

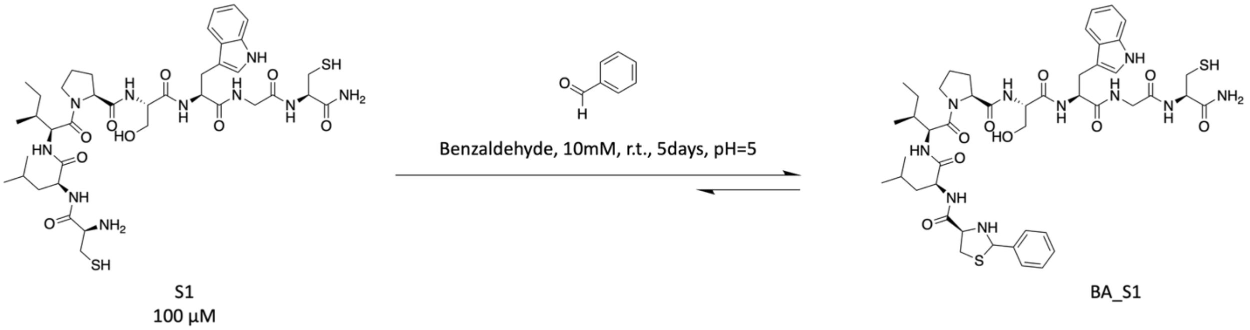

Scheme S6. NCys protection of **S1** by benzaldehyde (BA).

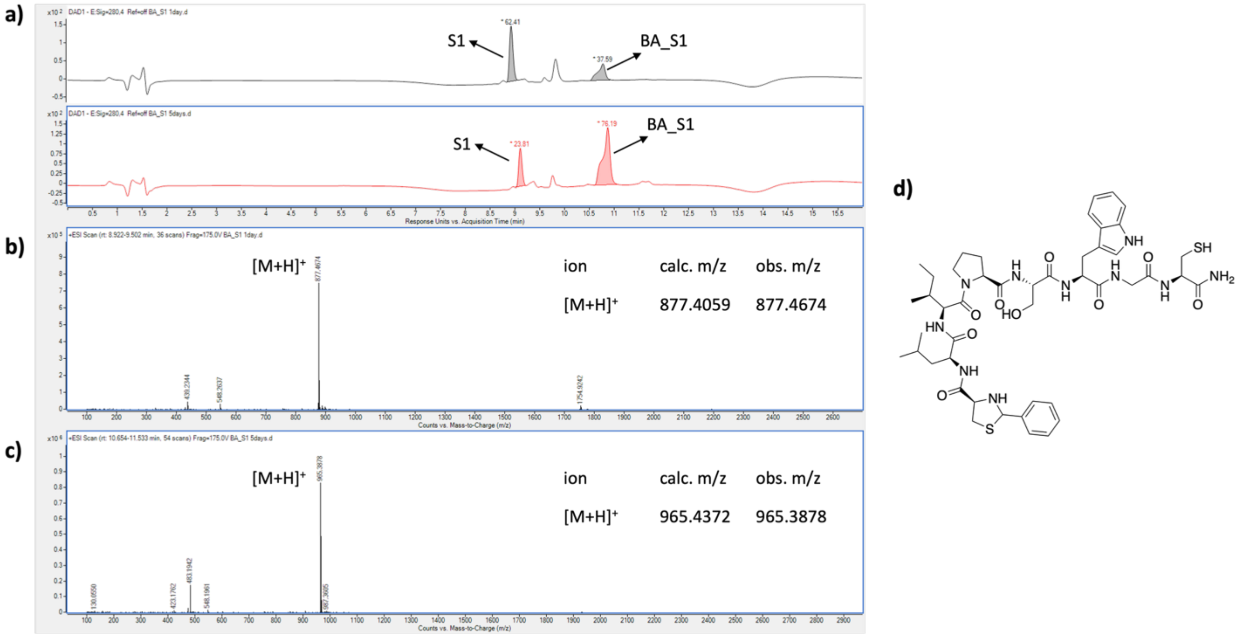

Figure S28. a) LC-MS UV (280 nm) traces of NCys protection of **S1** by benzaldehyde after 1 and 5 days, b) mass spec readout of starting peptide **S1**, c) mass spec readout of conjugate protect **BA_S1**, d) chemical structure of **BA_S1**

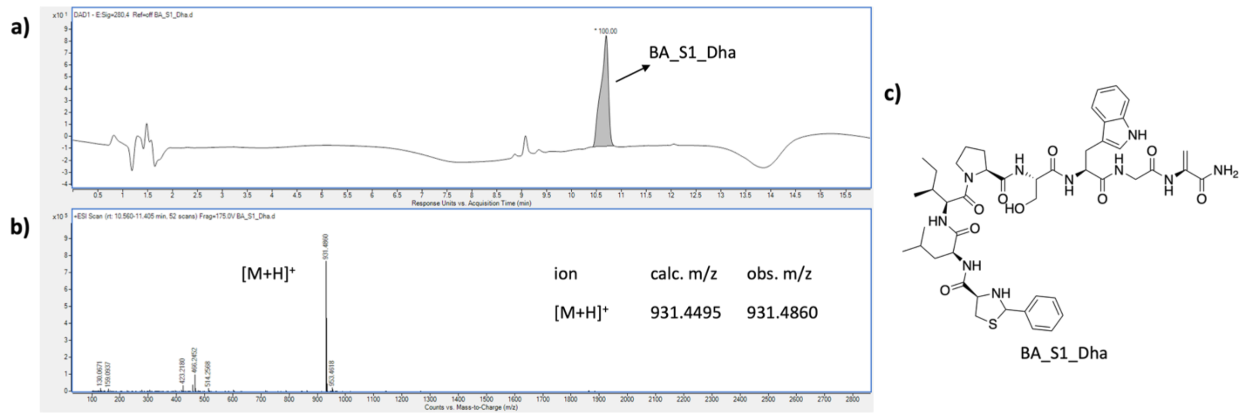

Figure S29. a) LC-MS UV (280 nm) trace of Cys-to-Dha conversion of **BA_S1**by MDBP, b) mass spec readout of peptide product **BA_S1_Dha**, c) chemical structure of **BA_S1_Dha**

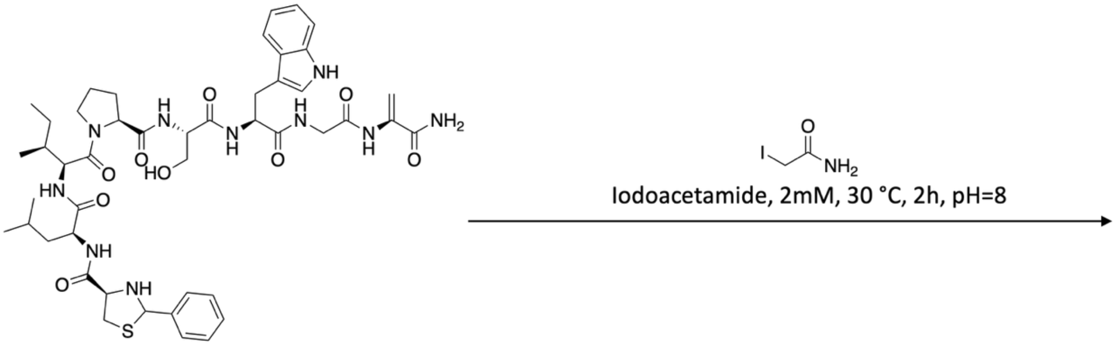

Scheme S7. Validation of complete Cys-to-Dha conversion by iodoacetamide labeling of **BA_S1_Dha**.

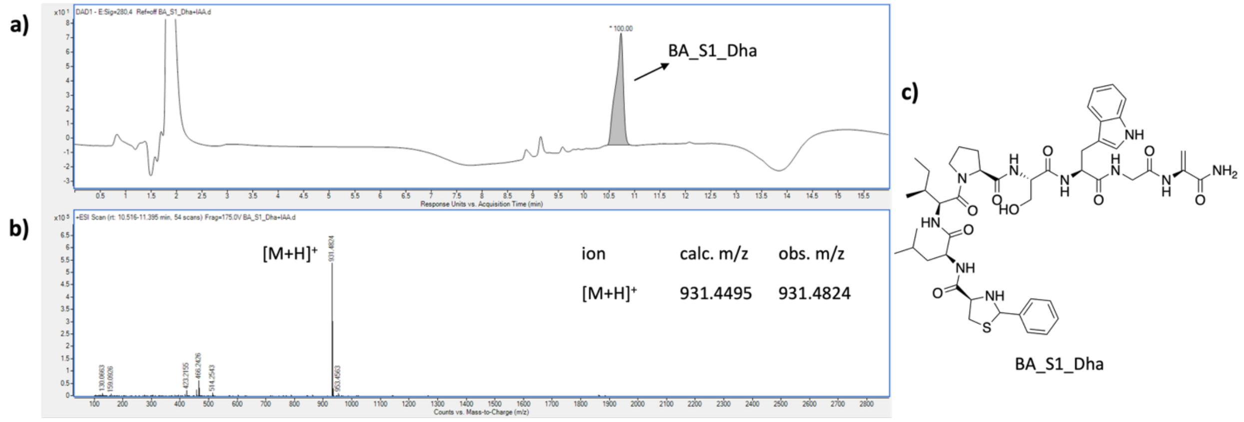

Figure S30. a) LC-MS UV (280 nm) trace of the reaction to validate no free cysteine available on model peptide **BA_S1_Dha** by labeling with iodoacetamide, b) mass spec readout of peptide product **BA_S1_Dha**, c) chemical structure of **BA_S1_Dha**

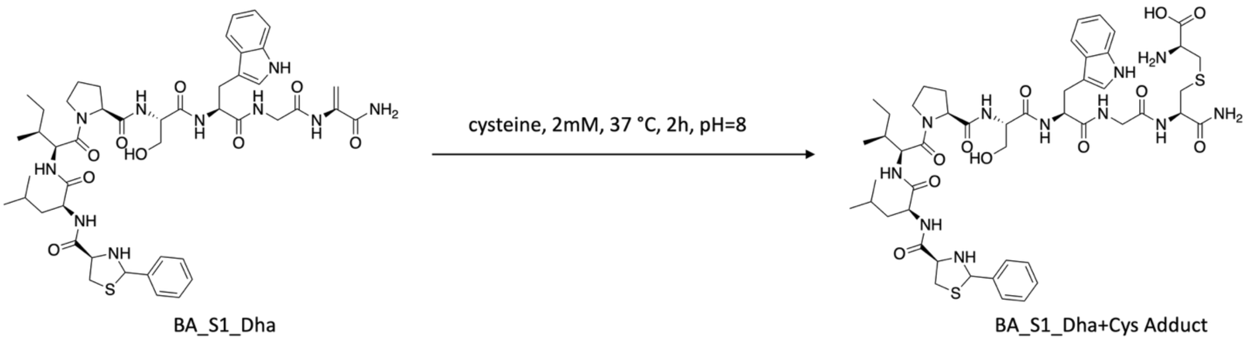

Scheme S8. Validation of dehydroalanine by cysteine labeling on **BA_S1_Dha**.

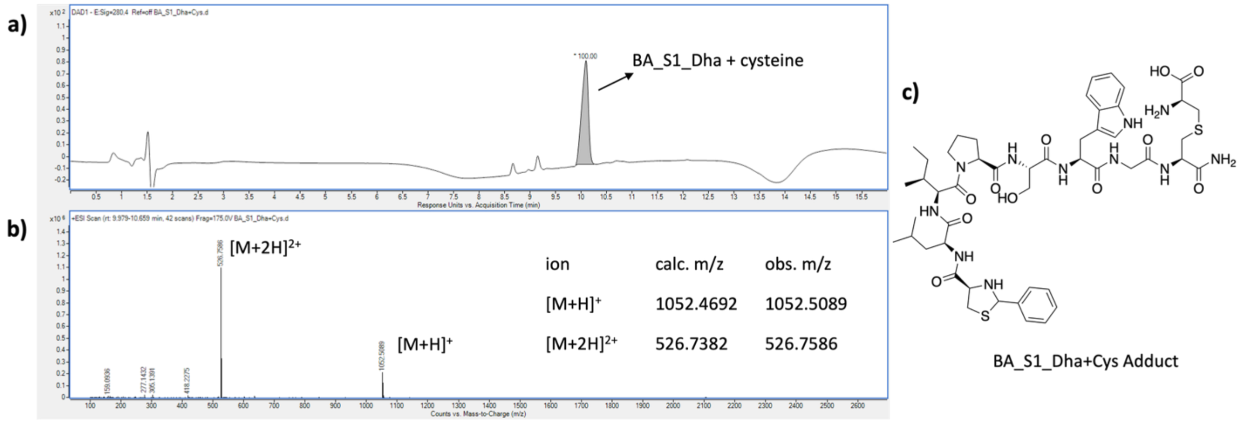

Figure S31. a) LC-MS UV (280 nm) trace of the cysteine labeling reaction of **BA_S1_Dha** , b) mass spec readout of peptide product **BA_S1_Dha+Cys Adduct**, c) chemical structure of **BA_S1_Dha+Cys Adduct**.

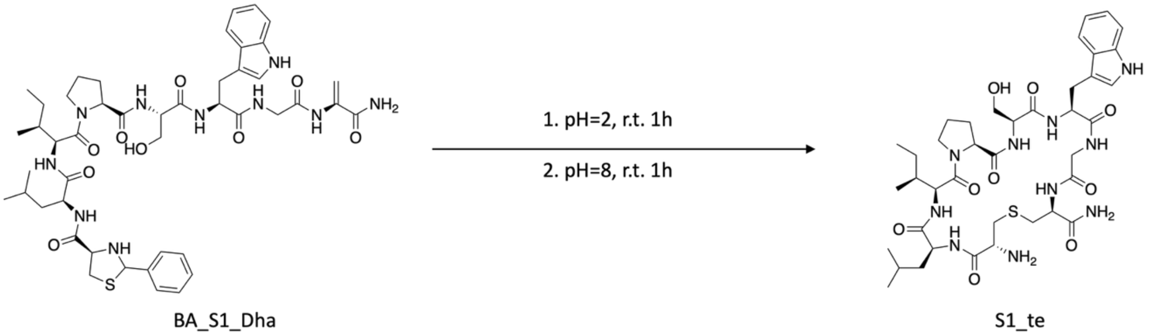

Scheme S9. Deprotection of NCys and cyclization of **BA_S1_Dha**.

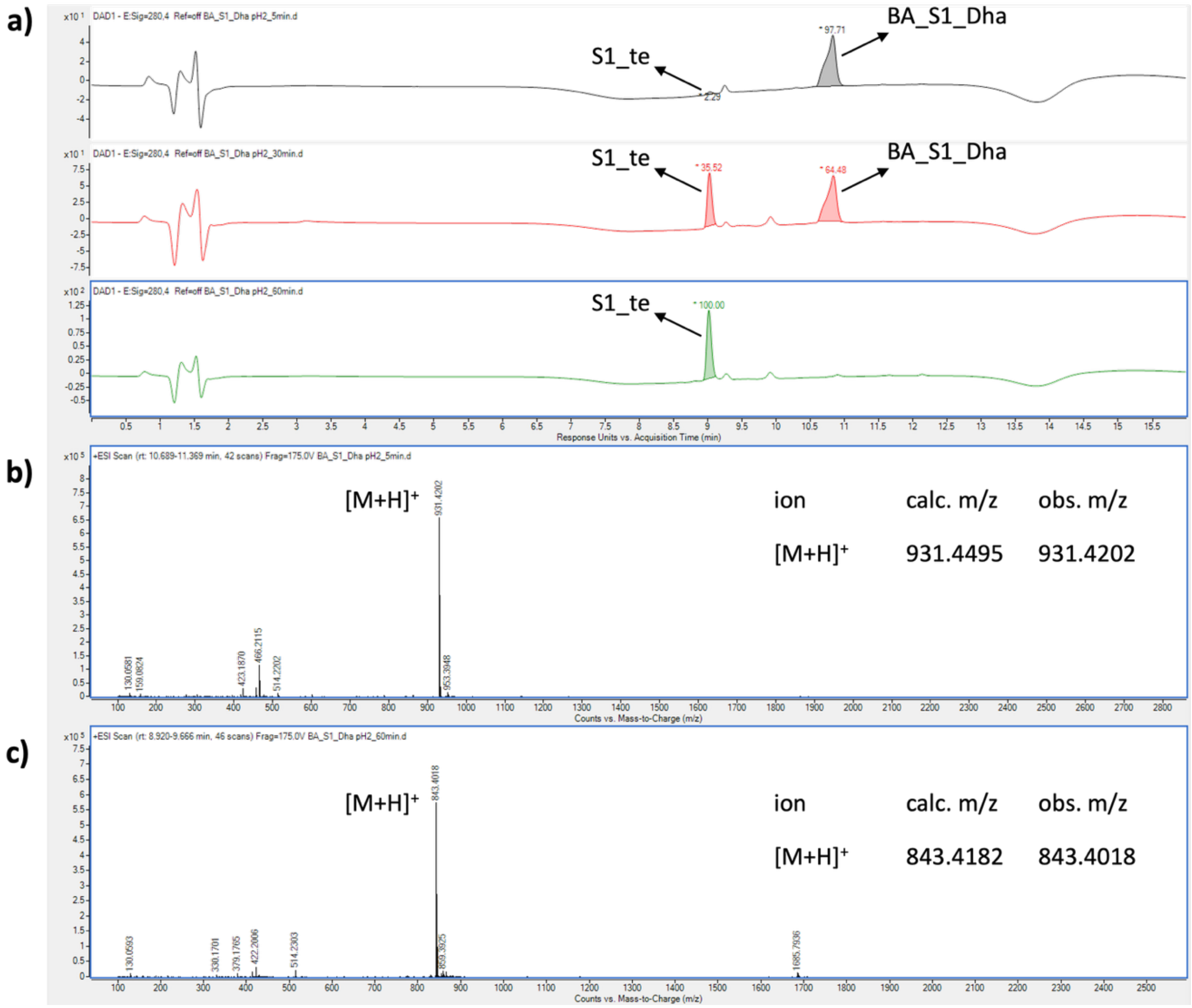

Figure S32. a) LC-MS UV (280 nm) traces of NCys deprotection and cyclization of **BA_S1_Dha** at pH 2 and time point of 5 min/30 min/60 min, b) mass spec readout of peptide **BA_S1_Dha**, c) mass spec readout of peptide product **S1_te**.

4.1.2 Cyclization of S1 (CLIPSWGC) through salicylaldehyde protection

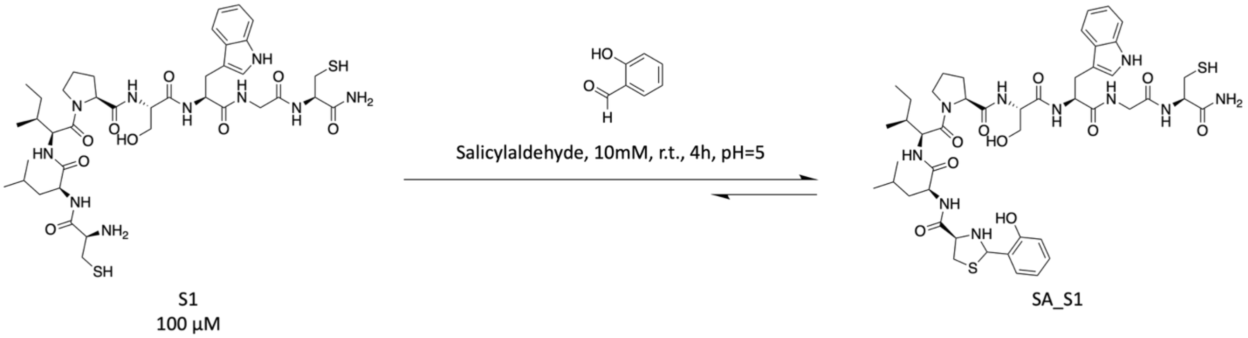

Scheme S10. NCys protection with salicylaldehyde (SA) on model peptide **S1**.

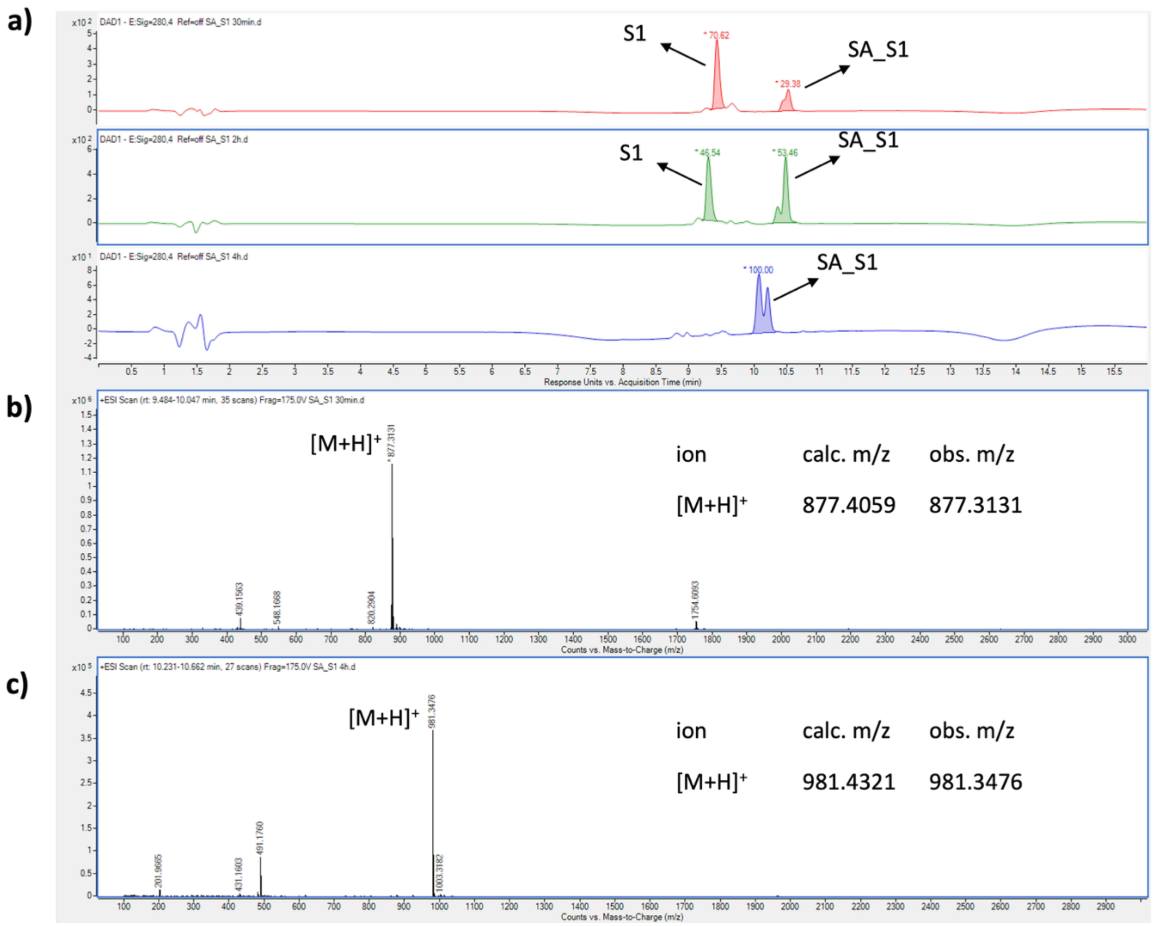

ion	calc. m/z	obs. m/z
$[M+H]^+$	877.4059	877.3131

ion	calc. m/z	obs. m/z
$[M+H]^+$	981.4321	981.3476

Figure S33. a) LC-MS UV (280 nm) traces of NCys protection of **S1** with salicylaldehyde (SA) at 0.5, 2 and 4 hrs, b) mass spec readout of starting peptide **S1**, c) mass spec readout of NCys protected peptide product **SA_S1**.

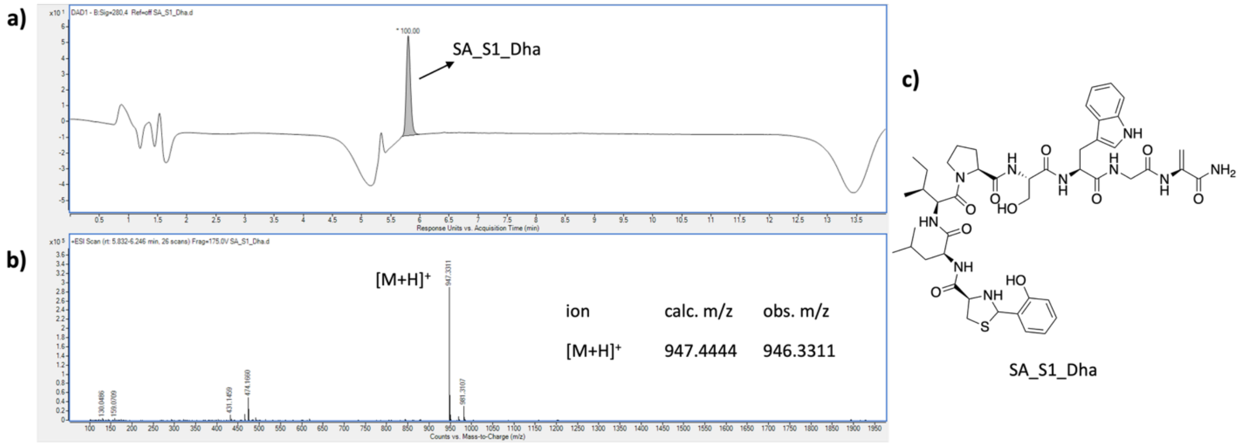

ion	calc. m/z	obs. m/z
$[M+H]^+$	947.4444	946.3311

Figure S34. a) LC-MS UV (280 nm) trace of Cys-to-Dha conversion of **SA_S1** by MDBP, b) mass spec readout of starting peptide **SA_S1_Dha**, c) chemical structure of **SA_S1_Dha**.

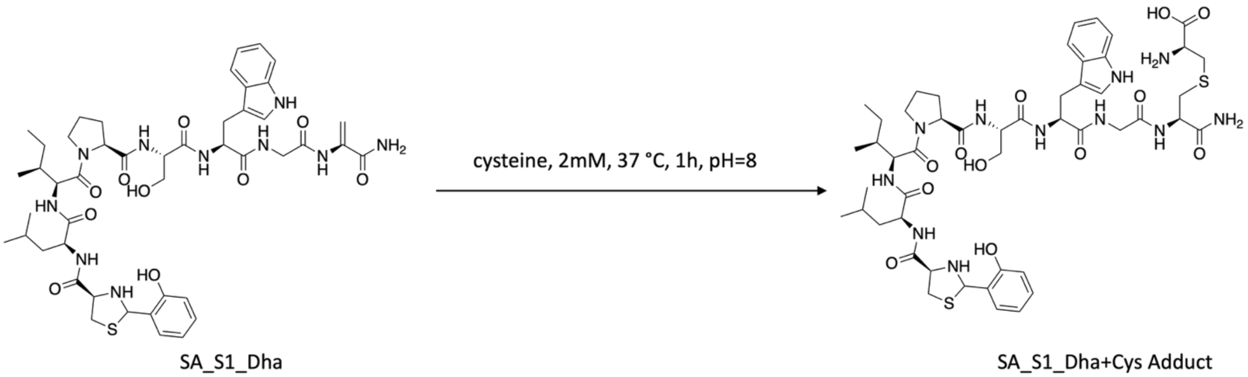

Scheme S11. Validation of dehydroalanine by cysteine labeling on **SA_S1_Dha**.

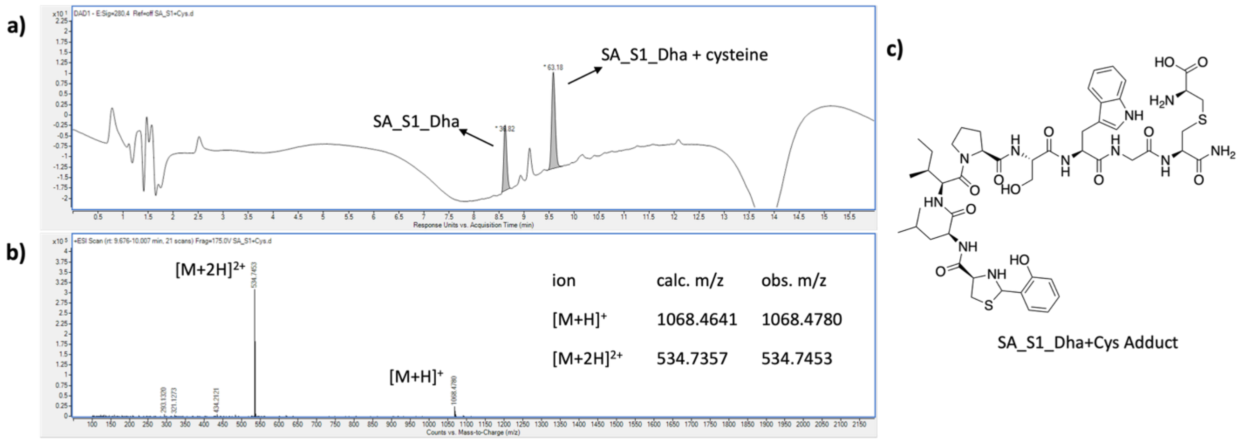

ion	calc. m/z	obs. m/z
$[M+H]^+$	1068.4641	1068.4780
$[M+2H]^{2+}$	534.7357	534.7453

Figure S35. a) LC-MS UV (280 nm) trace of the reaction to validate Dha installation on **SA_S1_Dha** by cysteine labeling, b) mass spec readout of peptide product **SA_S1_Dha+Cys Adduct**, c) chemical structure of **SA_S1_Dha+Cys Adduct**.

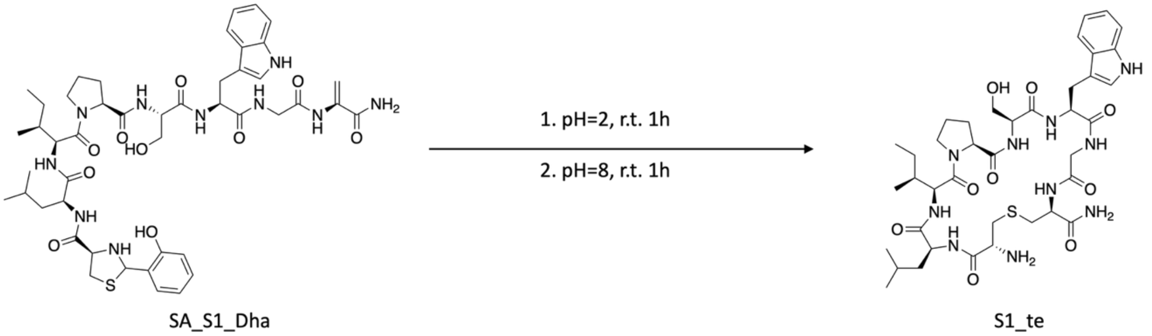

Scheme S12. NCys deprotection and cyclization of **SA_S1_Dha**.

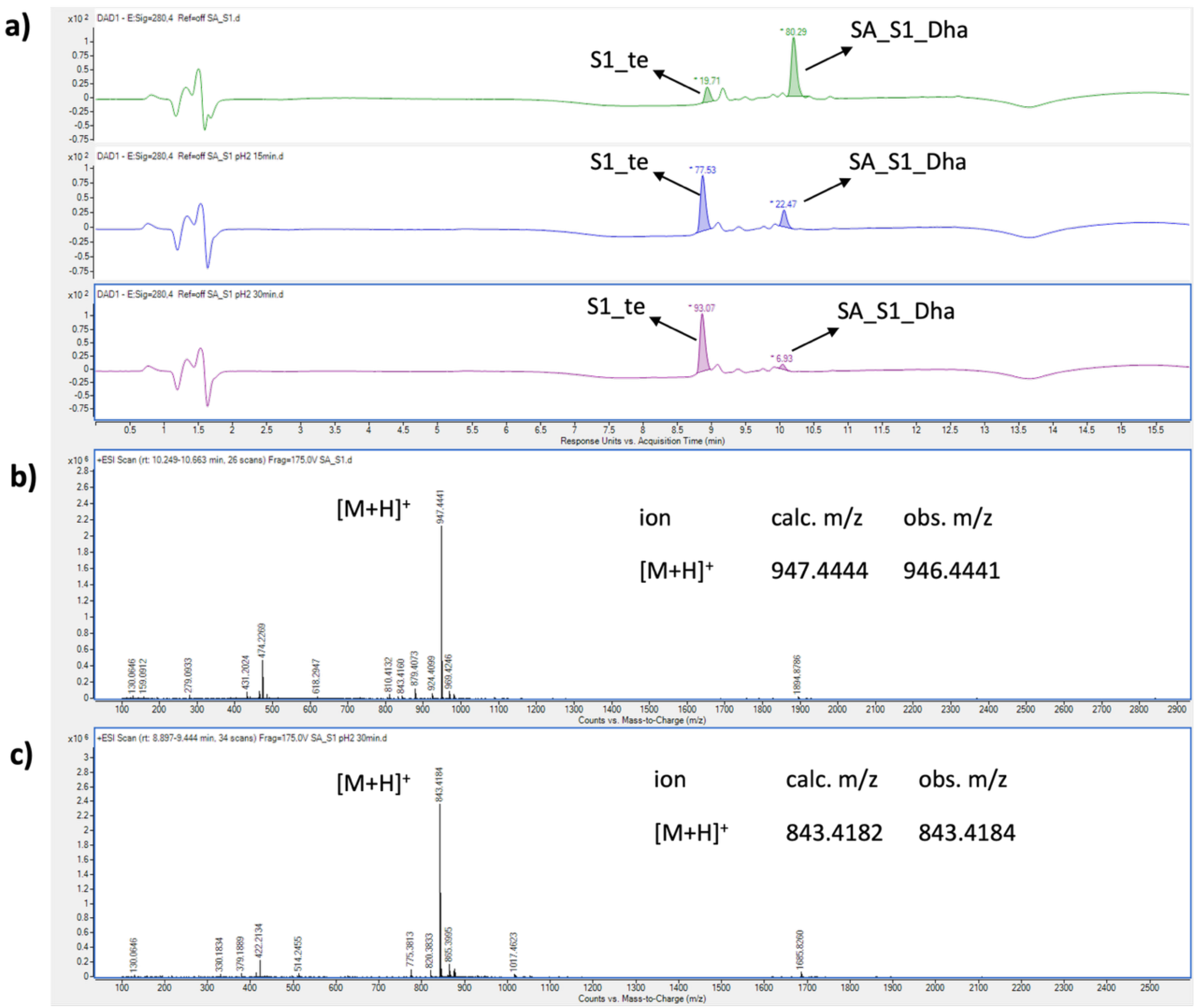

Figure S36. a) LC-MS UV (280 nm) trace of NCys deprotection and cyclization of **SA_S1_Dha** at pH 2 and time point of 5 min/15 min/30 min, b) mass spec readout of peptide **SA_S1_Dha**, c) mass spec readout of peptide product **S1_te**.

4.1.3 Cyclization of model peptide S1 (CLIPSWGC) through 2-FPBA protection

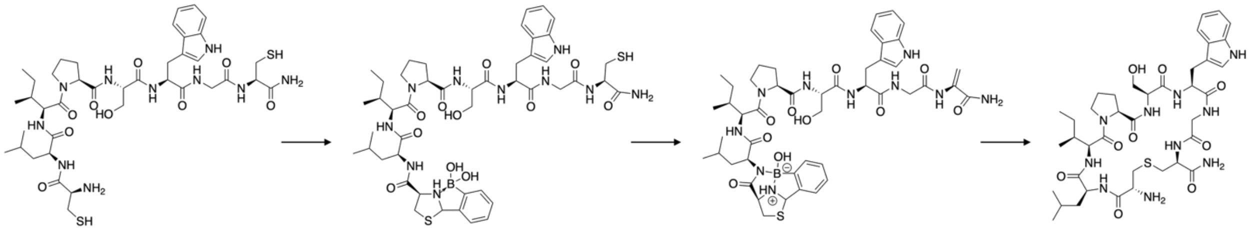

Scheme S13. Synthesis of **S1_te** through Cys-Dha addition using 2-FPBA for NCys protection.

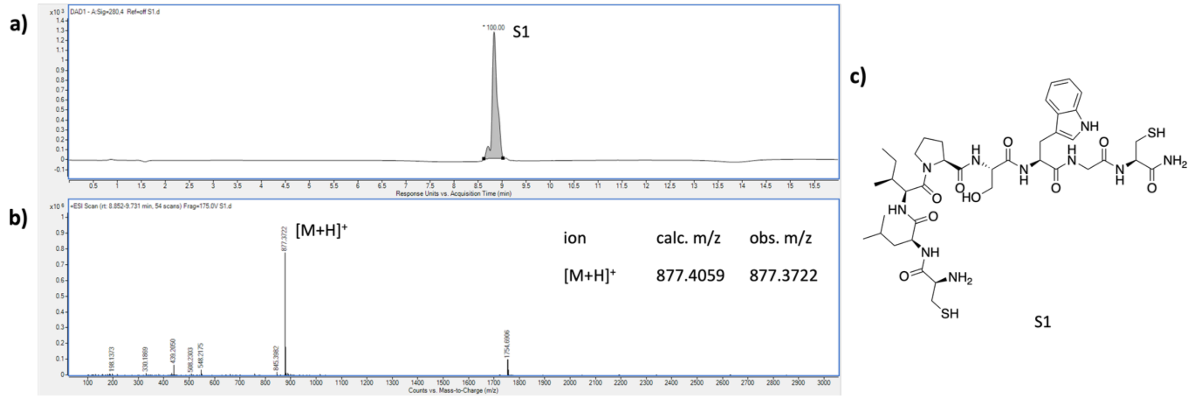

ion	calc. m/z	obs. m/z
$[M+H]^+$	877.4059	877.3722

Figure S37. a) LC-MS UV (280 nm) trace of **S1**, b) mass spec readout of peptide **S1**, c) chemical structure of peptide **S1**.

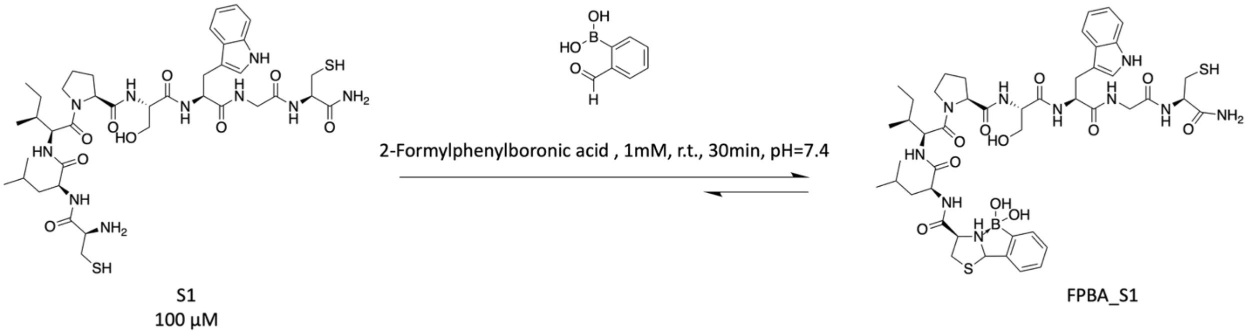

Scheme S14. NCys protection by 2-FPBA on model peptide **S1**.

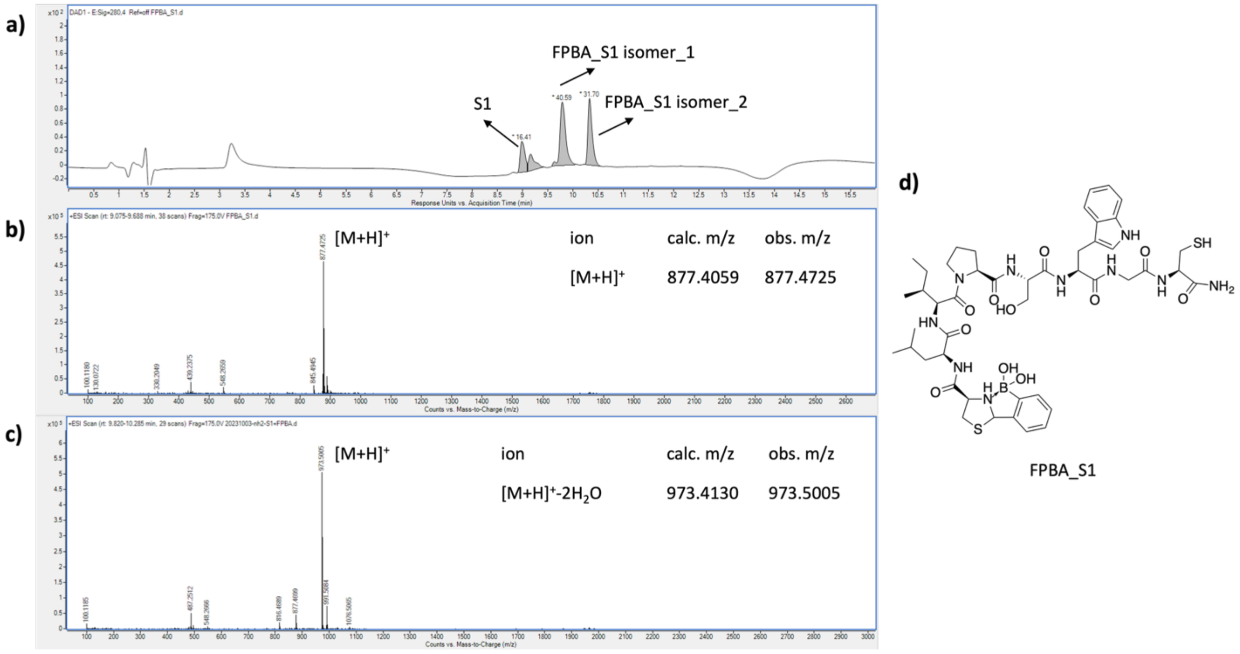

ion	calc. m/z	obs. m/z
$[M+H]^+$	877.4059	877.4725

ion	calc. m/z	obs. m/z
$[M+H]^+-2H_2O$	973.4130	973.5005

Figure S38. a) LC-MS UV (280 nm) trace of NCys protection on **FPBA_S1** by FPBA, b) mass spec readout of starting peptide **S1**, c) mass spec readout of NCys protected peptide product **FPBA_S1**, d) chemical structure of peptide **FPBA_S1**.

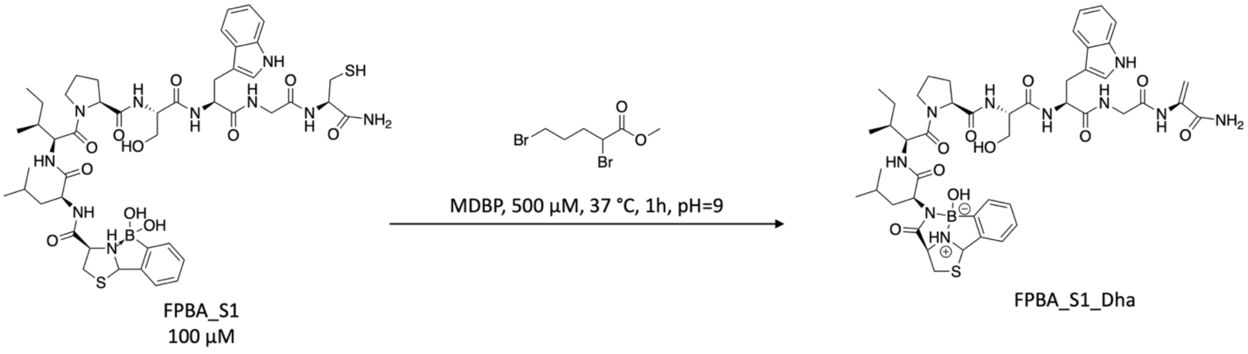

Scheme S15. Cys-to-Dha conversion by MDBP on model peptide **FPBA_S1**.

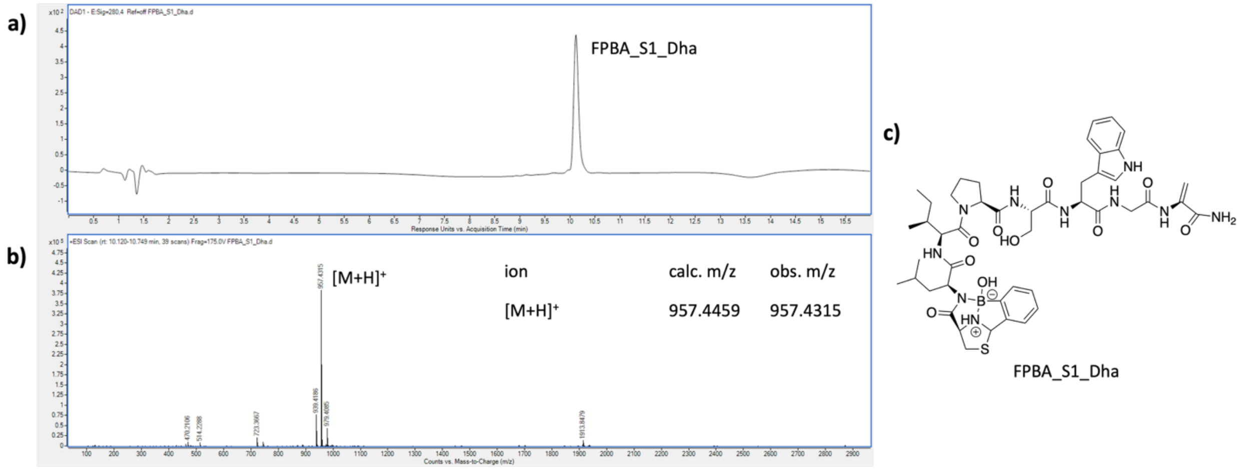

ion	calc. m/z	obs. m/z
$[M+H]^+$	957.4459	957.4315

Figure S39. a) LC-MS UV (280 nm) trace of the Cys-to-Dha conversion of **FPBA_S1** by MDBP, b) mass spec readout of starting peptide **FPBA_S1_Dha**, c) chemical structure of peptide **FPBA_S1_Dha**.

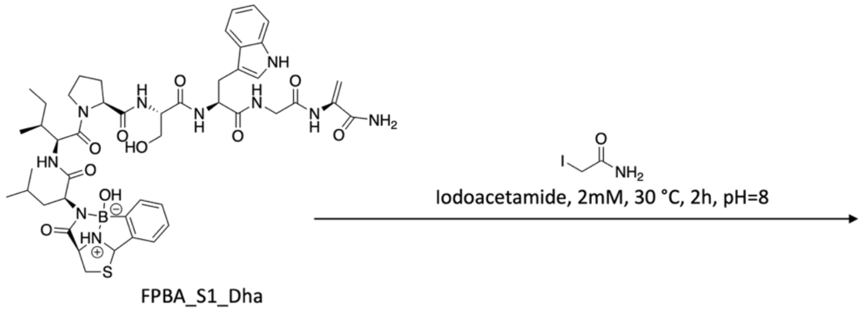

Scheme S16. Validation of complete Cys-to-Dha conversion by labeling **FPBA_S1_Dha** with iodoacetamide.

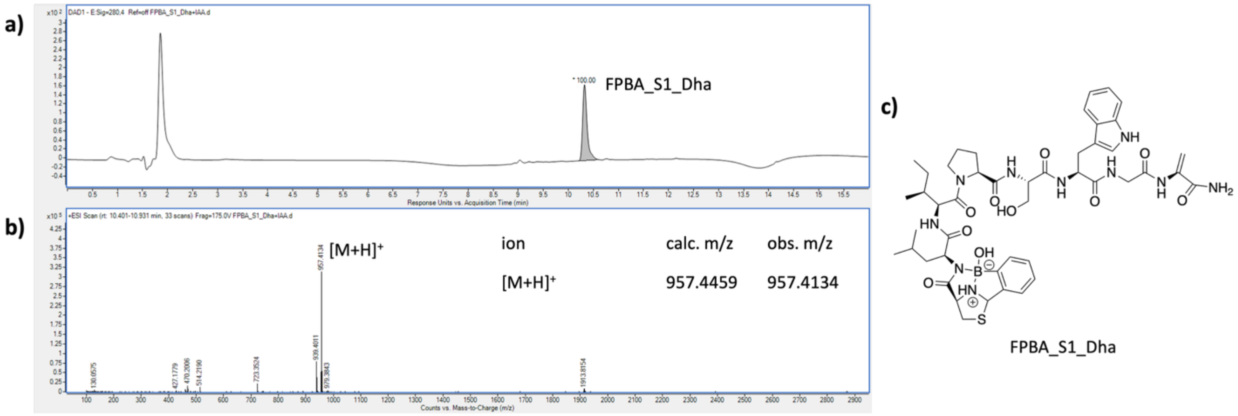

ion	calc. m/z	obs. m/z
$[M+H]^+$	957.4459	957.4134

Figure S40. a) LC-MS UV (280 nm) trace of the iodoacetamide labeling reaction of **FPBA_S1_Dha**, b) mass spec readout of peptide product **FPBA_S1_Dha**, c) chemical structure of **FPBA_S1_Dha.**

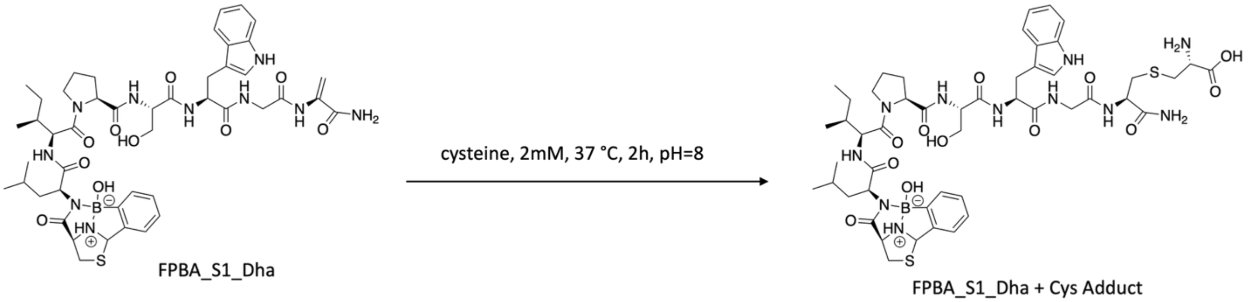

Scheme S17. Validation of dehydroalanine by cysteine labeling on **FPBA_S1_Dha**.

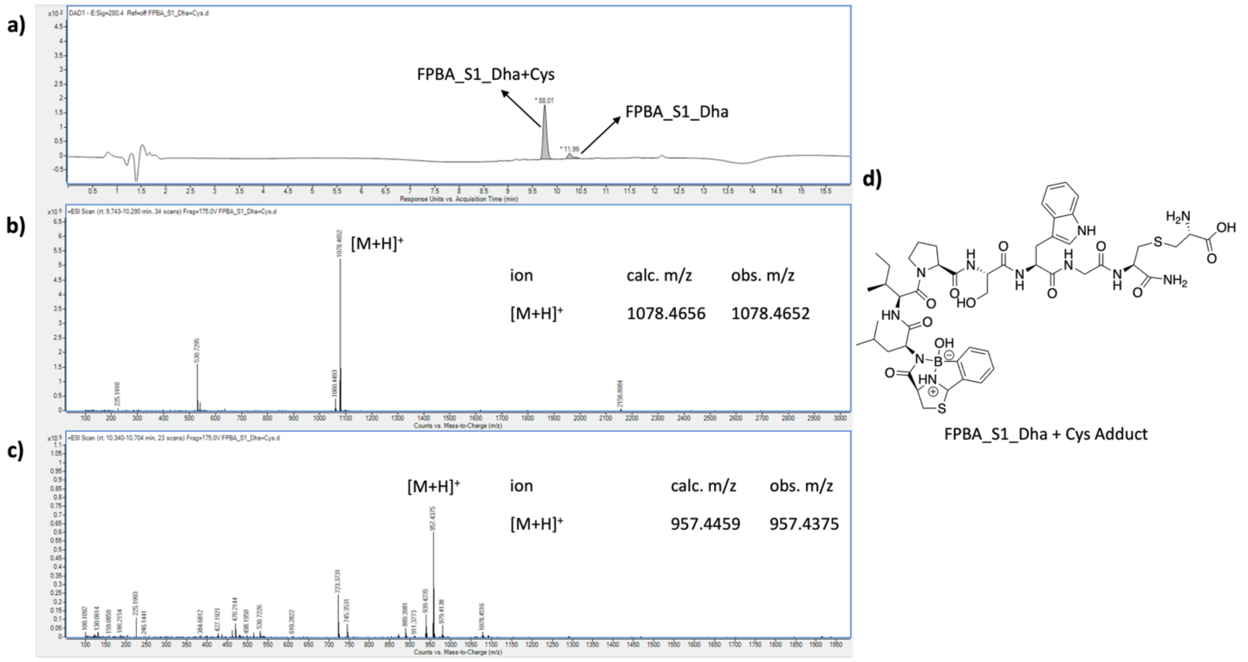

Figure S41. a) LC-MS UV (280 nm) trace of **FPBA_S1_Dha** labeling by cysteine, b) mass spec readout of **FPBA_S1_Dha+Cys Adduct**, c) chemical structure of **FPBA_S1_Dha+Cys Adduct**.

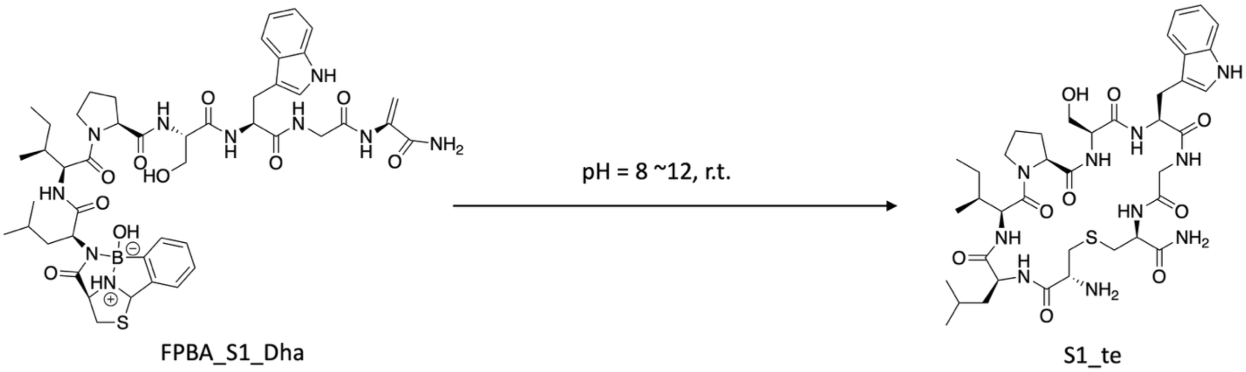

Scheme S18. NCys deprotection and cyclization of **FPBA_S1_Dha**.

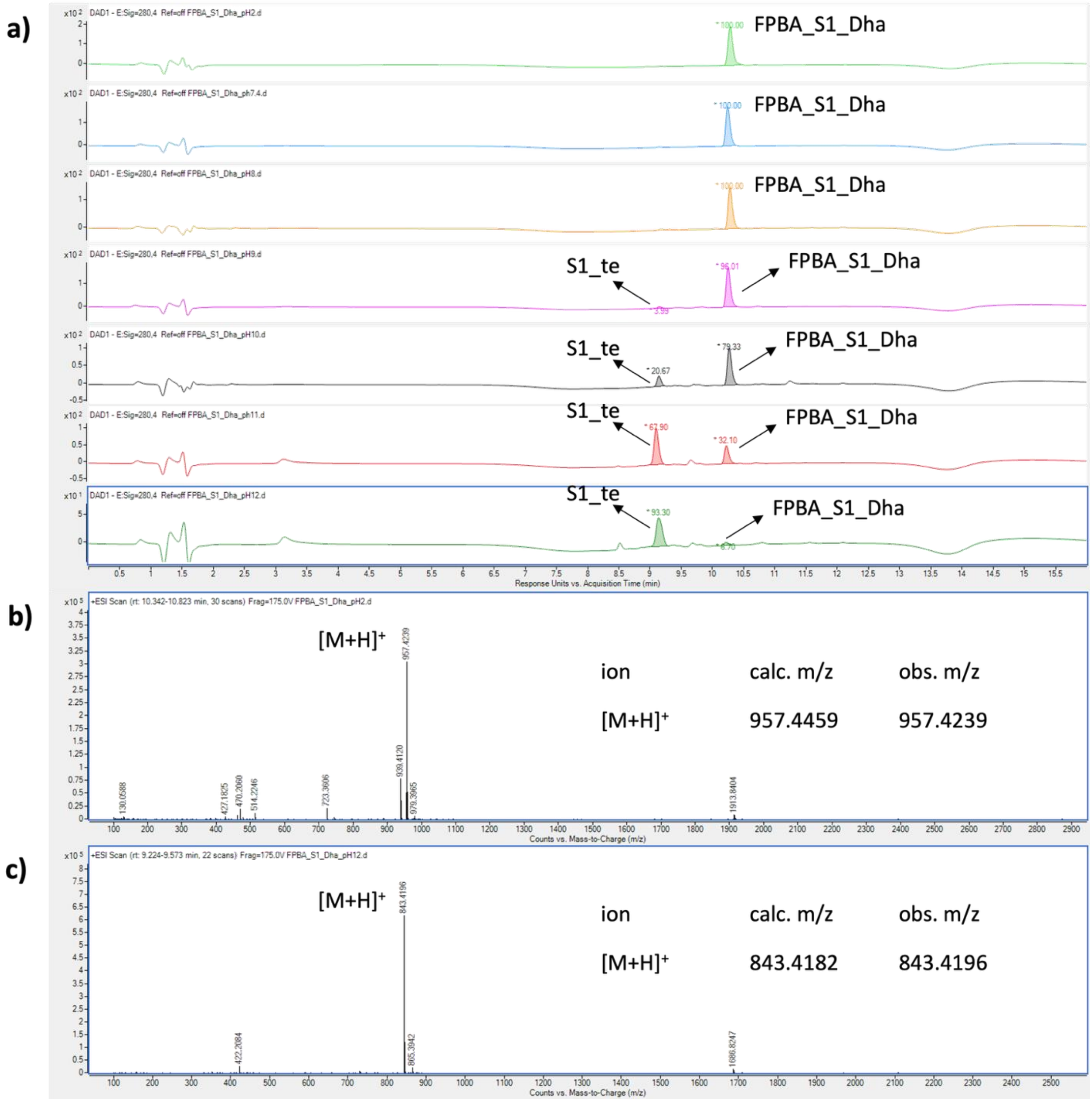

Figure S42. a) LC-MS UV (280 nm) trace of NCys deprotection and cyclization of **FPBA_S1_Dha** by adjusting the pH to 2-12 b) mass spec readout of peptide **FPBA_S1_Dha**, c) mass spec readout of peptide product **S1_te**.

4.2 Cyclization of model peptide R1 (CTWTDQFDVVTTC)

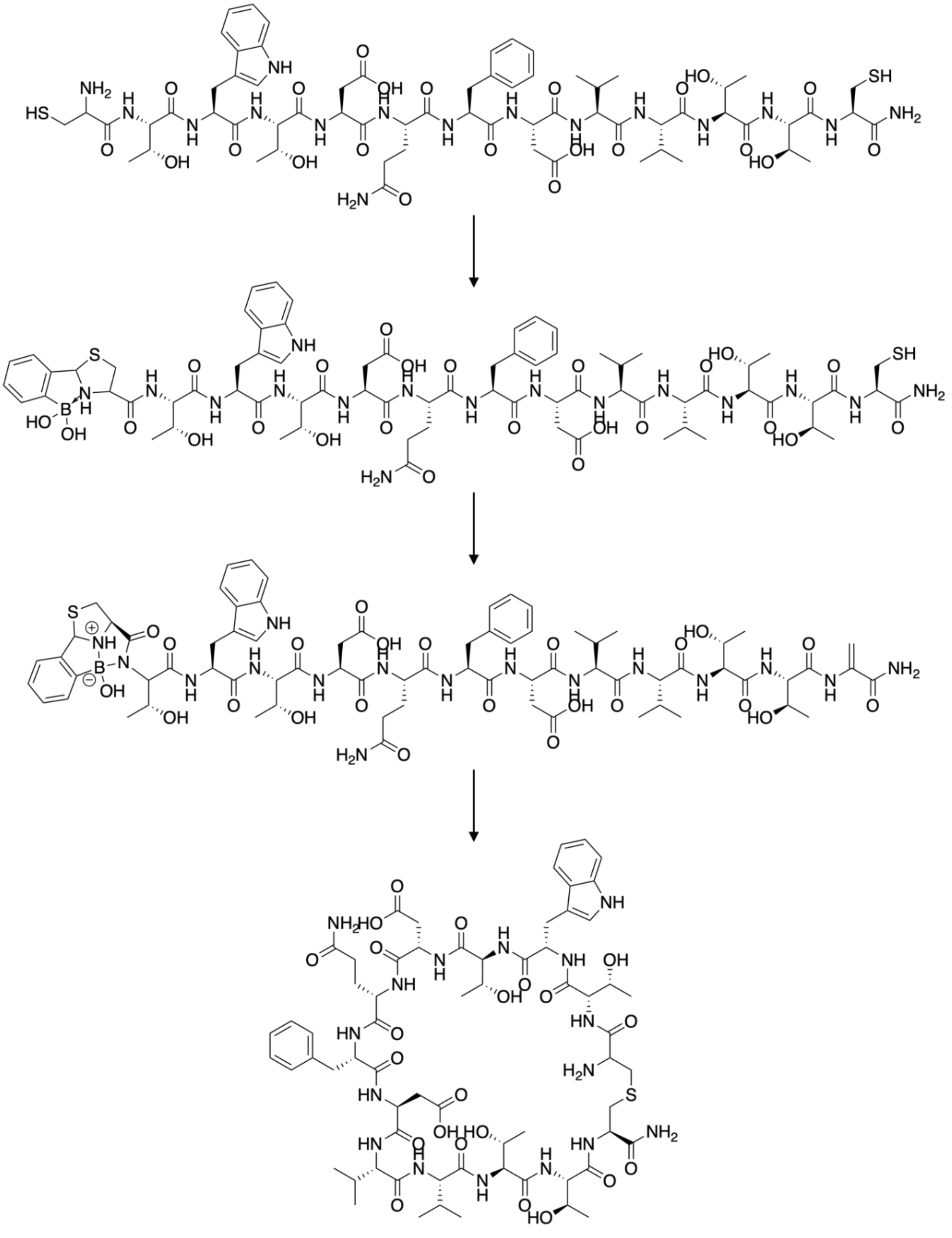

Scheme S19. Synthesis of **R1_te** using 2-FPBA for NCys protection.

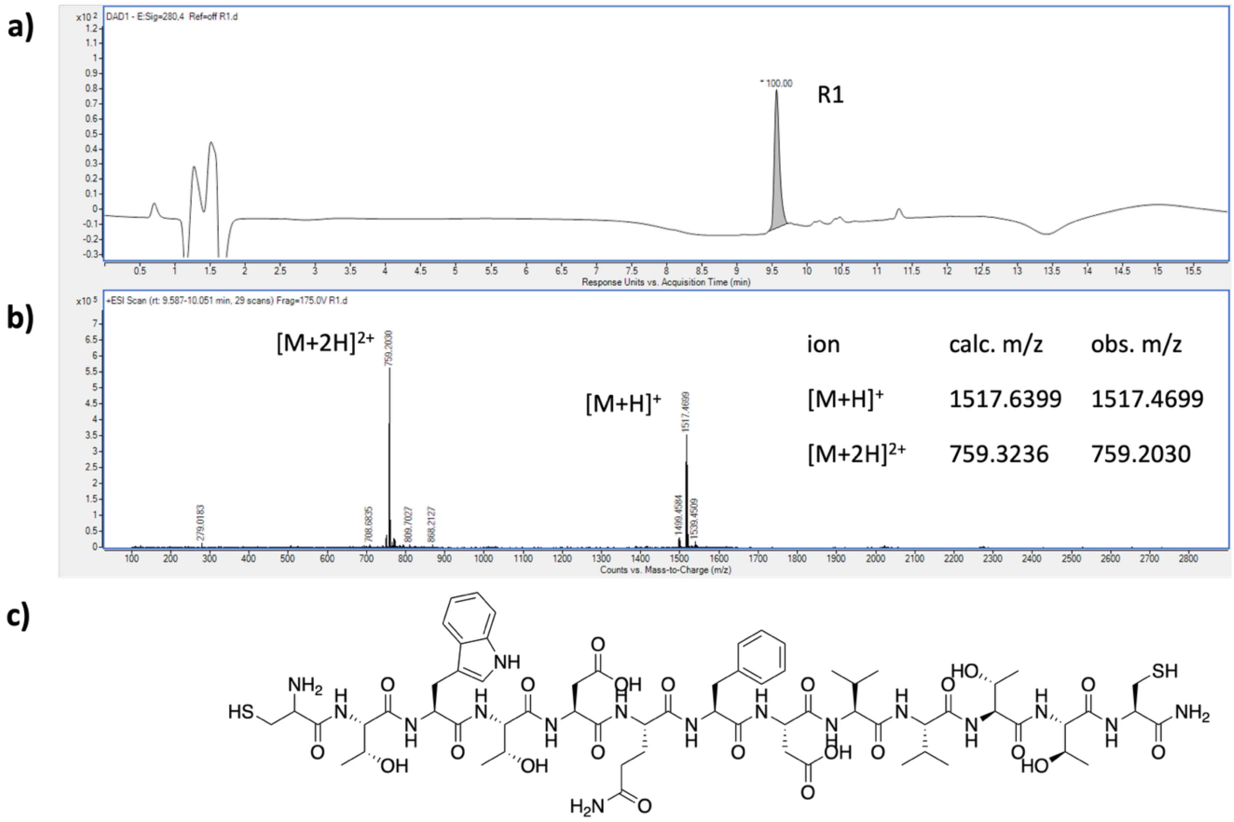

ion	calc. m/z	obs. m/z
$[M+H]^+$	1517.6399	1517.4699
$[M+2H]^{2+}$	759.3236	759.2030

Figure S43. a) LC-MS UV (280 nm) trace of **R1**, b) mass spec readout of peptide **R1**, c) chemical structure of peptide **R1**.

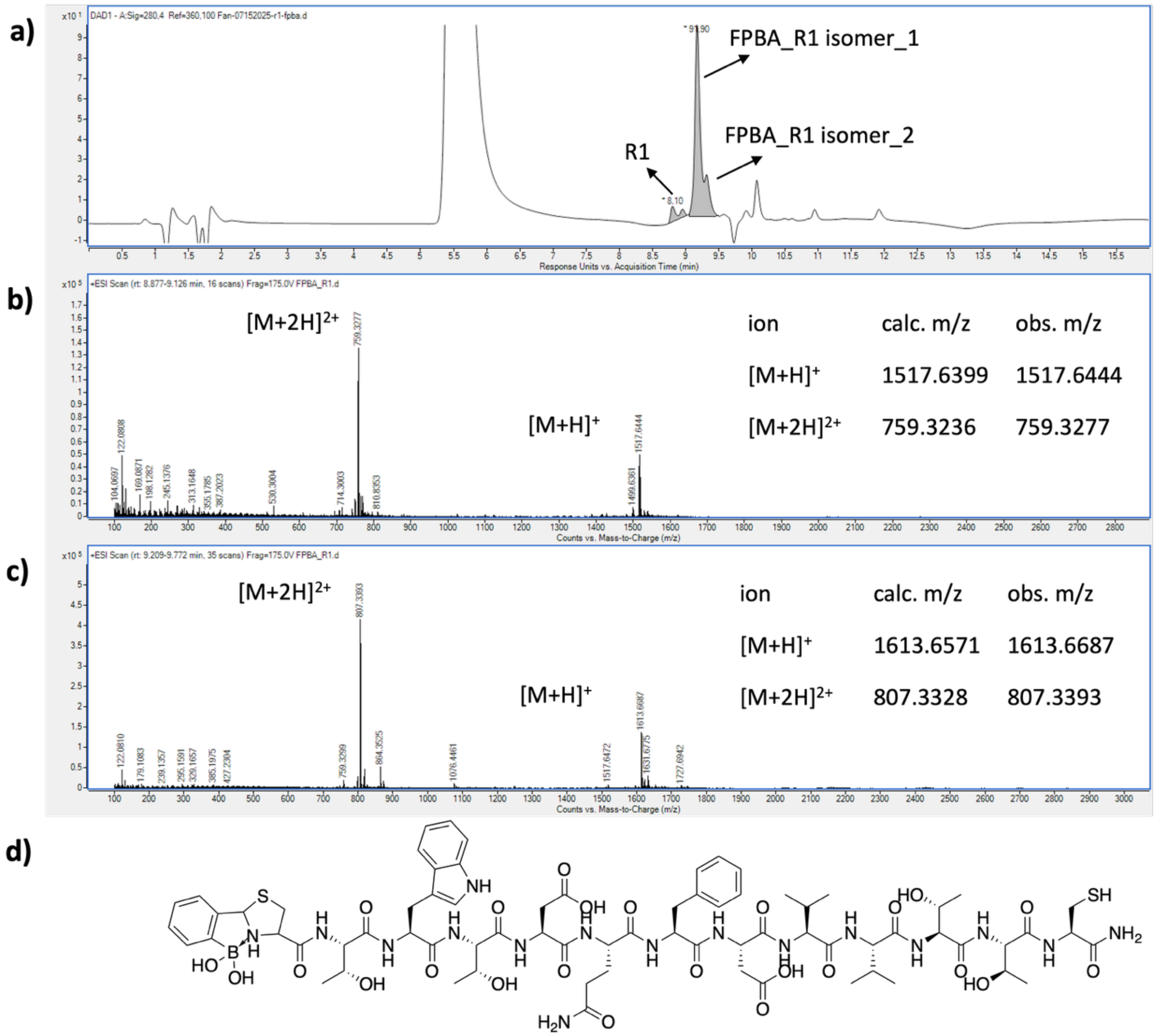

b)

ion	calc. m/z	obs. m/z
$[M+H]^+$	1517.6399	1517.6444
$[M+2H]^{2+}$	759.3236	759.3277

c)

ion	calc. m/z	obs. m/z
$[M+H]^+$	1613.6571	1613.6687
$[M+2H]^{2+}$	807.3328	807.3393

Figure S44. a) LC-MS UV (280 nm) trace of the reaction to protect the NCys on model peptide **FPBA_R1** by FPBA, b) mass spec readout of starting peptide **R1**, c) mass spec readout of NCys protected peptide product **FPBA_R1**, d) chemical structure of peptide **FPBA_R1**.

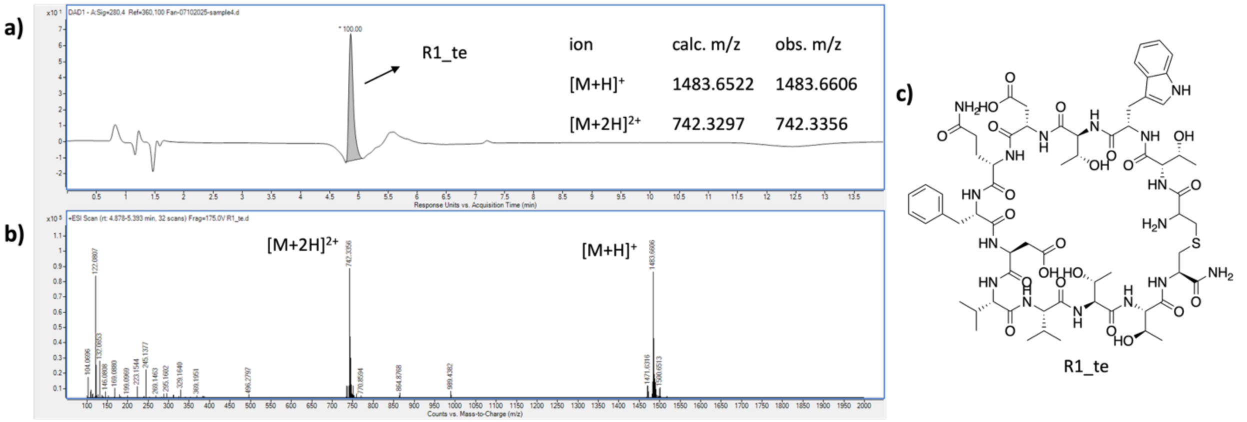

ion	calc. m/z	obs. m/z
[M+H]$^{+}$	1483.6522	1483.6606
[M+2H]$^{2+}$	742.3297	742.3356

Figure S45. a) LC-MS UV (280 nm) trace of **R1_te**, b) mass spec readout of peptide **R1_te**, c) chemical structure of peptide **R1_te**.

4.3 Cyclization of Model Peptide P2 (CYQLNYFWRTCGGGDap(Fam))

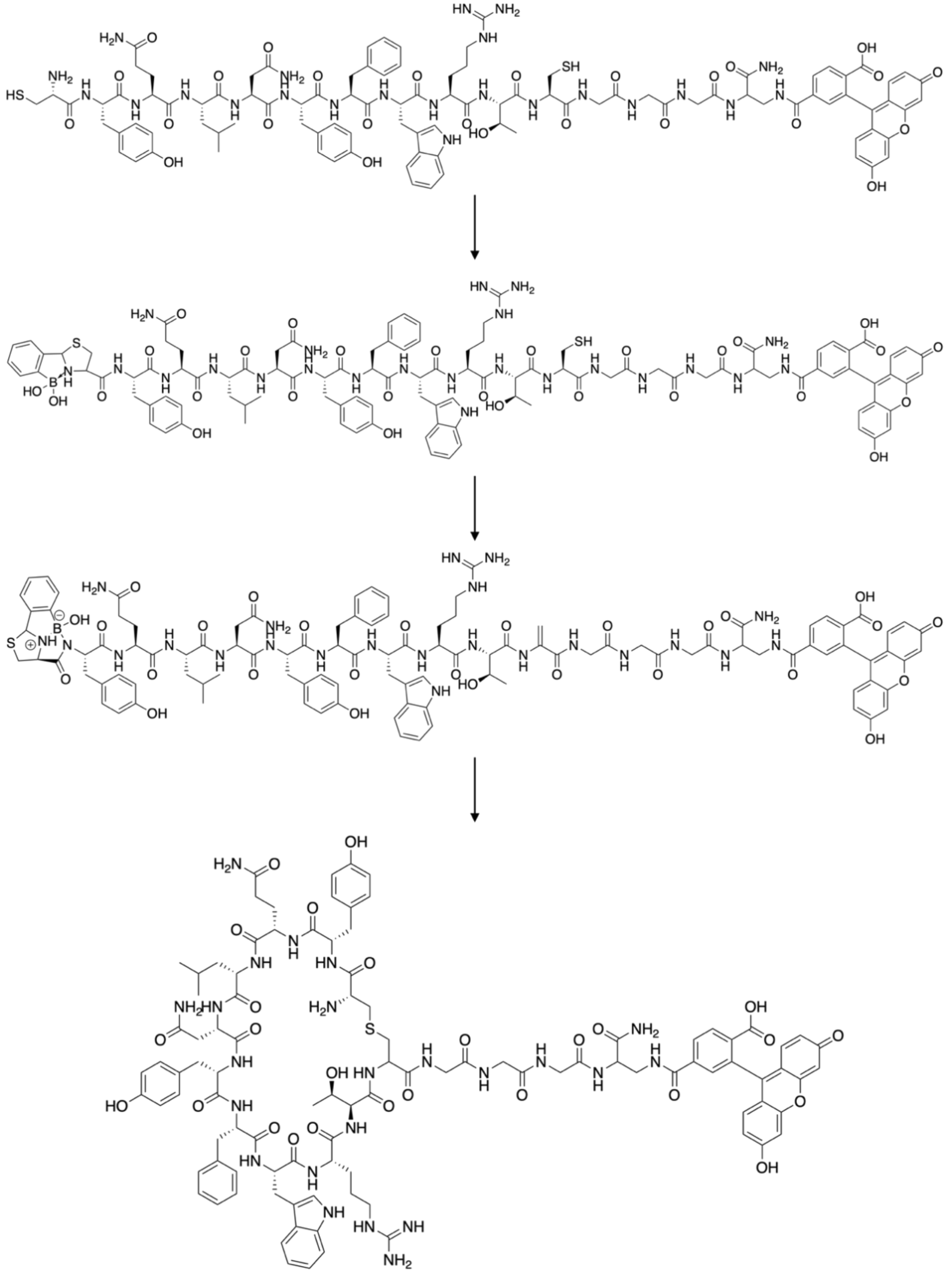

Scheme S20. Synthesis of **P2_te** using 2-FPBA for NCys protection.

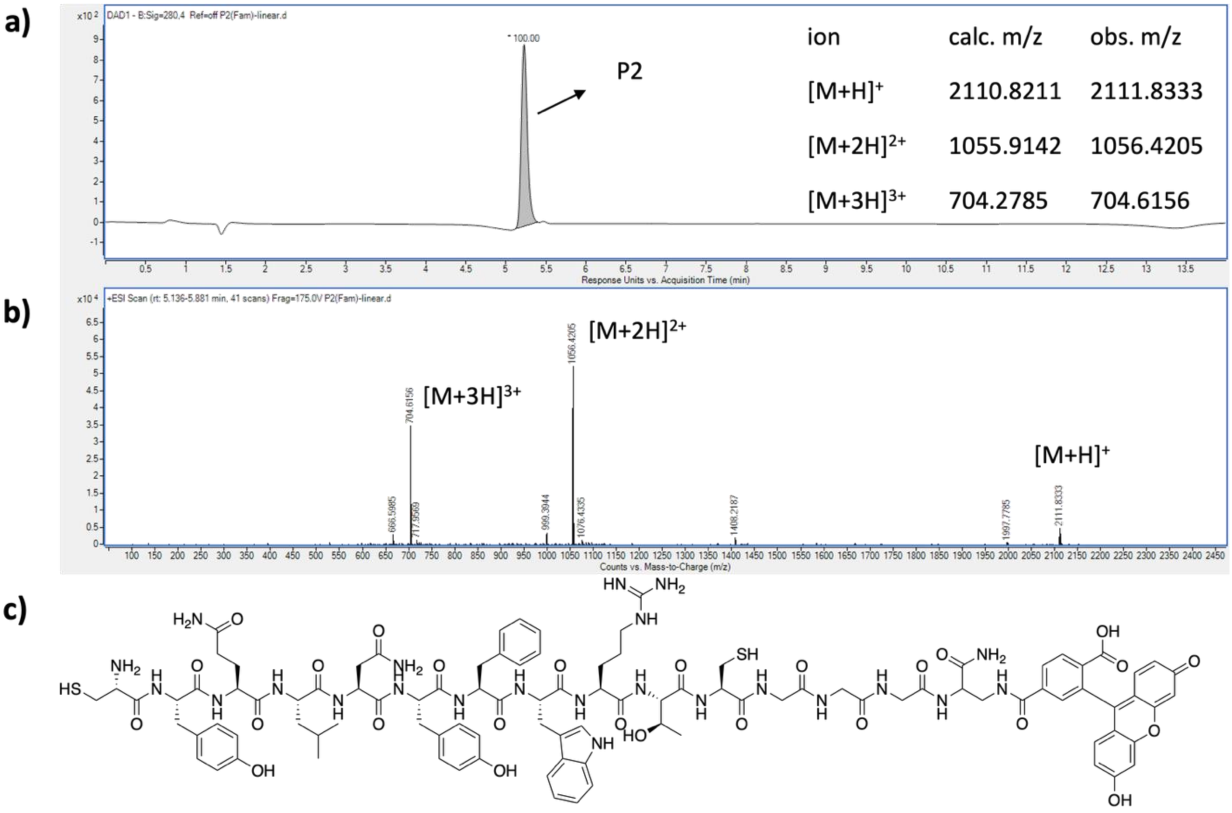

ion	calc. m/z	obs. m/z
$[M+H]^+$	2110.8211	2111.8333
$[M+2H]^{2+}$	1055.9142	1056.4205
$[M+3H]^{3+}$	704.2785	704.6156

Figure S46. a) LC-MS UV (280 nm) trace of **P2**, b) mass spec readout of peptide **P2**, c) chemical structure of peptide **P2**.

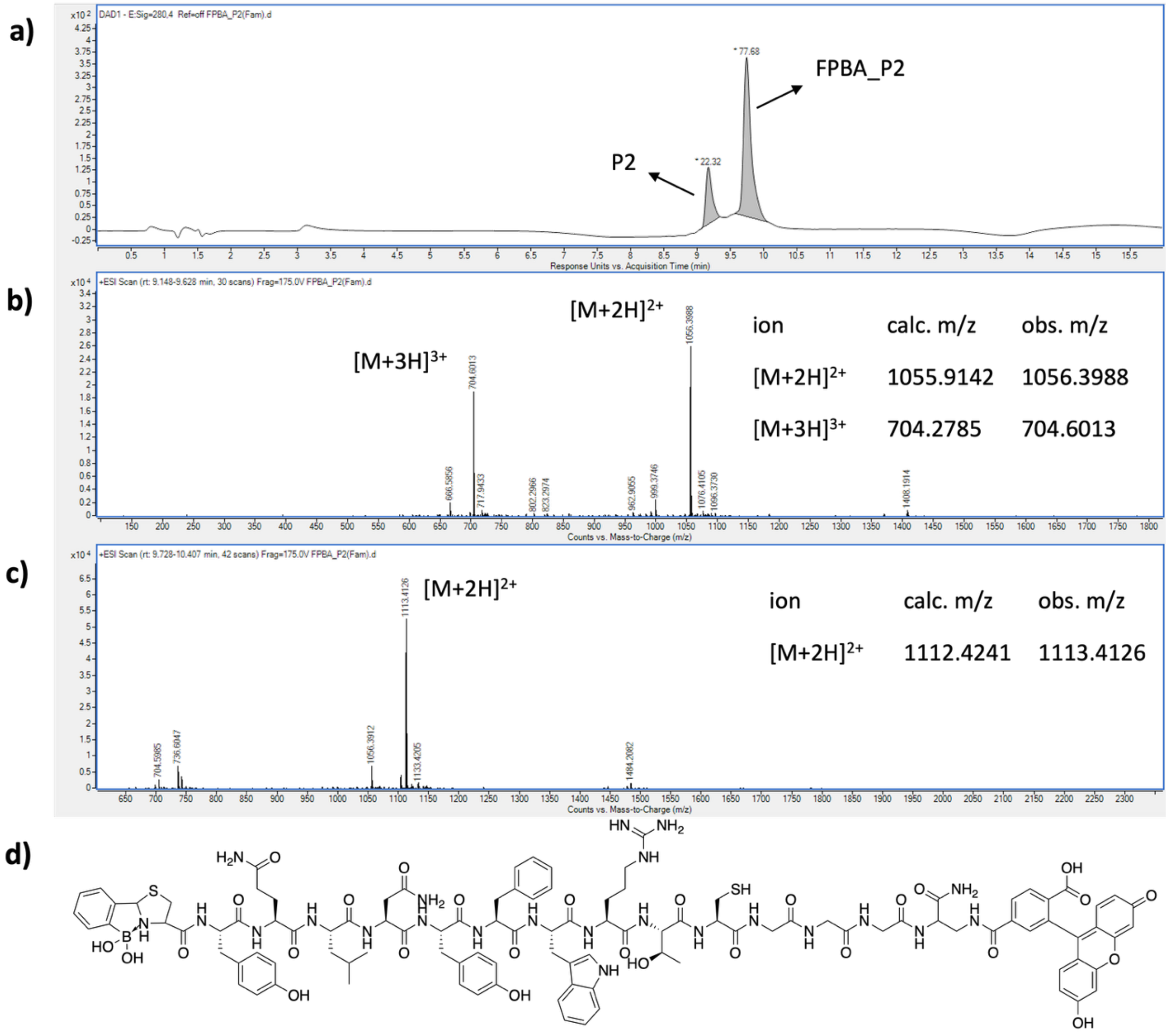

ion	calc. m/z	obs. m/z
$[M+2H]^{2+}$	1055.9142	1056.3988
$[M+3H]^{3+}$	704.2785	704.6013

ion	calc. m/z	obs. m/z
$[M+2H]^{2+}$	1112.4241	1113.4126

Figure S47. a) LC-MS UV (280 nm) trace of NCys protection of **FPBA_P2** by FPBA, b) mass spec readout of starting peptide **P2**, c) mass spec readout of NCys protected peptide product **FPBA_P2**, d) chemical structure of peptide **FPBA_P2**.

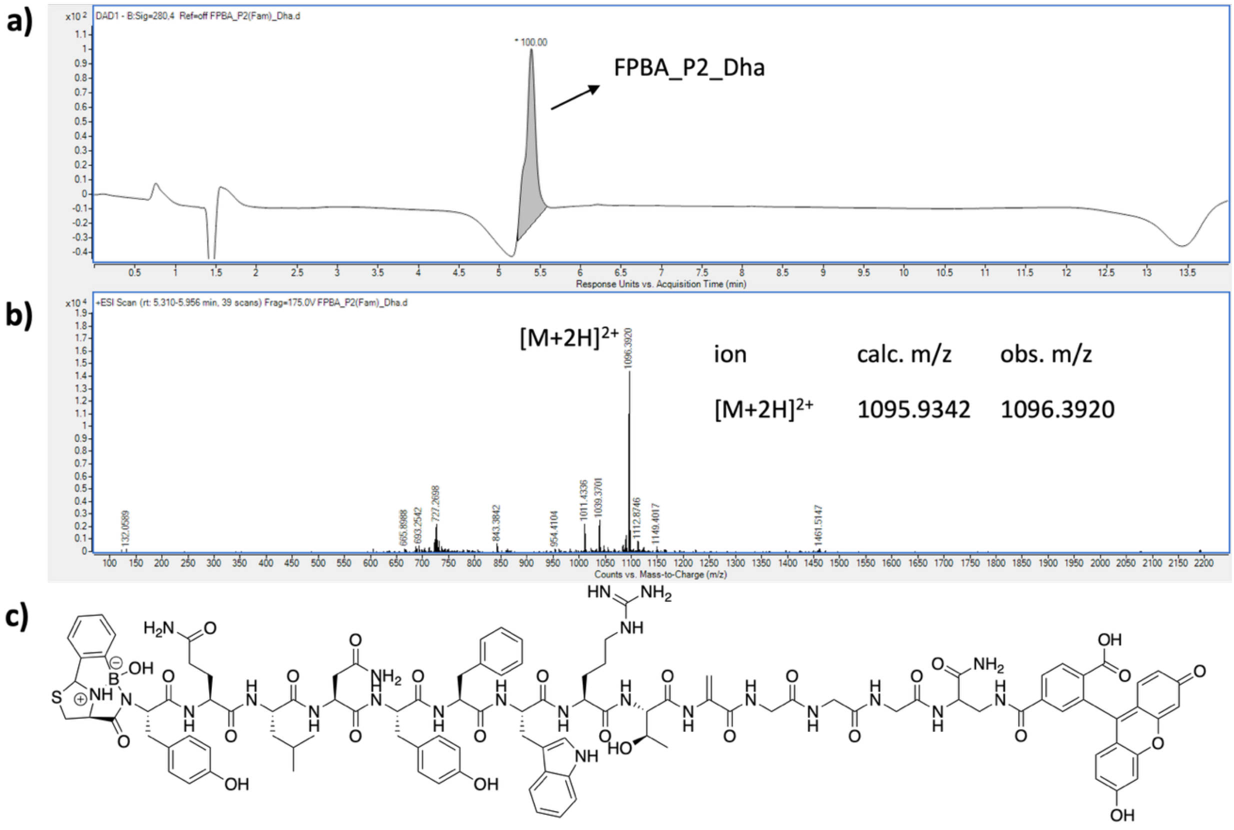

Figure S48. a) LC-MS UV (280 nm) trace of Cys-to-Dha conversion on **FPBA_P2**, b) mass spec readout of starting peptide **FPBA_P2_Dha**, c) chemical structure of peptide **FPBA_P2_Dha**.

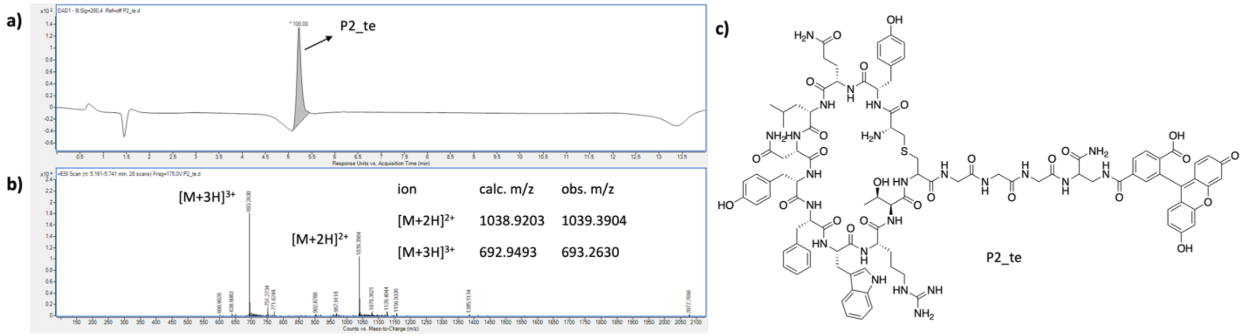

Figure S49. a) LC-MS UV (280 nm) trace of **P2_te**, b) mass spec readout of starting peptide **P2_te**, c) chemical structure of peptide **P2_te**.

4.4 Lanthipeptide Structure Validation with Positive Controls

4.4.1 Cyclization structure validation with model peptide N6MP1 (CLKPEWGC)

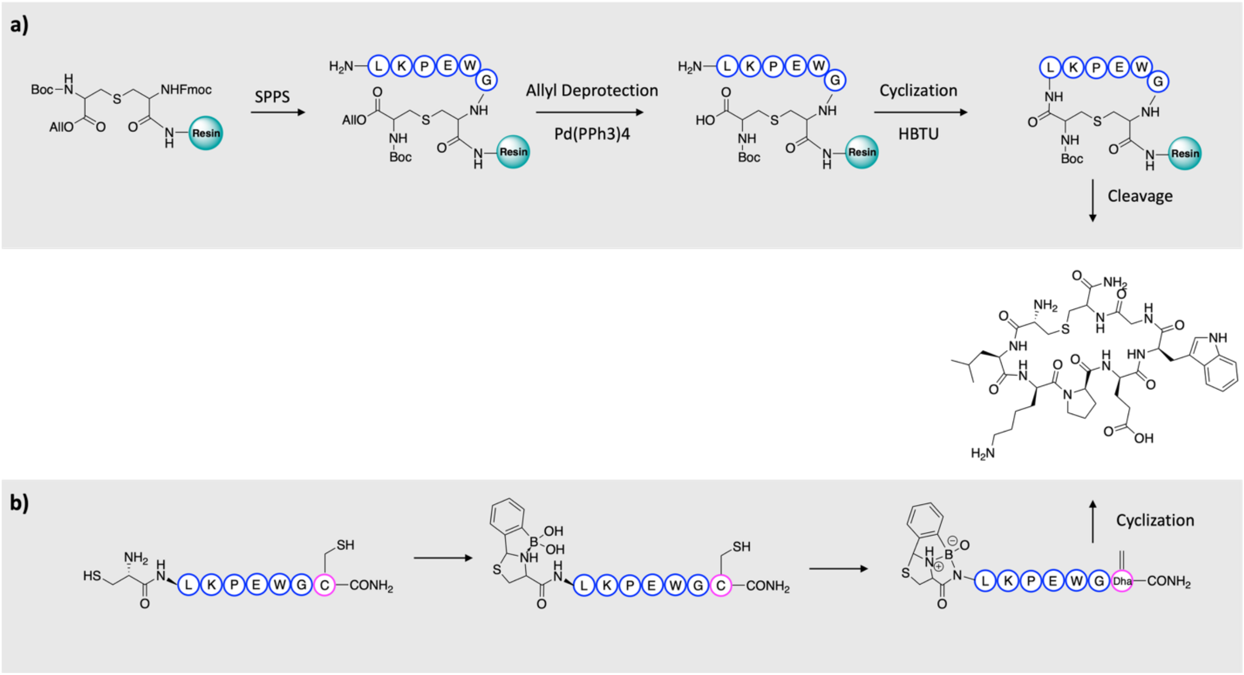

Scheme S21. Synthesis of **N6MP1_te**. a) by SPPS using lanthionine building block; b) by NCys-Dha cyclization using **2-FPBA** for NCys protection.

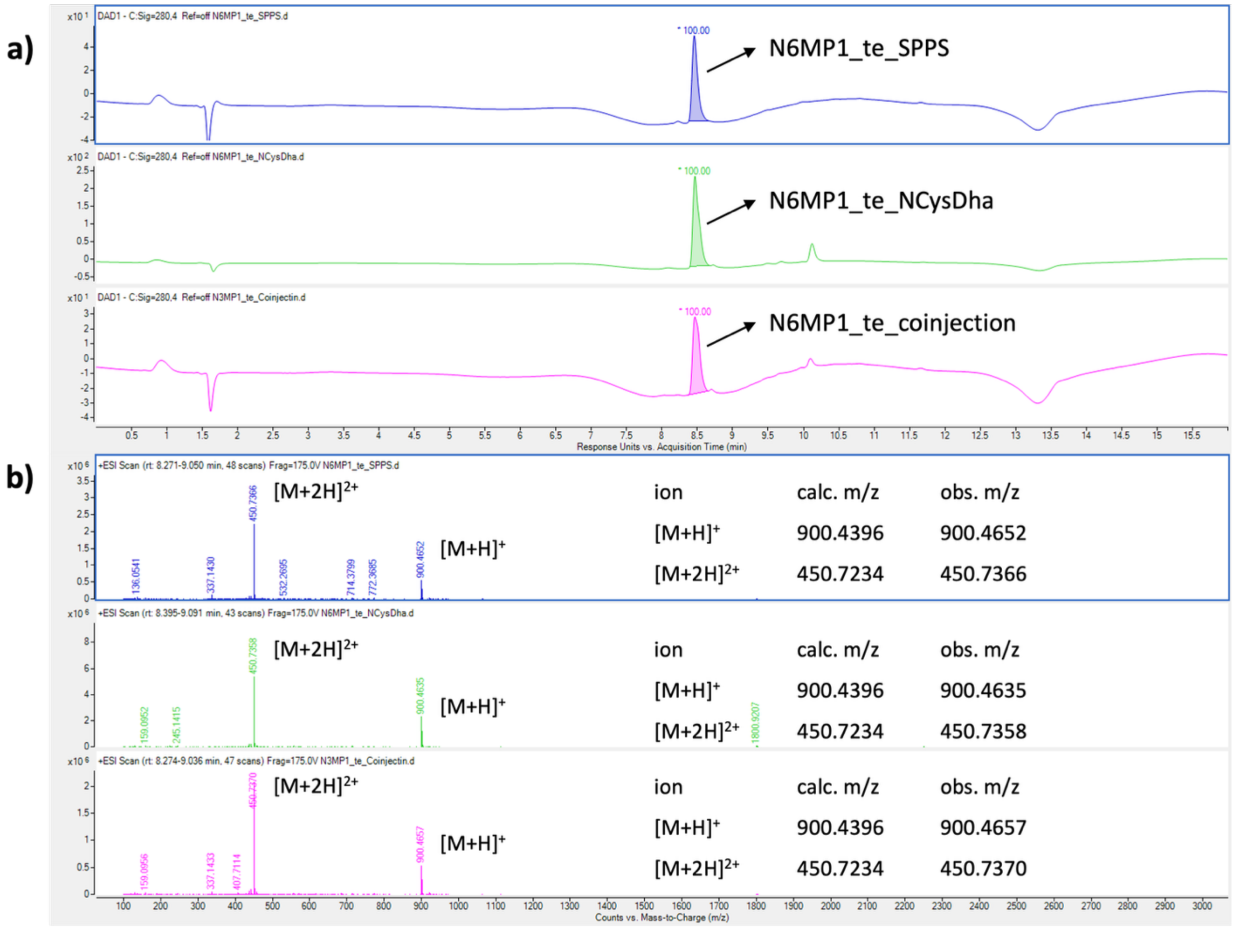

ion	calc. m/z	obs. m/z
[M+H]$^{+}$	900.4396	900.4652
[M+2H]$^{2+}$	450.7234	450.7366

ion	calc. m/z	obs. m/z
[M+H]$^{+}$	900.4396	900.4635
[M+2H]$^{2+}$	450.7234	450.7358

ion	calc. m/z	obs. m/z
[M+H]$^{+}$	900.4396	900.4657
[M+2H]$^{2+}$	450.7234	450.7370

Figure S50. a) LC-MS UV (280 nm) trace of **N6MP1_te** synthesized by SPPS using lanthionine building block, synthesized by NCys-Dha cyclization, and coinjection, b) mass spec readout of peptide **N6MP1_te**.

4.4.2 Cyclization structure validation with hit peptide FK1 (CLDPETGEC)

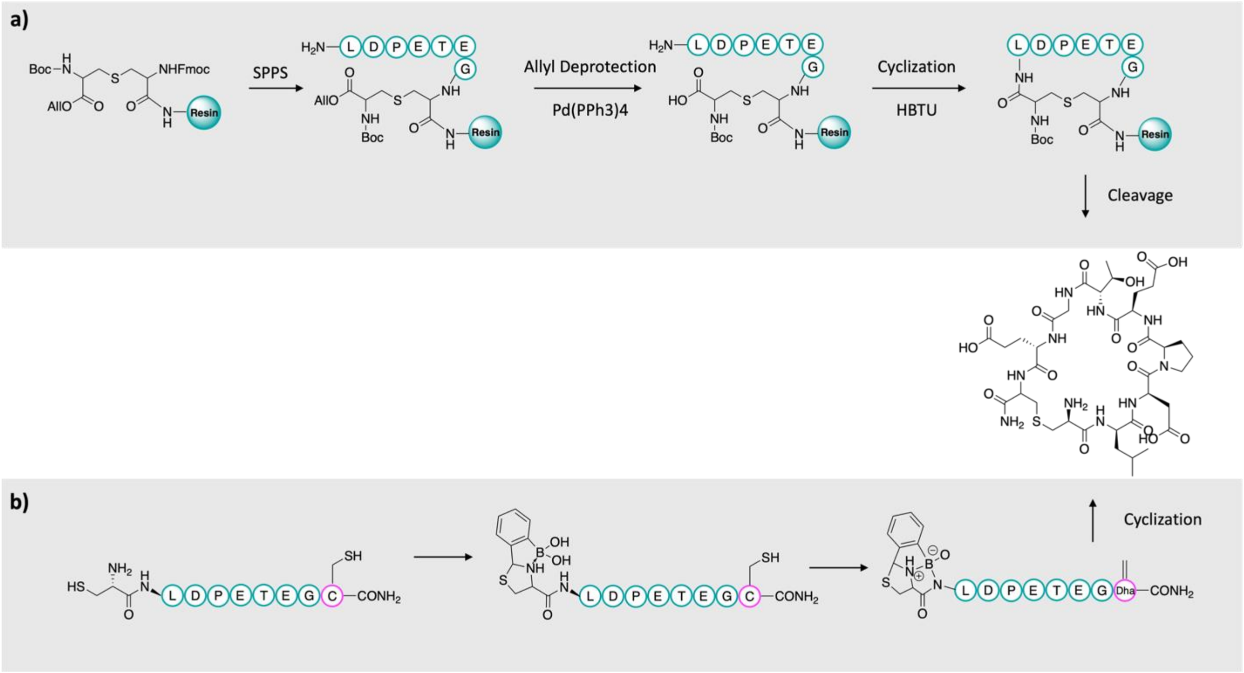

Scheme S22. Synthesis of **FK1_te**. a) by SPPS using lanthionine building block; b) by NCys-Dha cyclization using **2-FPBA** for NCys protection.

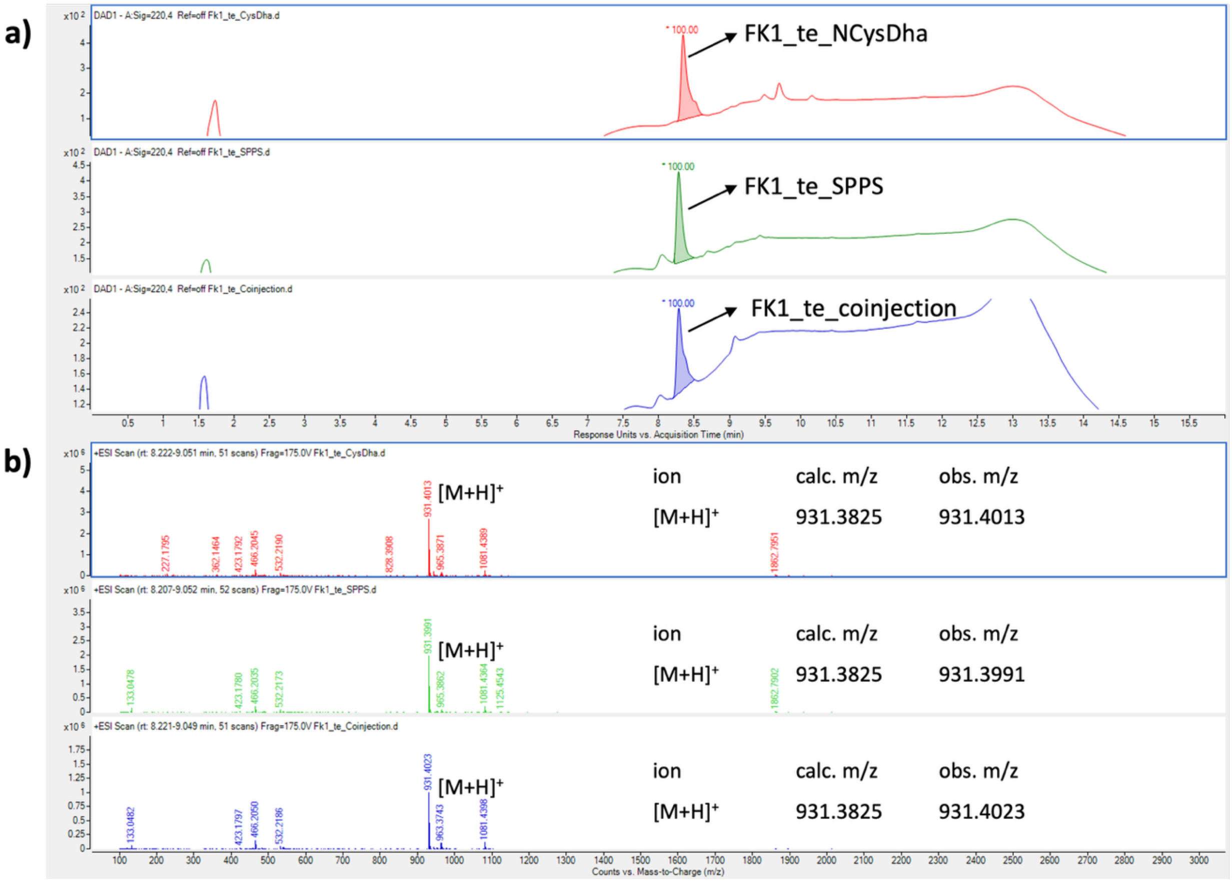

ion	calc. m/z	obs. m/z
$[M+H]^+$	931.3825	931.4013

ion	calc. m/z	obs. m/z
$[M+H]^+$	931.3825	931.3991

ion	calc. m/z	obs. m/z
$[M+H]^+$	931.3825	931.4023

Figure S51. a) LC-MS UV (220 nm) trace of **FK1_te** synthesized by NCys-Dha cyclization, by SPPS using lanthionine building block and the coinjection, b) mass spec readout of peptide **FK1_te**.

5. Cyclization on CX$_9$C_pIII Protein

NCys CX$_9$C_pIII fusion protein was generated by treating the MIEGRCX9C_pIII protein with Factor Xa protease (NEB, # P8010) at room temperature for 6h in the cleavage buffer (20 mM Tris-HCl, with 100 mM NaCl and 2 mM $CaCl_2$, pH=8.0). Then CX$_9$C_pIII protein (100 µM in Tris buffer, pH=8) was reduced with 1mM TCEP buffer R (20 mM ammonium bicarbonate, pH= 8.0) at room temperature for 1h to give reduced CX$_9$C_pIII protein (Figure S52).

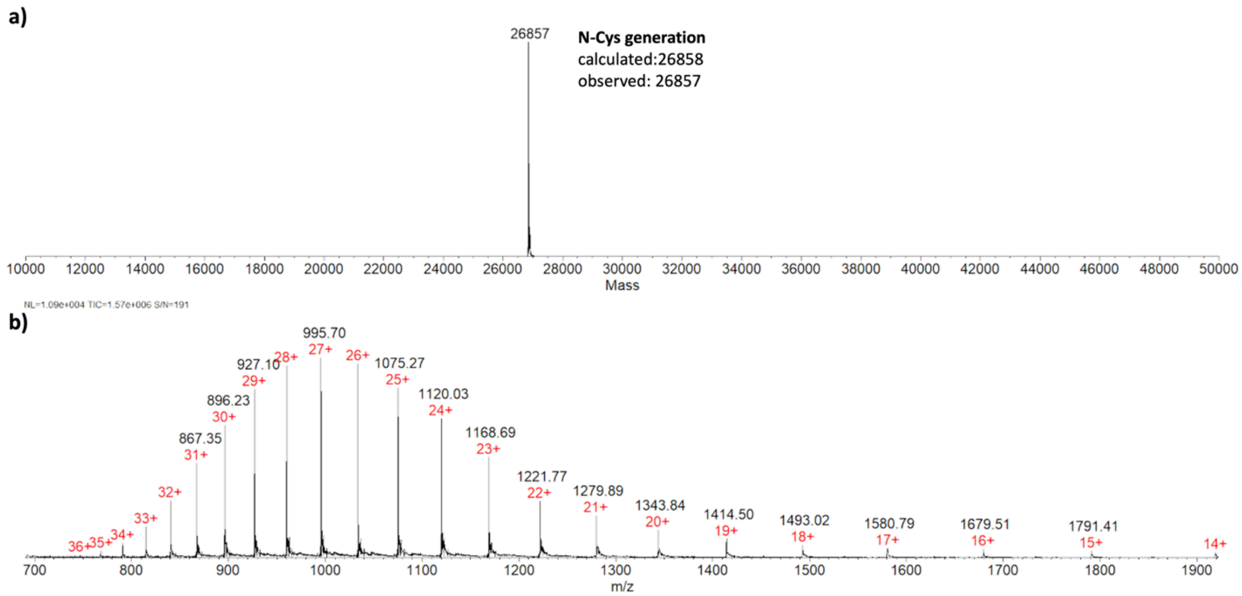

Figure S52. a) Deconvoluted mass and b) crude mass envelope of CX₉C_pIII protein.

50 μL of reduced CX₉C_pIII protein (100 μM in Tris buffer with 10 equivalents of TCEP, pH=8) was diluted with 50 μL of PBS (pH 7.4), and mixed with 1 μL of 2-FPBA (100 mM stock solution in DMF), resulting 50 μM of CX₉C_pIII protein and 1 mM of 2-FPBA in PBS buffer pH=7.4. The mixture was mixed well by pipetting several times, incubated at room temperature for 1h, and the reaction was monitored by LC-MS. After incubation, 61.75% conversion of FPBA_CX₉C_pIII was observed, since the condensation reaction of 2-FPBA and NCys is reversible, the reaction mixture was moved to next step without removing the excess amount of 2-FPBA. The molecular weight of protein increased by 98 Da after 2-FPBA protection, which is consistent with the mass change for thiazolidine boronate formation (calculated mass change Δm-2H_2O = +98 Da). The result indicates that the CX₉C_pIII protein reacts with 10 equivalents of 2-FPBA to form a thiazolidine protected FPBA_CX₉C_pIII protein as the observed product (Figure S53).

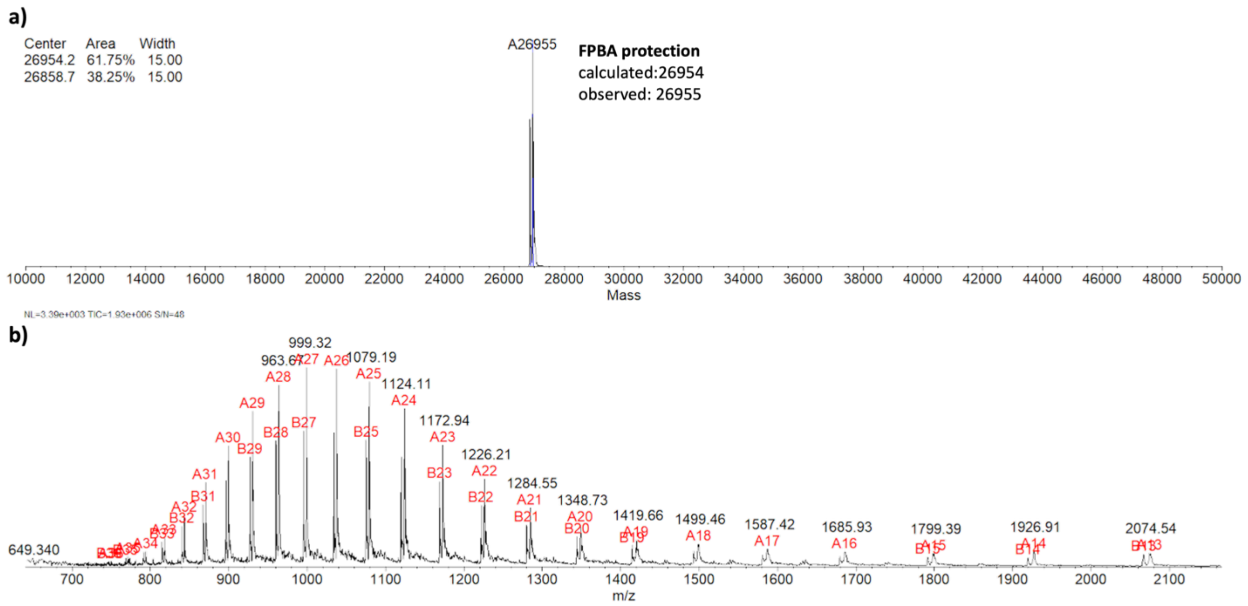

Figure S53. a) Deconvoluted mass and b) crude mass envelope of FPBA_CX₉C_pIII protein.

10 µL of FPBA_CX₉C_pIII protein reaction mixture was diluted with 90 µL of NaPi (100mM, pH=9), and mixed with 1 µL of MDBP (50 mM stock solution in DMF), resulting 5 µM of FPBA_CX₉C_pIII protein and 500 µM of MDBP in NaPi buffer pH=9. The mixture was mixed well by pipetting several times, and incubated at 37 °C for 1h, and the reaction was monitored by LC-MS. The molecular weight of protein decreased by 34 Da after the internal cysteine was converted to dehydroalanine by MDBP, which is consistent with the mass change for dehydroalanine formation (calculated mass change Δm = -34 Da). The result indicates that the FPBA_CX₉C_pIII protein reacts with 500 µM MDBP to generate a site-selective dehydroalanine on pIII protein N-terminal CX₉C fusion peptide, resulting FPBA_CX₉C_Dha_pIII protein as the observed product (Figure S54).

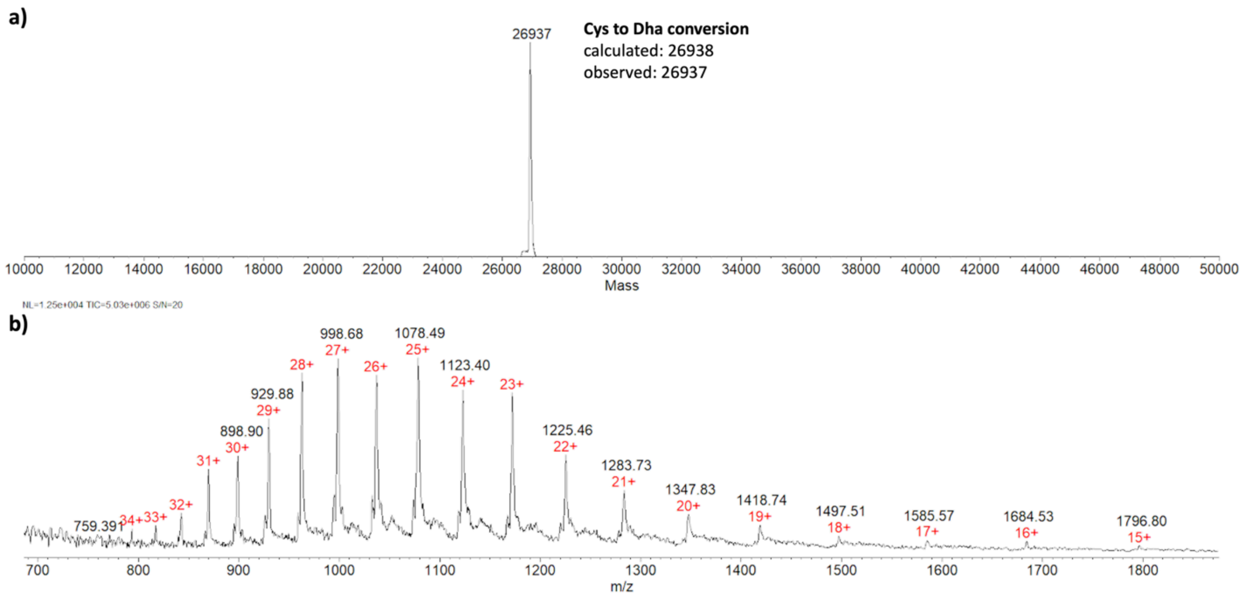

Figure S54. a) Deconvoluted mass and b) crude mass envelope of FPBA_CX$_9$C_Dha_pIII protein.

The excess amount of small molecules was removed by Bio-Spin P6 column (BioRad, CA), then the buffer pH was adjusted to 10 for deprotection of N-terminus protector, with the incubation at 37 °C for 1h. The reaction was monitored by LC-MS. The molecular weight of protein decreased by 113 Da after the NCys was deprotected, which is consistent with the mass change for removal of thiazolidine boronate (calculated mass change Δm = -113 Da). The result indicates that the lanthionine bridged CX$_9$C fusion peptide was generated on the N-terminus of pIII protein, resulting in CX$_9$C_te_pIII protein as the observed product (Figure S55).

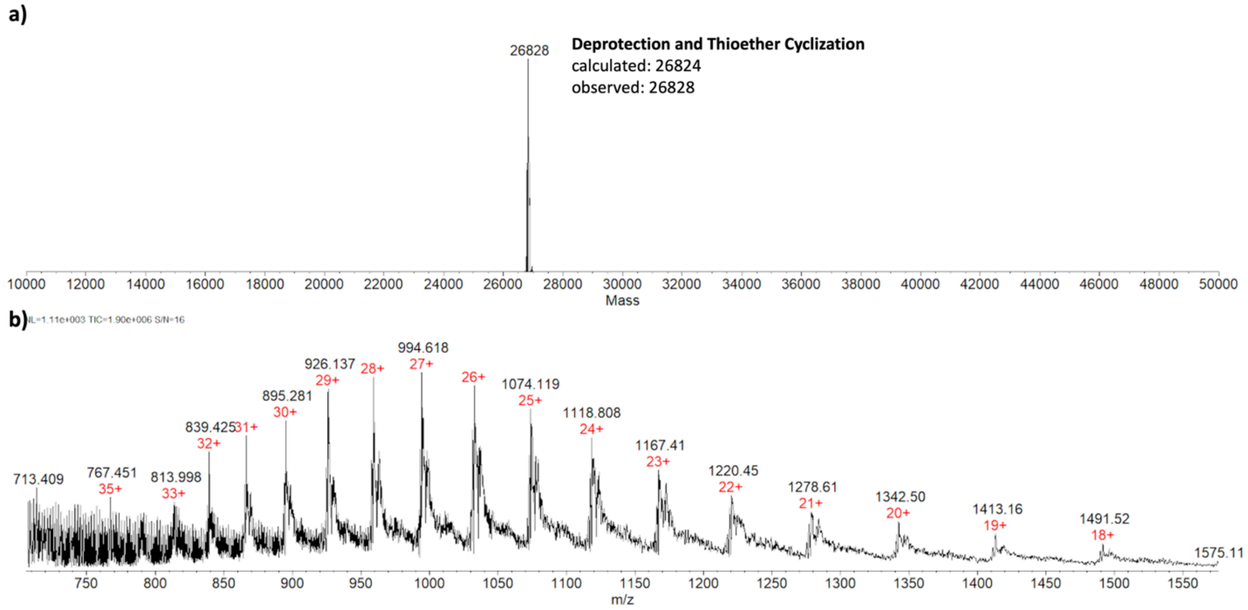

Figure S55. a) Deconvoluted mass and b) crude mass envelope of CX_9C_te_pIII protein.

6. Biopanning

6.1 Construction of Phage Libraries

The Ph.D. Peptide Display Cloning System (NEB, E8101S) was used to construct the peptide libraries. For the library construction, the following library-coding sequence was used: CATGTTTCGGCCGAACCTCCACCACAMNNMNNMNNMNNMNNMNNMNNACACCGG CCCTCAATTGCAGCGTAGTCTGGAACGTCGTAGGGGTAAGAGTGAGAATAGAAAGG TACCCGGGCATG. The library insert DNA was prepared by annealing 5 µg of the library oligonucleotide (Genewiz, MA) with 3 molar equivalents of the universal extension primer. Then the annealed duplex was extended using Klenow fragment (NEB #M0210), then subjected to restriction enzyme digestion with KpnI-HF (NEB, #R3142) and EagI-HF (NEB, #R3505), then followed by phenol/chloroform extraction, ethanol purification and 8% nondenaturing polyacrylamide gel purification. In parallel, the M13KE vector was digested with the same enzyme and purified by 1% agarose gel. The digested/purified cut DNA duplex was ligated with digested/purified vector with T4 DNA Ligase (NEB, #M0202). The ligation mixture was then electroporated into TOP10 competent cells. After outgrowth in SOC, titering of the outgrowths to obtain the complexity of the library (4.5×10^8 pfu). Finally, phage amplification was accomplished by incubating the electroporated cells at 37 °C with shaking at 250 r.p.m for 4-4.5 h. Phage was recovered from the supernatant by adding 1/5 volume of 20% PEG/2.5 M NaCl and incubating for 1 hour at 4 ºC. The precipitated phage was resuspended in TBS buffer pH 7.4 and stored at 4°C for further use.

6.2 Chemical Modification of Phage Libraries

20 µL of the prepared phage library (10^{13} pfu/mL) was reduced with 1 mM TCEP in 80 µL of buffer R (20 mM ammonium bicarbonate, pH= 8.0). The reducing reaction was carried out at room temperature for 1 h with 100 rpm shaking. The reduced phage particles were precipitated with 1/5 volume of 20% PEG/2.5 M NaCl on ice for 1 h, then the precipitated phage was pelleted at 4°C by centrifugation at 14000 rpm for 20 min. For N-terminal cysteine protection, the supernatant was discarded and the phage pellet was re-suspended in 99 µL of PBS (pH = 7.4), then 1 µL of 2-FPBA (100mM stock in DMF) was added. The reaction was mixed and incubated at room temperature for 30 min. Upon completion, to remove the excess amount of the 2-FPBA, the phage was precipitated using 1/5 volume of 20% PEG/2.5 M NaCl on ice for 1 h, then the precipitated phage was pelleted at 4°C by centrifugation at 14000 rpm for 20 min. To convert the internal cysteine to dehydroalanine, the supernatant was discarded and the phage pellet was re-suspended in 99 µL of NaPi (100mM, pH =9), then 1 µL of MDBP (100mM stock in DMF) was added. The reaction was mixed and incubated at 37 °C for 60 min. For N-terminal protector removal and cyclization, the supernatant was discarded and the phage pellet was re-suspended in 90 µL of PBS

(pH = 10), the reaction was mixed and incubated at 37 °C for 60 min. After completion, the modified phage mixture was neutralized to pH 7 by adding 10 µL of 0.2 M glycine-HCl, pH= 2.2.

To evaluate the potential toxicity of each chemical modification step to the phage particles, infectivity was monitored by titering throughout the entire cyclization modification stepwise. A naïve phage library (100 µL, 10^{13} pfu/mL) was used as the starting point. After each modification step, including N-Cys generation by Factor Xa cleavage, TCEP reduction to expose two free Cys, FBPA capping NCys, internal Cys converted to Dha by MDBP, final deprotection and cyclization, an aliquot of the phage solution was subjected to standard titering for quantification.

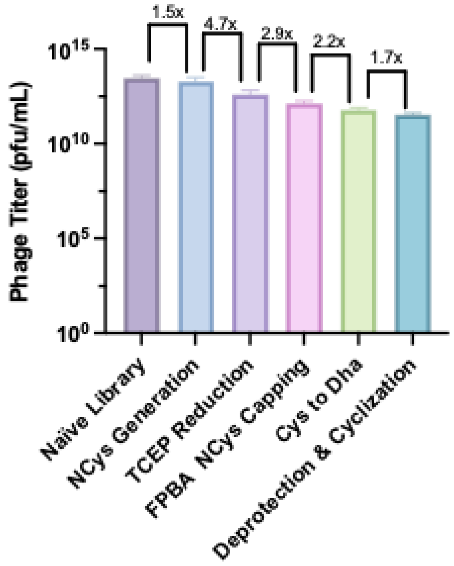

Figure S56. Impact of sequential chemical modifications on phage infectivity.

To evaluate whether the thioether modification introduces sequence bias at the library level, next-generation amplicon sequencing was performed before and after thioether chemical modification on phage. The naïve phage library was first subjected to amplicon sequencing to establish the baseline. The same library was then subjected to thioether cyclic chemical modification under the same conditions as previously described. Following modification, the residual unmodified disulfide phage particles were selectively captured using iodoacetamide–biotin (biotin-IA), then removed by streptavidin pull-down. The remaining phage population, corresponding to thioether-cyclized library members, was recovered and subjected to amplicon sequencing (Figure S57). For each dataset, amino acid frequencies were calculated independently at every randomized position of the library. Two complementary analyses were performed. First, the frequency of each of the 20 canonical amino acids was quantified at every position within the library. Second, a property-based analysis was performed by categorizing amino acids into 5 groups according to their physicochemical characteristics, including positively charged group (Arg, Lys, His), negatively charged group (Asp, Glu), polar uncharged group (Ser, Thr, Asn, Gln), nonpolar group (Ala, Val, Leu, Ile, Met), aromatic residues (Phe, Trp, Tyr) and special residues (Gly, Pro, Cys). All library modification and sequencing analyses were performed in two independent experimental replicates. Across all randomized positions, amino acid frequencies remained highly diverse after thioether modification. No enrichment or depletion trends were observed for specific residues or physicochemical classes. The positional distributions in the modified library closely matched those of the naïve library. These results demonstrate that the thioether modification does not introduce detectable sequence bias at the library level (Figure S58).

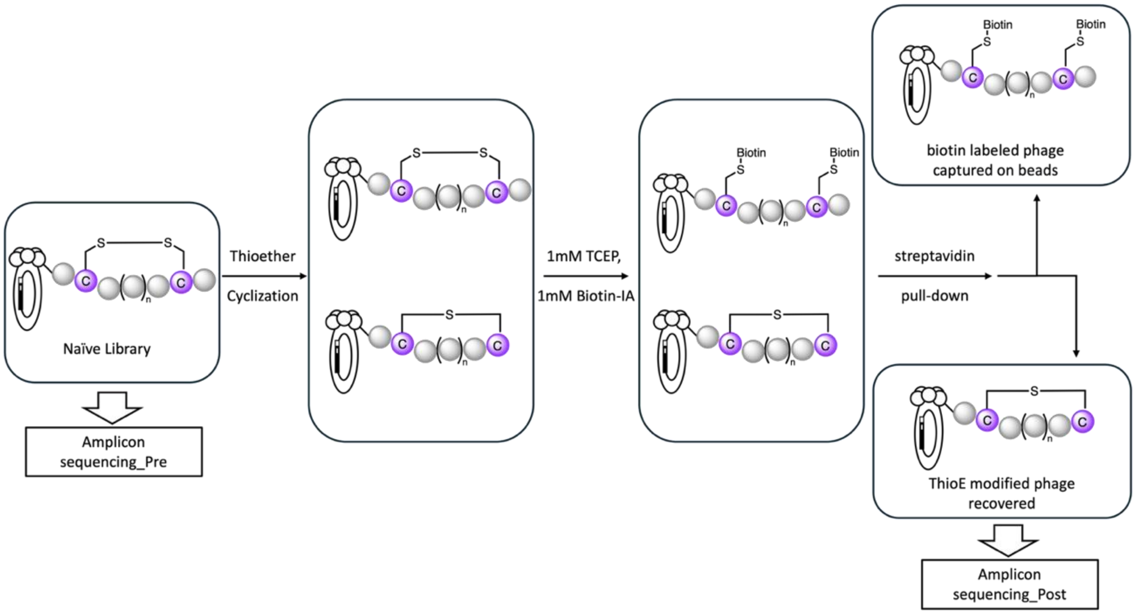

Figure S57. Workflow for lanthionine-bridged macrocyclic phage library amplicon sequencing analysis.

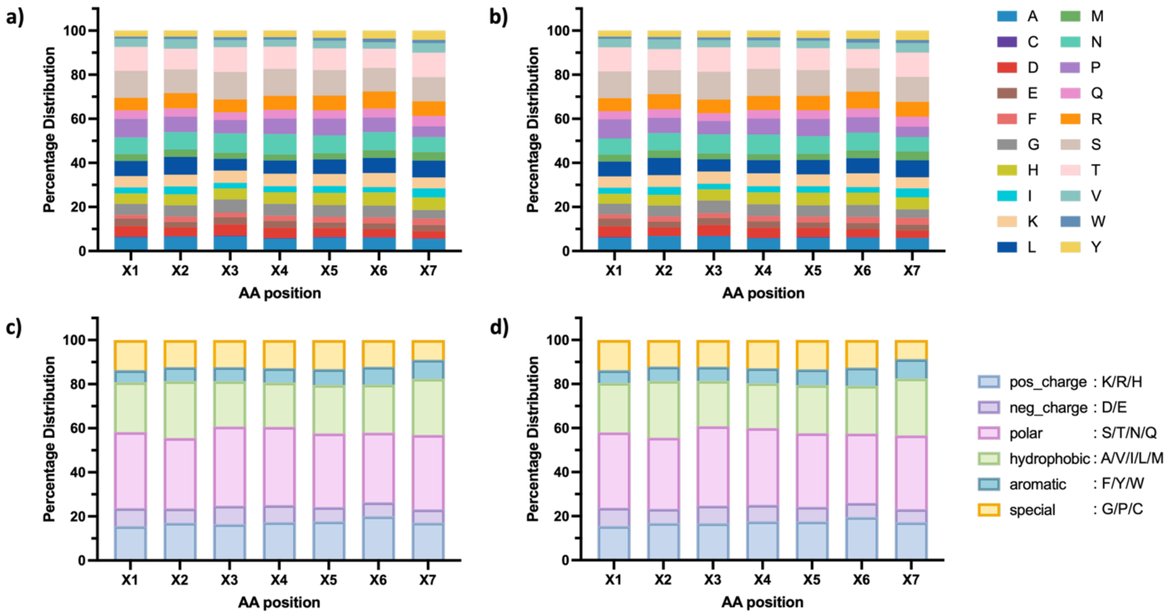

Figure S58. Amplicon sequencing analysis of library composition before and after thioether modification. a) Amino acid distribution at each randomized position in the naïve library; b) Amino acid distribution at each randomized position in the thioether cyclized library；c) physicochemical property distribution (positive, negative, polar, nonpolar, special) in the naïve library; d) physicochemical property distribution in the thioether cyclized library.

Table S3. Summary of amplicon sequencing analysis of the phage library before and after lanthionine cyclization.*

	Pre Modification		**Post Modification**	
Total Counts	121,492		102,140	
Unique sequence counts	118,315		99,907	
Unique sequence percentage	97.4%		97.8%	
No.	**Top30 Sequence**			
	Sequence	**counts**	**Sequence**	**counts**
1	CGANPDPIC	5	CSASRQSAC	4
2	CKLKSASYC	4	CELSKSSMC	3
3	CLVDNQGGC	4	CKRSLLSLC	3
4	CDEAKAFTC	4	CKSLYDKHC	3
5	CGTSGNRIC	4	CLSLSKTVC	3
6	CSVNGNTEC	4	CPGPRMTGC	3
7	CFTMHNLRC	3	CQRERLTNC	3
8	CKREHAIAC	3	CRTTLVGTC	3
9	CSSRSDWRC	3	CSNVTRGYC	3
10	CSTDSASYC	3	CSTPDASMC	3
11	CTSLKGPNC	3	CSTTTRGAC	3
12	CHPSGTHYC	3	CTTDSFSLC	3
13	CGDDLHSKC	3	CAIRANLSC	3
14	CTNAKGENC	3	CAANSVKYC	3
15	CDRSPDRAC	3	CEATRTMSC	3
16	CELSNNRMC	3	CHDTNTGGC	3
17	CFRSSPRTC	3	CLSNRAHSC	3
18	CGANRSDLC	3	CPTSQKSRC	3
19	CGLKSTGGC	3	CSRSQSLFC	3
20	CSHTSTPTC	3	CTGQPAKTC	3
21	CSVRTSYHC	3	CSPYHNREC	3
22	CSVYDTRKC	3	CAIRDPHKC	3
23	CWQTENRPC	3	CASQWSKMC	3
24	CFRENTRTC	3	CDERSQKNC	3
25	CKTSRLNYC	3	CDLTDLTHC	3
26	CSKPKMPQC	3	CDNKDLGTC	3
27	CTKARSMNC	3	CEGLQKRHC	3
28	CAGKPGLQC	3	CGYAREPVC	3
29	CANKAATKC	3	CMADSTTPC	3
30	CASEEPRIC	3	CNAVFNKEC	3

*For each sequencing pool, total read counts, unique sequenced read counts, percentage of unique sequences, and the top 30 most abundant sequences with corresponding read counts are reported. Pre-modification pool represents the naïve disulfide library, whereas post-modification pool corresponds to the chemically modified thioether library.

To determine whether the chemical modification on phage introduces sequence-dependent bias for phage infectivity, ten individual phage clones were randomly selected from the naïve library by isolating single plaques. The selected clones were amplified independently and subjected to the same lanthionine-bridged cyclization chemical modification conditions. Phage titers were quantified for each clone both before and after chemical modification by titering. Comparison of the relative infectivity across all ten independent clones showed comparable levels of phage toxicity after chemical modification, with no statistically significant variation between sequences. These results indicate that the thioether chemical modification does not preferentially impair or enrich specific peptide sequences and therefore does not introduce detectable sequence bias at the level of phage infectivity (Figure S57).

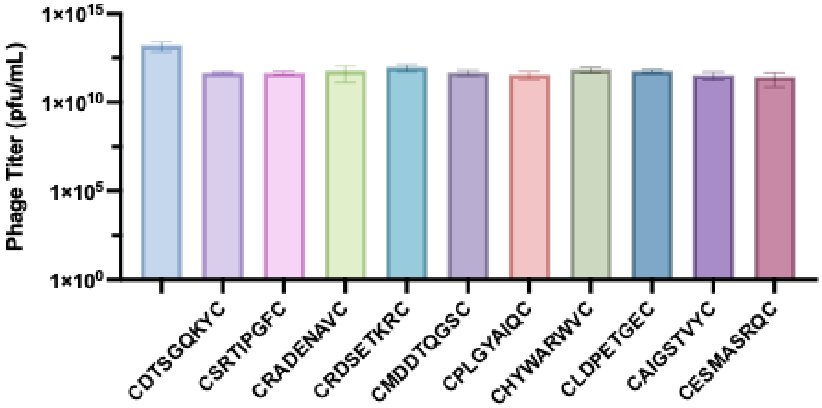

Figure S59. Sequence-independence of thioether modification for phage infectivity assessed by individual phage clones

For the thioether modification efficiency on phage, we used a phage ELISA assay to quantitatively evaluate the efficiency of phage modification by Iodoacetamide-biotin (Thermo Scientific, IL) with and without lanthionine-bridged modification. To coat the well, streptavidin (0.1 mg/mL in 0.1 M $NaHCO_3$ pH 8.6, 100 µL/well) was added into 96-well plate (Corning^{TM}, 3361) and incubated overnight at 4°C. Wells incubated with buffer only were used as a negative control. After incubation, the solution in wells was removed and the wells were blocked with 5mg/mL BSA in PBS (room temperature, 1h) and then washed six times with PBST. Chemically modified phage samples (100 µL, 10^9 pfu/mL) were added to the wells and incubated for 1 h at room temperature. After 6 times of washing with PBST, an anti-M13 antibody-HRP fusion (1:10,000 dilution) was added and incubated at room temperature for 1 h. The wells were washed with PBST for 6 times and then 100 µL TMB (Thermo scientific, 34028) was added into the plate. After incubation at room temperature for 15 min, 100 µL 2M sulfuric acid was added to stop the reaction. The absorbance at 450 nm was read for all treated wells. All experiments were repeated at least three times and consistent results were obtained

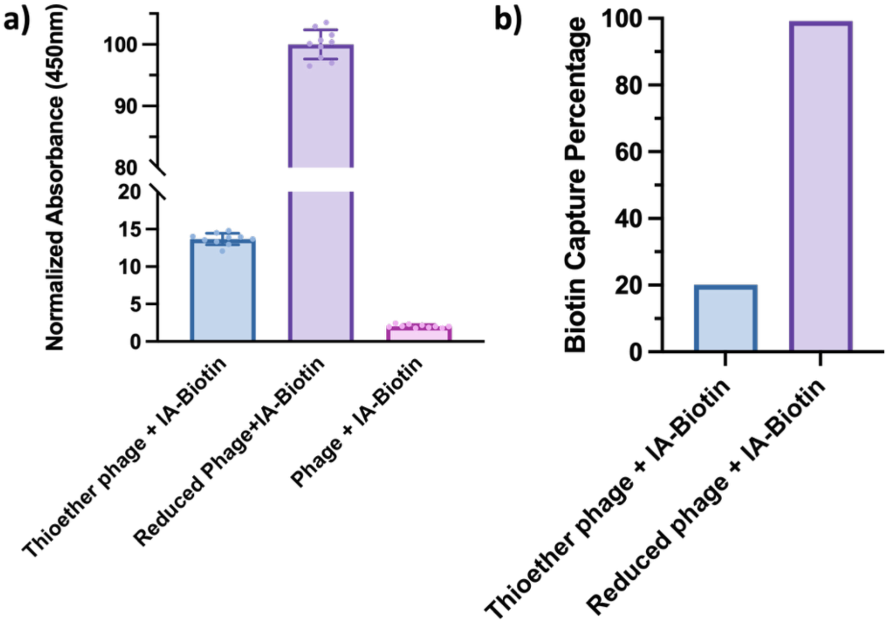

Figure S60. Phage pulldown assay to quantify the efficiency of lanthionine-bridged cyclization chemical modification. a) ELISA assay of streptavidin pull-down with phage library, b) streptavidin magnetic beads pull-down followed by titering gives a similar result.

For the phage pull-down assay, chemically modified phage was quantified through titering and then diluted to 10^7 pfu/mL. Then 100 µL of the diluted phage solution was mixed with 100 µL blocking buffer (2 mg/mL BSA, 0.2% Tween-20 in PBS) and incubated for 30 min at room temperature. In parallel, pre-washed streptavidin beads (20 µL for each phage sample) were incubated with the same buffer at room temperature for 30 min before mixing with the blocked phage samples. After incubation at room temperature for 30 min, the beads together with the biotinylated phage were precipitated using a magnetic stand and the phage count in the supernatant was determined via titering. The percentage of biotin capture was calculated as:

Biotin capture (%) = [(input-output)/input]×100%

The results show that IA-Biotin modification of the reduced phage was quite efficient, normalized as 100% phage pulldown on Elisa assay (Figure S60). This near quantitative phage modification justifies the use of **IA-Biotin** as a positive control in the ELISA assay and magnetic beads based pull-down assay. These data demonstrate the thioether cyclization of the fused CX_7C peptide on phage is efficient with an average modification efficiency of over 85%.

6.3 Phage Panning Against Keap1 Protein

20 µL of streptavidin-coated magnetic beads (Dynabeads M-280 streptavidin, Invitrogen) were washed three times with 500 µL of PBS. The washed beads were re-suspended completely with 100 µL PBS, and 2 µg of biotinylated Keap1 was added. The mixture was incubated on a shaker with 80 rpm at room temperature for 30 min. After the biotinylated Keap1 immobilized, the magnetic beads were washed three times with 500 µL of PBST (PBS, pH=7.4, 0.1% Tween-20), then re-suspended in 500 µL of a blocking buffer (1 mg/mL BSA, PBS, pH=7.4, 0.1% Tween-20). Then the blocking protein was incubated on the Tube Revolver Rotator (Thermofisher, MA) at room temperature for 30min. In parallel, a modified phage library was also blocked for 30 min at room temperature. Then the library was mixed with the magnetic beads for binding and incubated at room temperature for 30 min. After binding, the unbounded phage was removed. The beads were washed ten times with a washing buffer (PBS, pH=7.4, 0.1% Tween-20). After washing, the beads were re-suspended in 200 µL of the elution buffer (0.2 M glycine-HCl, pH= 2.2). After 10 min elution, the supernatant was separated from the beads, and neutralized with 800 µL of neutralization buffer (1 M Tris-HCl, pH=9.0) resulting in 1 mL of output. A small aliquot from the input and output pools were subjected to titering to quantify the phage population. For the next round of selection, 500 µL of output was subjected to amplification following the standard amplification protocol from NEB.

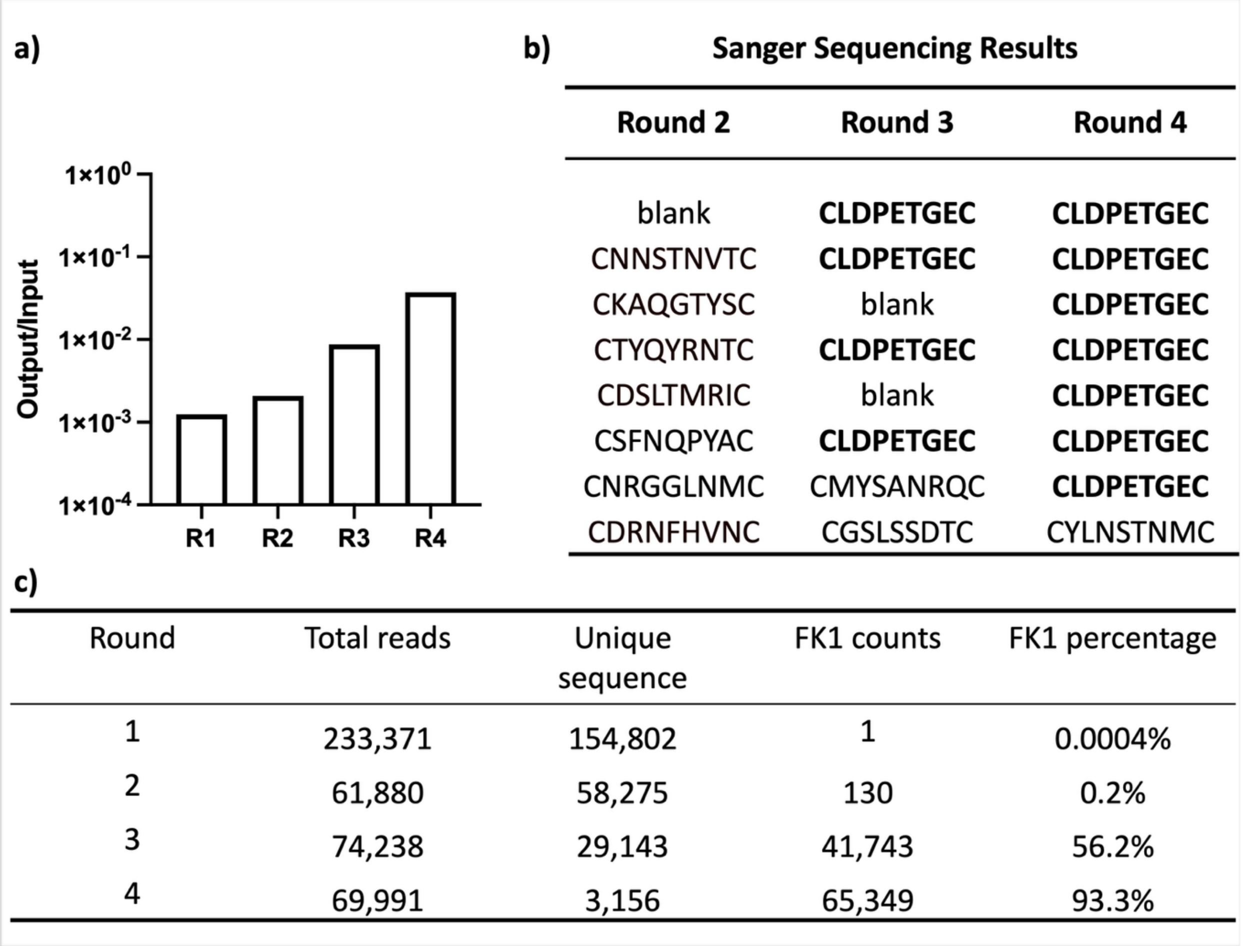

b) **Sanger Sequencing Results**

Round 2	Round 3	Round 4
blank	**CLDPETGEC**	**CLDPETGEC**
CNNSTNVTC	**CLDPETGEC**	**CLDPETGEC**
CKAQGTYSC	blank	**CLDPETGEC**
CTYQYRNTC	**CLDPETGEC**	**CLDPETGEC**
CDSLTMRIC	blank	**CLDPETGEC**
CSFNQPYAC	**CLDPETGEC**	**CLDPETGEC**
CNRGGLNMC	CMYSANRQC	**CLDPETGEC**
CDRNFHVNC	CGSLSSDTC	CYLNSTNMC

c)

Round	Total reads	Unique sequence	FK1 counts	FK1 percentage
1	233,371	154,802	1	0.0004%
2	61,880	58,275	130	0.2%
3	74,238	29,143	41,743	56.2%
4	69,991	3,156	65,349	93.3%

Figure S61. Biopanning against Keap1 protein using the thioether modified CX$_7$C phage library. a) phage recovery for each round after panning, b) Sanger sequencing results from Round 2-4, c) summary of amplicon sequencing results showing gradual enrichment of FK1.

Amplicon sequencing was performed on libraries from R0 (naïve library), R3, and R4 output pool after Keap1 screening. Amino acid frequencies were calculated at each randomized position, and residues were grouped into physicochemical classes as previously described. R0 showed highly diverse amino acid and property distributions across all positions. In contrast, positional enrichment was observed in R3 and became more pronounced in R4. These results indicate that sequence enrichment occurs during Keap1 screening rather than during chemical modification.

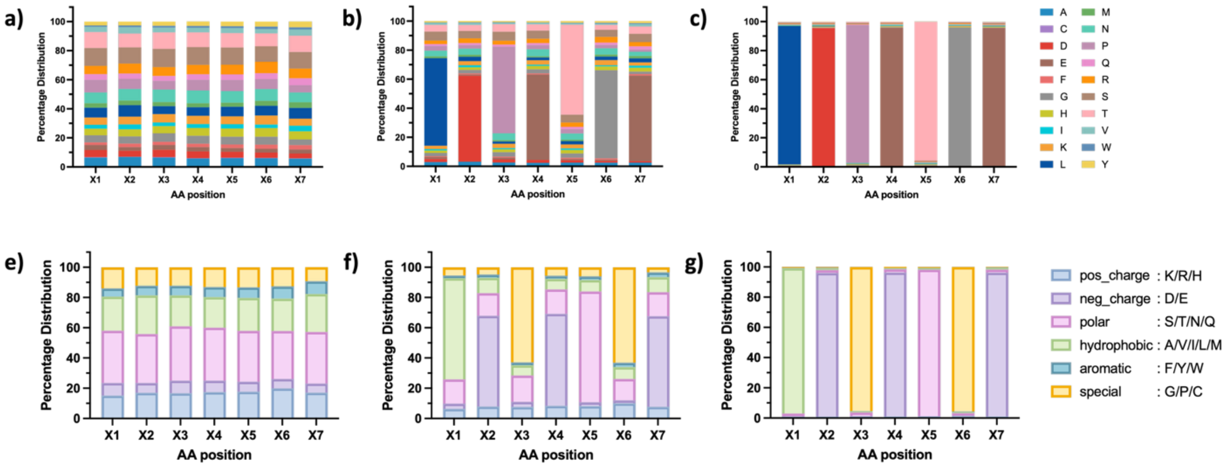

Figure S62. Amino acid and physicochemical property distributions across panning rounds. a)–c) Amino acid distribution at each randomized position in R0 (naïve library), R3, and R4, respectively. d)–f) Physicochemical property distribution (positively charged, negatively charged, polar uncharged, nonpolar, special) in R0, R3, and R4, respectively.

6.4 Peptide Hit Synthesis

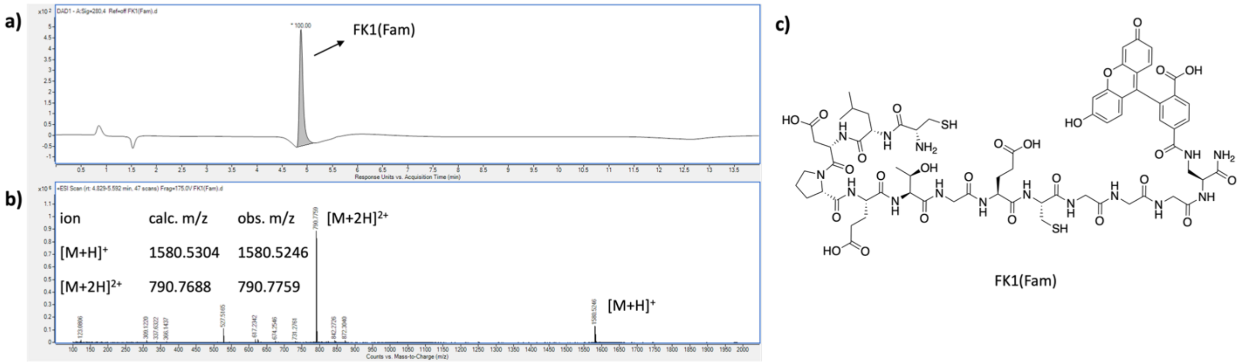

ion	calc. m/z	obs. m/z
$[M+H]^+$	1580.5304	1580.5246
$[M+2H]^{2+}$	790.7688	790.7759

Figure S63. a) LC-MS UV (280 nm) trace of **FK1(Fam)**, b) mass spec readout of starting peptide **FK1(Fam)**, c) chemical structure of peptide **FK1(Fam)**.

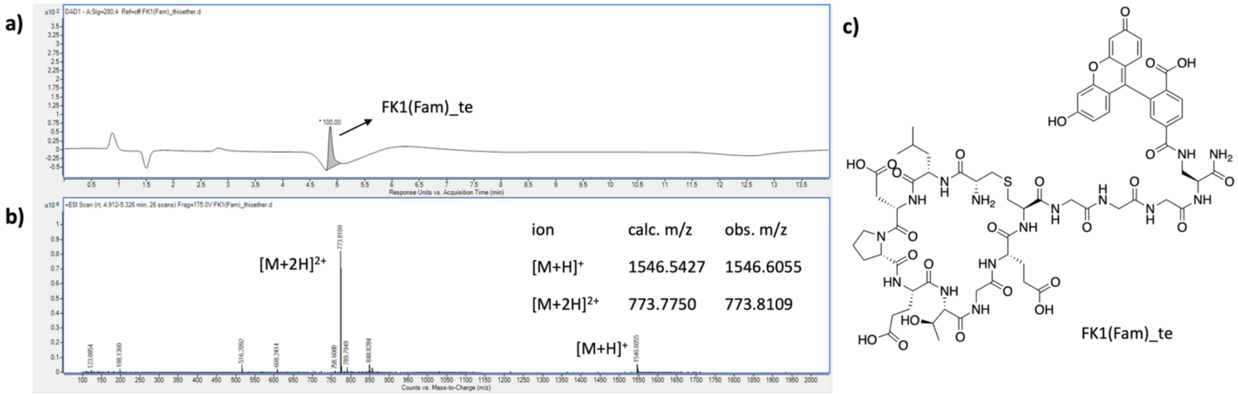

ion	calc. m/z	obs. m/z
$[M+H]^+$	1546.5427	1546.6055
$[M+2H]^{2+}$	773.7750	773.8109

Figure S64. a) LC-MS UV (280 nm) trace of **FK1(Fam)_te**, b) mass spec readout of **FK1(Fam)_te**, c) chemical structure of peptide **FK1(Fam)_te**.

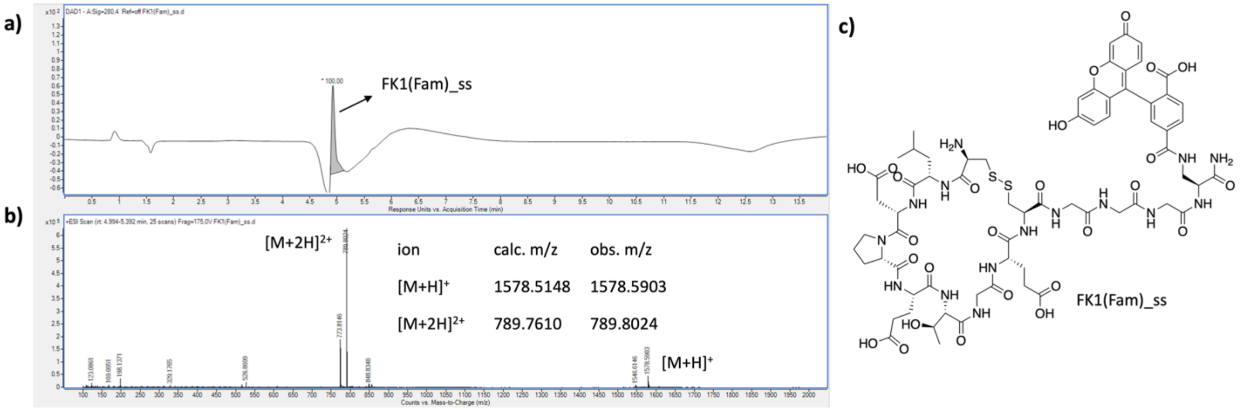

ion	calc. m/z	obs. m/z
$[M+H]^+$	1578.5148	1578.5903
$[M+2H]^{2+}$	789.7610	789.8024

Figure S65. a) LC-MS UV (280 nm) trace of **FK1(Fam)_ss**, b) mass spec readout of **FK1(Fam)_ss**, c) chemical structure of **FK1(Fam)_ss**.

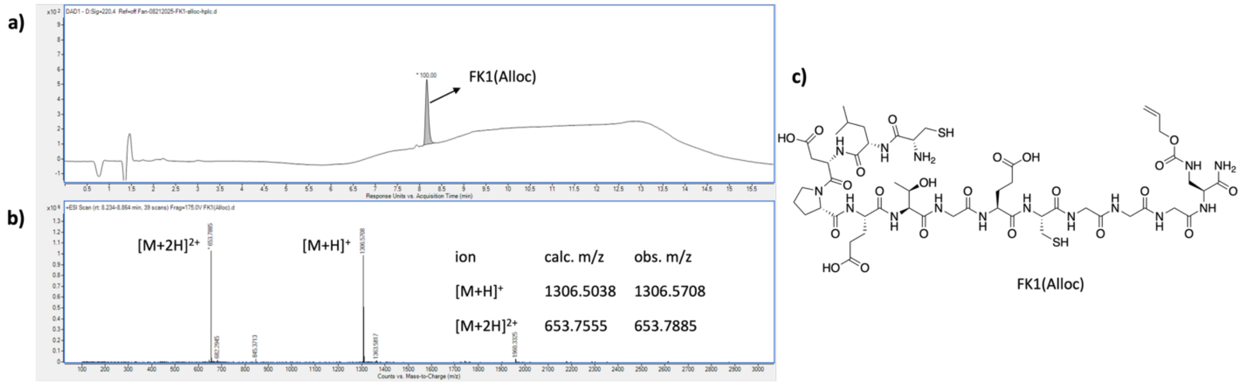

ion	calc. m/z	obs. m/z
$[M+H]^+$	1306.5038	1306.5708
$[M+2H]^{2+}$	653.7555	653.7885

Figure S66. a) LC-MS UV (220 nm) trace of **FK1(Alloc)**, b) mass spec readout of **FK1(Alloc)**, c) chemical structure of **FK1(Alloc)**.

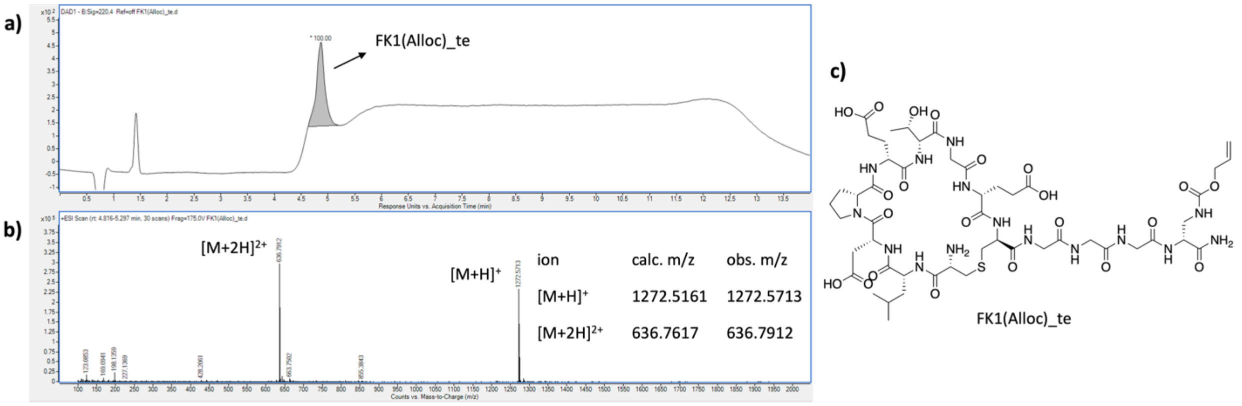

ion	calc. m/z	obs. m/z
$[M+H]^+$	1272.5161	1272.5713
$[M+2H]^{2+}$	636.7617	636.7912

Figure S67. a) LC-MS UV (220 nm) trace of **FK1(Alloc)_te**, b) mass spec readout of **FK1(Alloc)_te**, c) chemical structure of **FK1(Alloc)_te**.

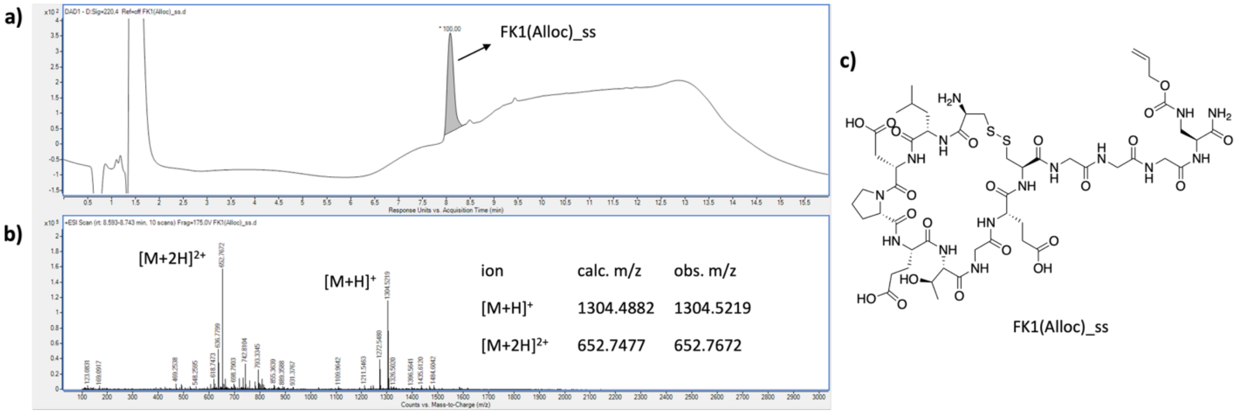

ion	calc. m/z	obs. m/z
$[M+H]^+$	1304.4882	1304.5219
$[M+2H]^{2+}$	652.7477	652.7672

Figure S68. a) LC-MS UV (220 nm) trace of **FK1(Alloc)_ss**, b) mass spec readout of **FK1(Alloc)_ss**, c) chemical structure of **FK1(Alloc)_ss**.

6.5 Peptide Hit Stability

6.5.1 Stability against reduction

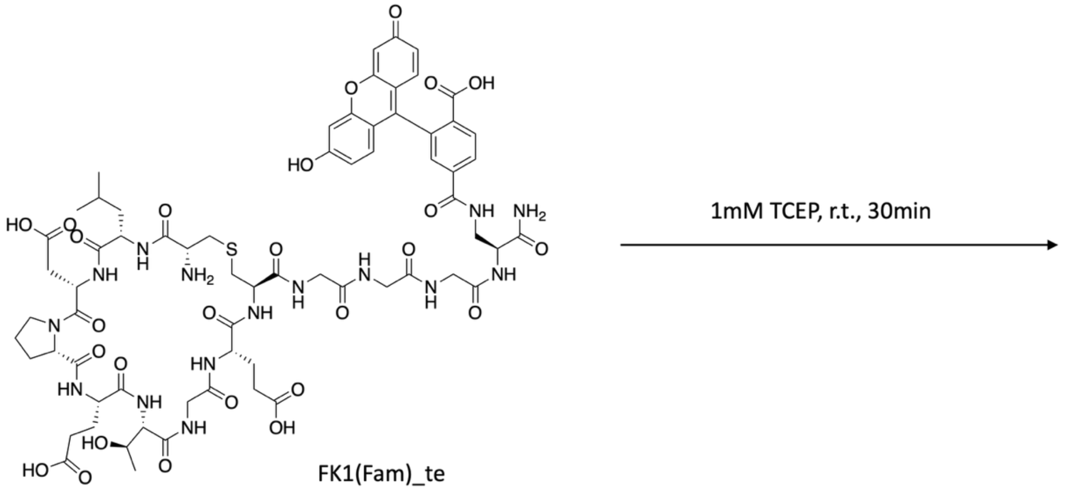

Scheme S23. Reduction of **FK1(Fam)_te** by TCEP.

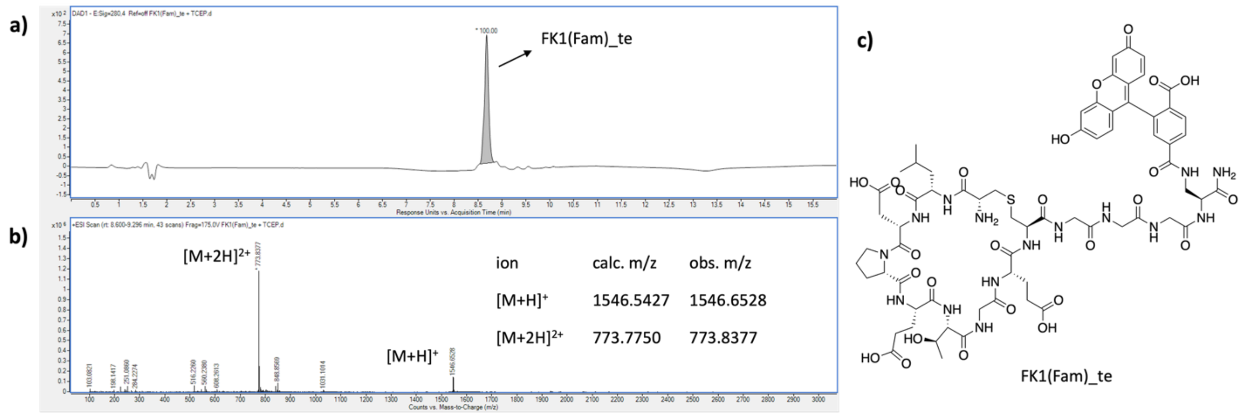

ion	calc. m/z	obs. m/z
$[M+H]^+$	1546.5427	1546.6528
$[M+2H]^{2+}$	773.7750	773.8377

Figure S69. a) LC-MS UV (280 nm) trace of **FK1(Fam)_te** treated with 1mM of TCEP, b) mass spec readout of **FK1(Fam)_te**, c) chemical structure of **FK1(Fam)_te**.

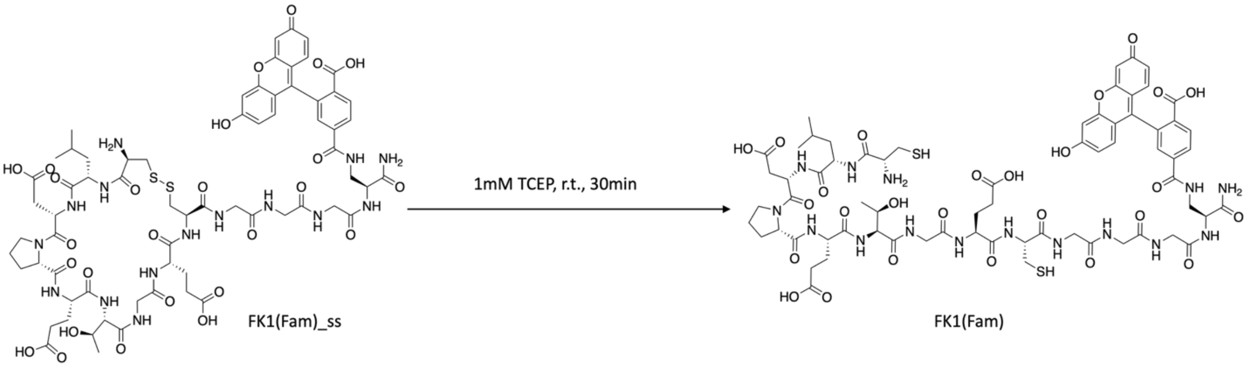

Scheme S24. Reduction of **FK1(Fam)_ss** by TCEP.

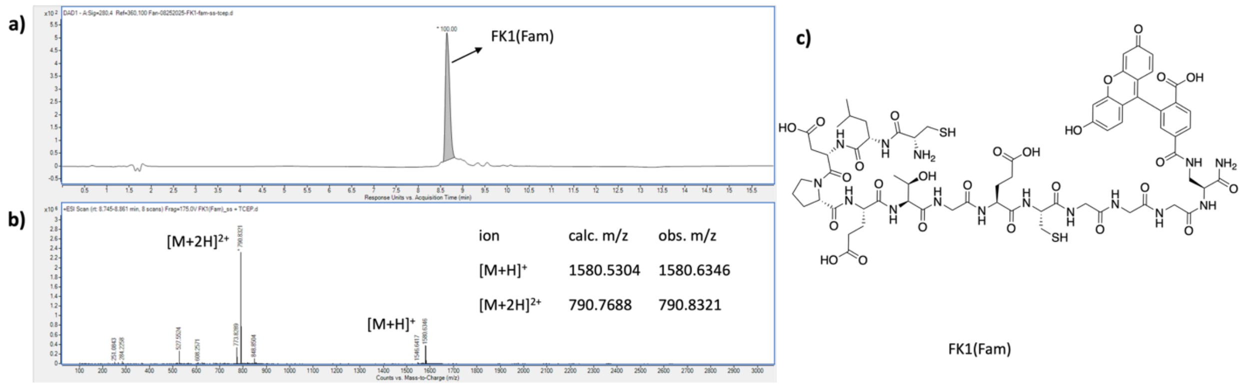

ion	calc. m/z	obs. m/z
$[M+H]^+$	1580.5304	1580.6346
$[M+2H]^{2+}$	790.7688	790.8321

Figure S70. a) LC-MS UV (280 nm) trace of **FK1(Fam)_ss** treated with 1mM of TCEP, b) mass spec readout of reduced peptide **FK1(Fam)**, c) chemical structure of **FK1(Fam)**.

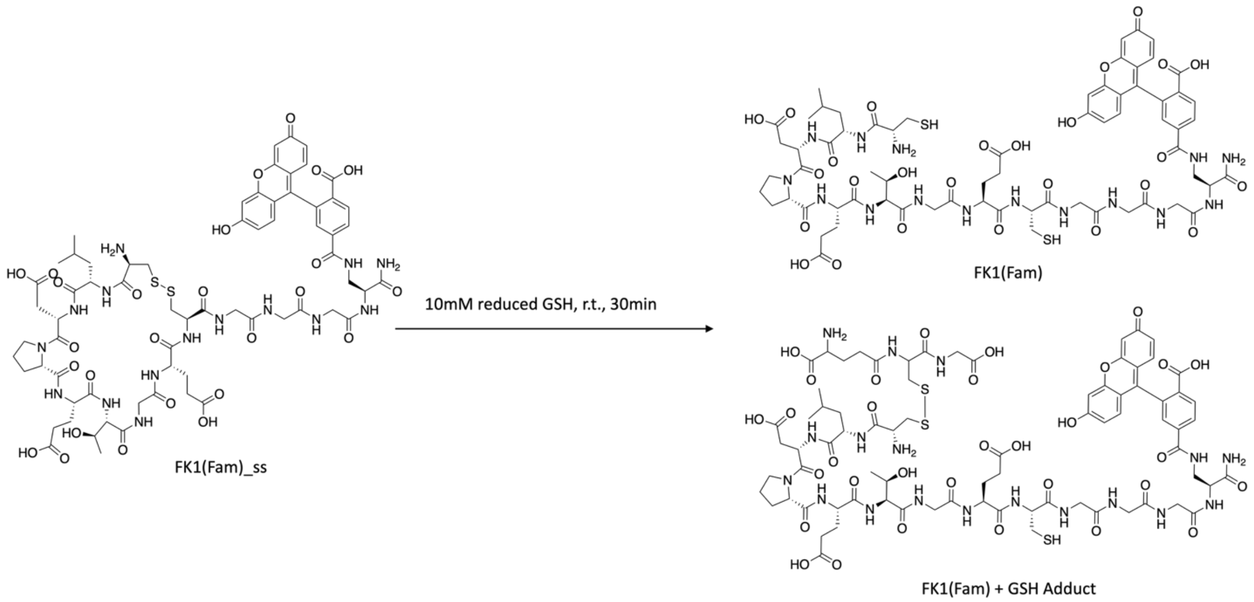

Scheme S25. Reduction of **FK1(Fam)_ss** by GSH.

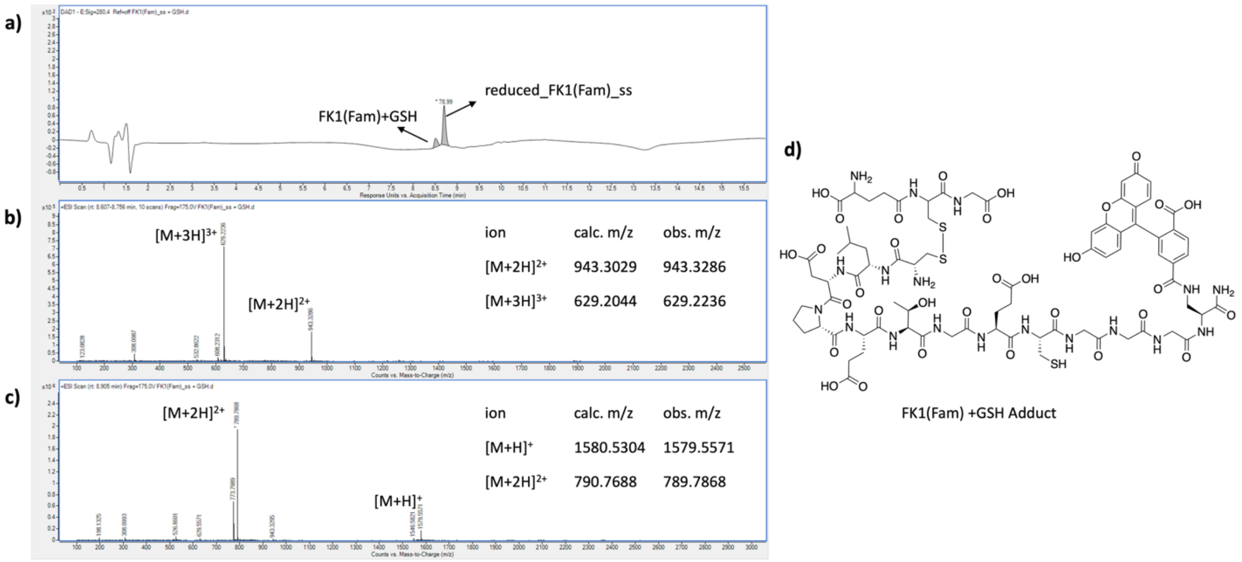

Figure S71. a) LC-MS UV (280 nm) trace of **FK1(Fam)_ss** treated with 10mM of GSH, b) mass spec readout of **FK1(Fam)+GSH Adduct**, c) chemical structure of peptide **FK1(Fam)+GSH Adduct**.

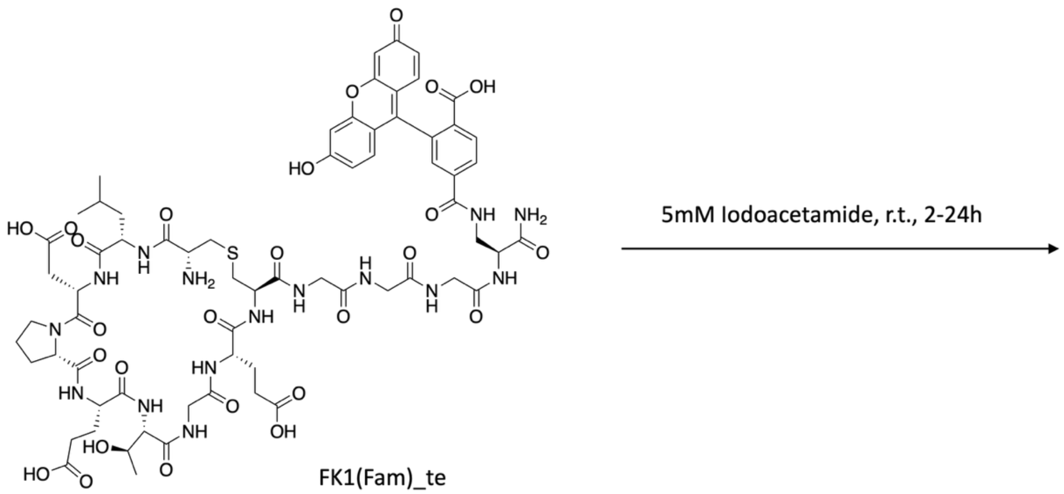

Scheme S26. Attempted alkylation of **FK1(Fam)_te** by iodoacetamide.

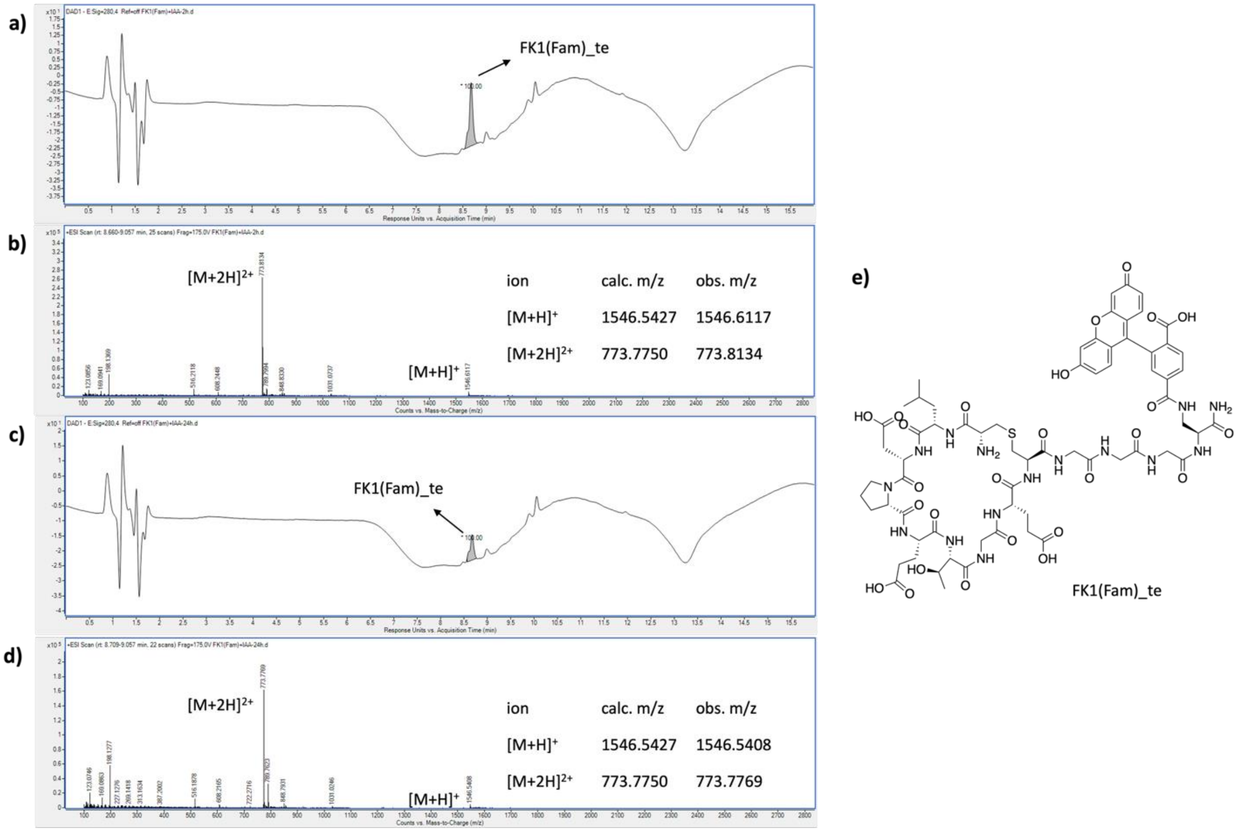

ion	calc. m/z	obs. m/z
$[M+H]^+$	1546.5427	1546.6117
$[M+2H]^{2+}$	773.7750	773.8134

ion	calc. m/z	obs. m/z
$[M+H]^+$	1546.5427	1546.5408
$[M+2H]^{2+}$	773.7750	773.7769

Figure S72. a) LC-MS UV (280 nm) trace of **FK1(Fam)_te** treated with 5mM of iodoacetamide after 2h incubation at room temperature, b) mass spec readout of peptide **FK1(Fam)_te**, c) LC-MS UV (280 nm) trace of **FK1(Fam)_te** treated with 5mM of iodoacetamide after 24h incubation at room temperature, d) mass spec readout of peptide **FK1(Fam)_te**, e) chemical structure of peptide **FK1(Fam)_te**.

6.5.2 Hit Peptide Stability in Human Serum

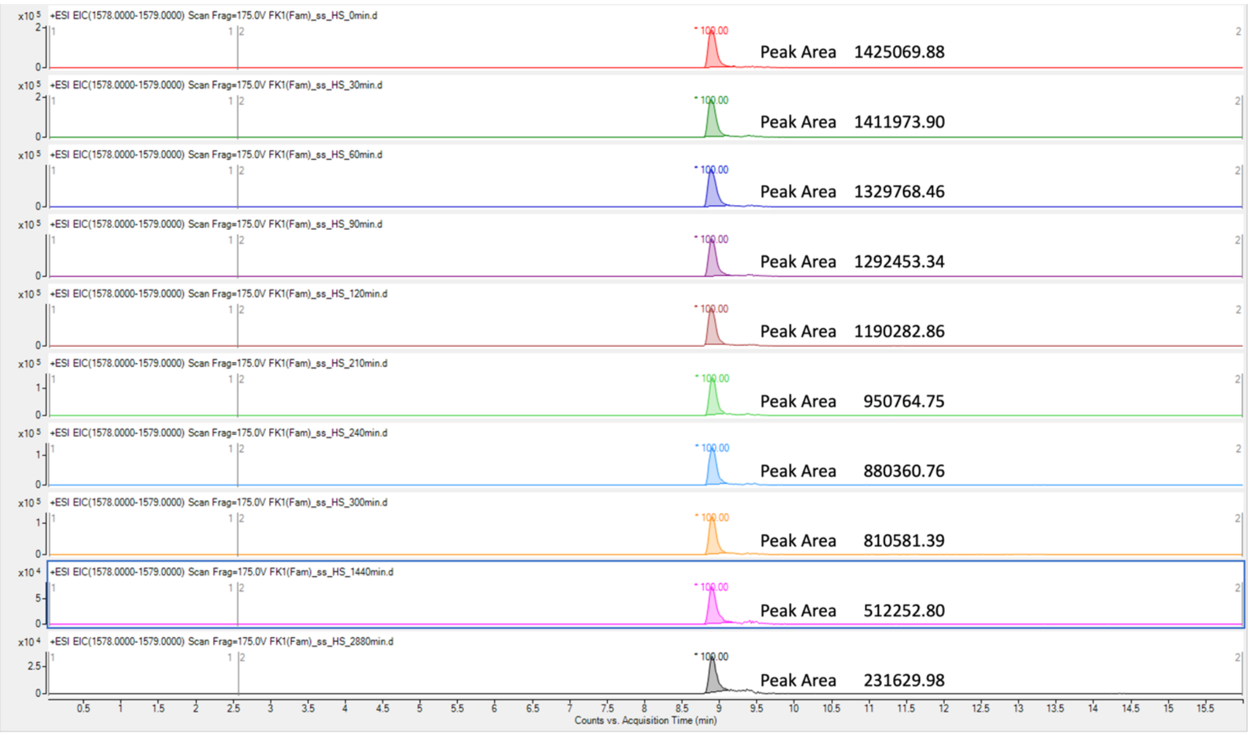

Figure S73. LC-MS UV (280 nm) trace of **FK1(Fam)_ss** incubated with human serum. The ion count of **FK1(Fam)_ss** was extracted at the time point of 0 min/ 30 min/ 60 min/ 90min/ 120min/ 210min/ 240min/ 300min/ 1440min/ 2880min.

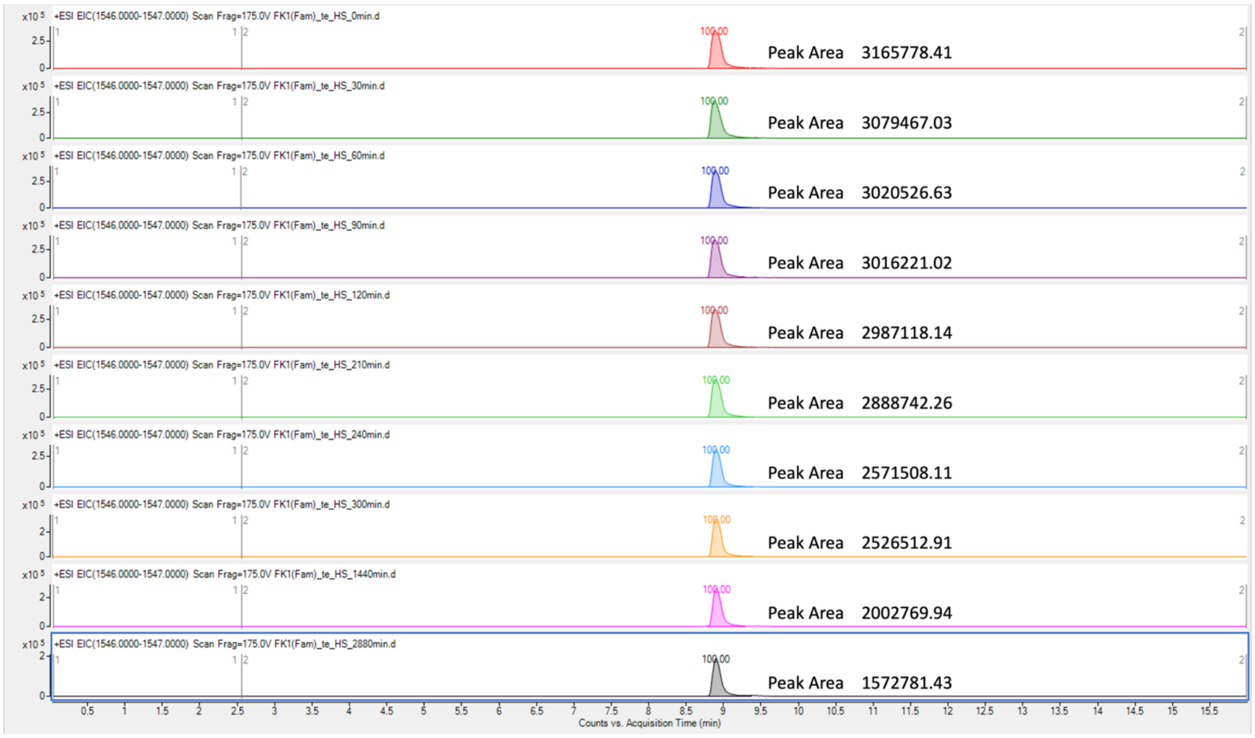

Figure S74. LC-MS UV (280 nm) trace of **FK1(Fam)_te** incubated with human serum. The ion count of **FK1(Fam)_te** was extracted at the time point of 0 min/ 30 min/ 60 min/ 90min/ 120min/ 210min/ 240min/ 300min/ 1440min/ 2880min.

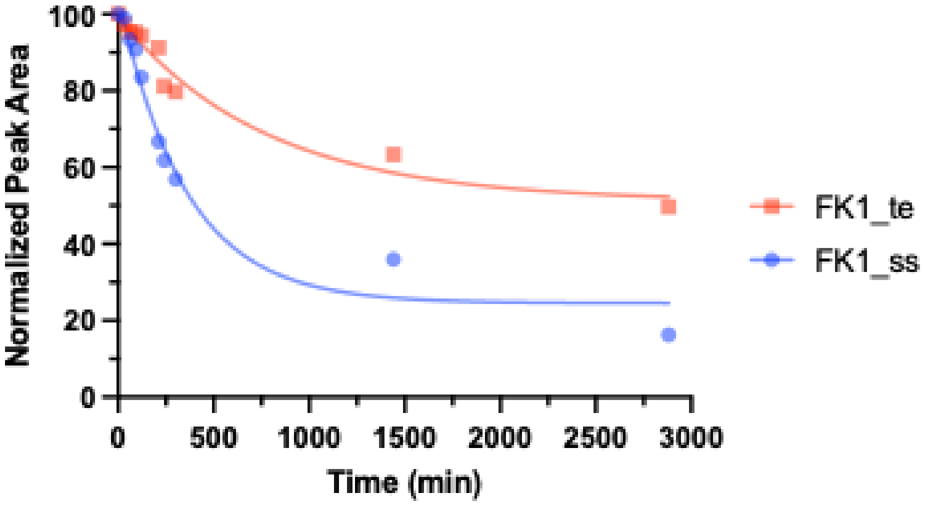

Figure S75. Normalized peak area plotted over time to compare serum stability of peptides.

6.6 Fluorescence Polarization Assay

Both fluorescence polarization binding assay and competition assay were performed in PBST (PBS with 0.1% tween-20) following the reference.[4] The fluorescence polarization values were measured in black 96-well plates with flat bottom (Costar, REF#3915, ME) using a SpectraMax M5 Microplate Reader (Molecular Devices, CA). The experiments were conducted in triplicates, and the results were averaged and analyzed. Each experiment was repeated at least three times, which gave consistent results. Representative results are presented in the paper with the FP value normalized against a fitted maximum. For the fluorescence polarization binding assay, a FAM labeled peptide was mixed with varying concentration of target protein (0 to 50 μM). The final peptide concentration was 200 nM in all samples. After incubated at room temperature for 30 min, the fluorescence polarization values were measured. Dissociation constants (K_d) were determined by plotting the fluorescence polarization value as a function of protein concentration, and the plots were fitted to the following equation.

$$y=FPmin+(FPmax-FPmin)*(K_d+Lst+x-sqrt((K_d+Lst+x)^2-4*Lst*x))/(2*Lst).$$

The Lst is the concentration of the FAM-labeled peptide and the x stands for the concentration of the protein.

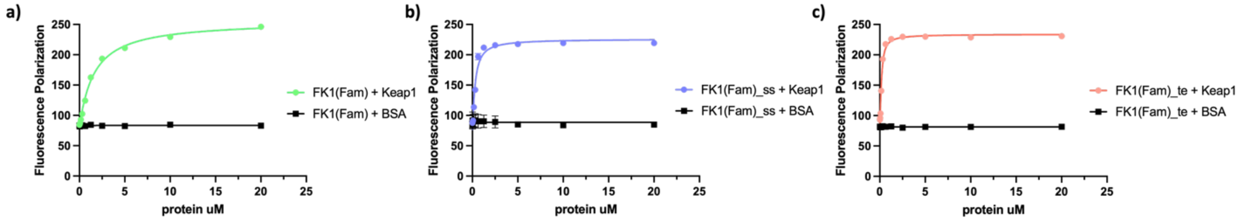

Figure S76. Fluorescence polarization of a) **FK1(Fam)**, b) **FK1(Fam)_ss**, and c) **FK1(Fam)_te**. Fluorescence polarization was recorded at 485 nm with proteins (Keap1 or BSA as a negative control) titrated into a 200 nM peptide solution.

For the competition assay, the concentration of the Keap1 and a FAM-labeled peptide was kept at 300 nM and 200 nM, respectively. This mixture was incubated (30 min) with a peptide competitor at varied concentrations and then the fluorescence polarization value was recorded. The IC_{50} was determined by fitting the dose-response curves to absolute IC_{50} via nonlinear regression using Prism. We note that under our experimental conditions, the IC_{50} values can be approximated as K_d as the reporter peptide was used at much lower concentrations.

6.7 Flow Cytometry Assay

The binding affinities of selected hit variants toward Keap1 were further validated using a bead-based flow cytometry assay. Biotinylated Keap1 protein was immobilized onto streptavidin magnetic beads according to the manufacturer's protocol. After washing and blocking with 1mg/mL of BSA in PBS, beads were incubated with a series of concentrations of FAM-labeled peptides in PBS buffer at room temperature for 30 min. Following incubation, fluorescence intensity was recorded in the FITC channel and gated on the bead population. Background fluorescence from beads without peptide was subtracted. Binding curves were generated by plotting mean fluorescence intensity versus peptide concentration. Data were fitted using nonlinear regression to a one-site specific binding model:

$$Y=B_{max}*X/(K_d+X)$$

where Y represents fluorescence intensity, X is peptide concentration, B_{max} is maximal binding, and K_d is the apparent dissociation constant. All measurements were performed in duplicate.

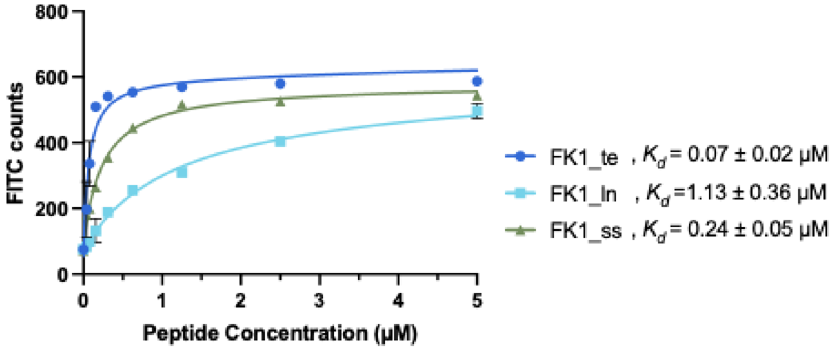

Figure S77. Flow cytometry binding curves of **FK1(Fam)**, **FK1(Fam)_ss** and **FK1(Fam)_te**. at FITC channel with Keap1 proteins.

7. NMR Spectra

^{1}H NMR spectra of ethyl (E)-N-((mesitylsulfonyl)oxy)acetimidate

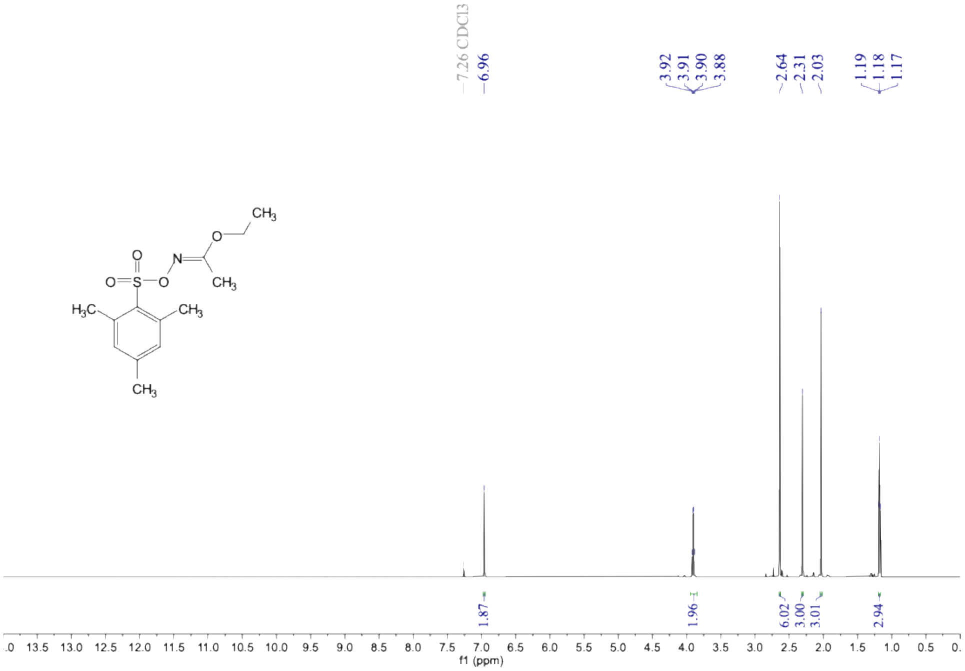

^{1}H NMR spectra of O-(mesitylsulfonyl)hydroxylamine (MSH)

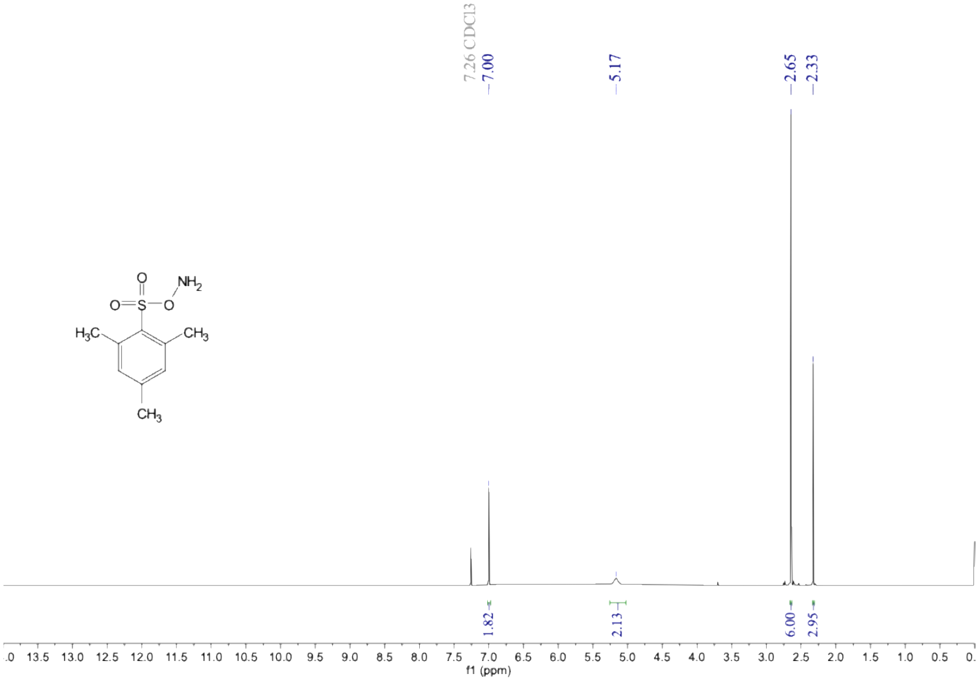

^{1}H NMR spectra of allyl (tert-butoxycarbonyl)-L-serinate

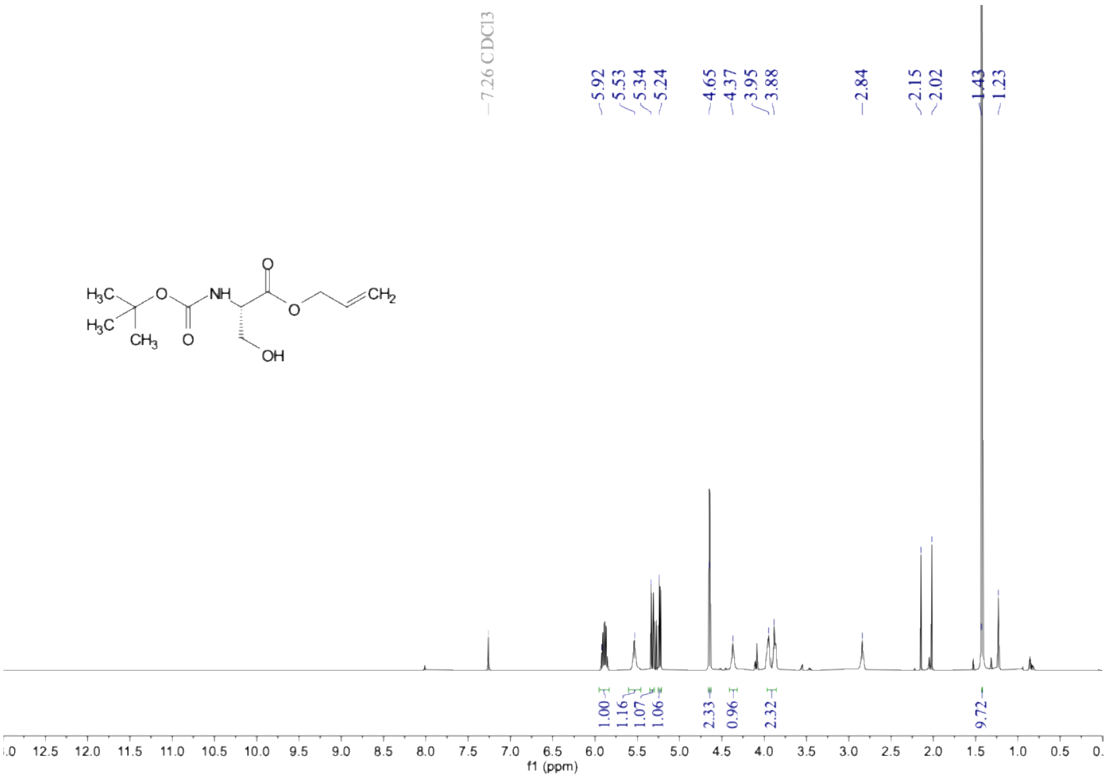

^{1}H NMR spectra of allyl (R)-3-bromo-2-((tert-butoxycarbonyl)amino)propanoate

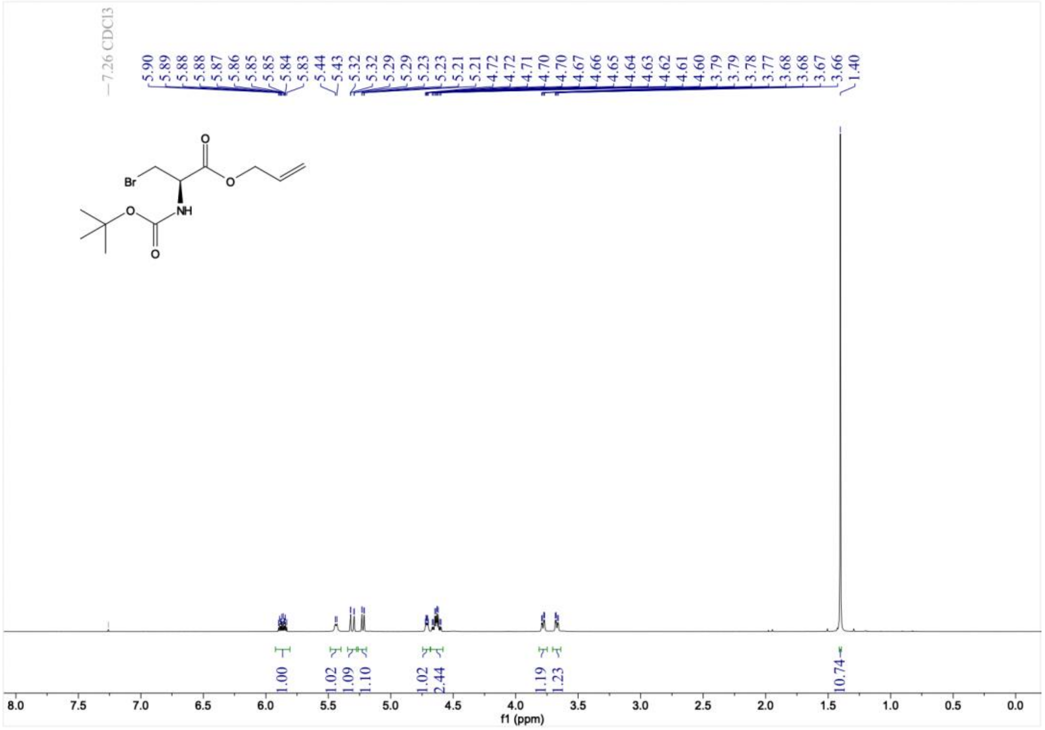

^{13}C NMR spectra of allyl (R)-3-bromo-2-((tert-butoxycarbonyl)amino)propanoate

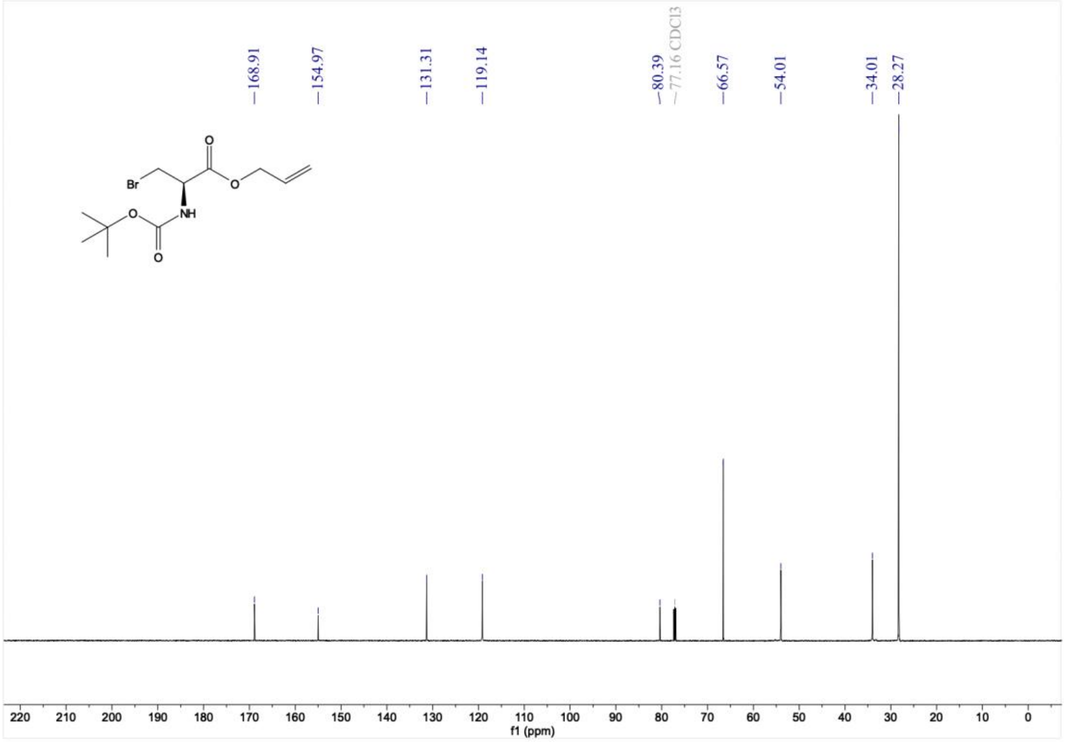

^{1}H NMR spectra of N-(((9H-fluoren-9-yl)methoxy)carbonyl)-S-(3-(allyloxy)-2-((tert-butoxycarbonyl)amino)-3-oxopropyl)cysteine

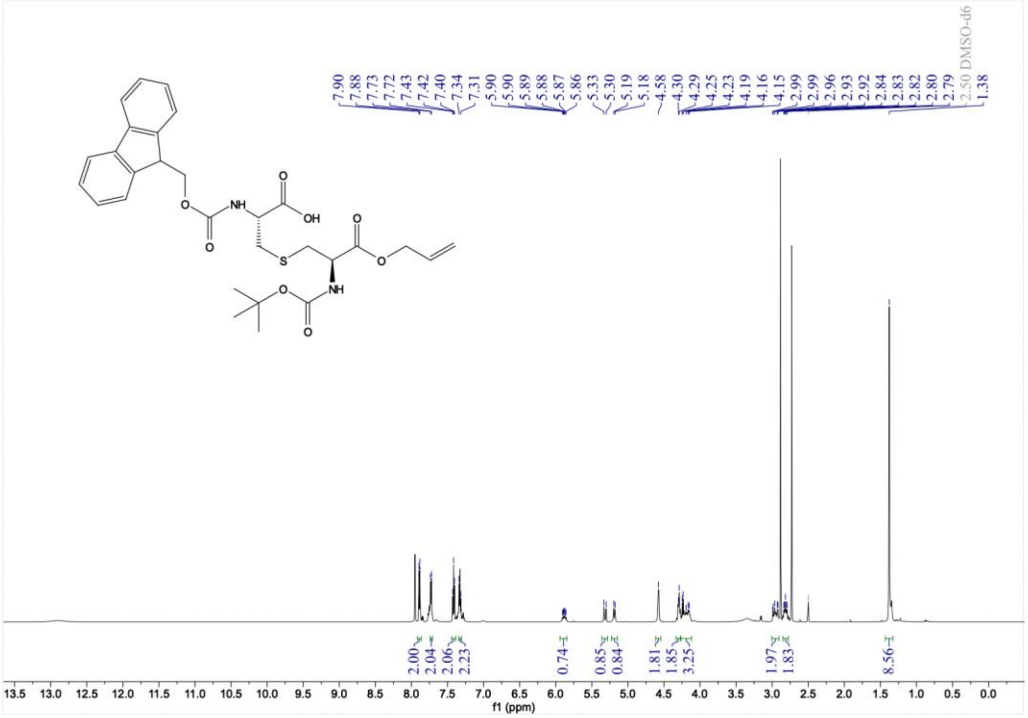

^{13}C NMR spectra of N-(((9H-fluoren-9-yl)methoxy)carbonyl)-S-(3-(allyloxy)-2-((tert-butoxycarbonyl)amino)-3-oxopropyl)cysteine

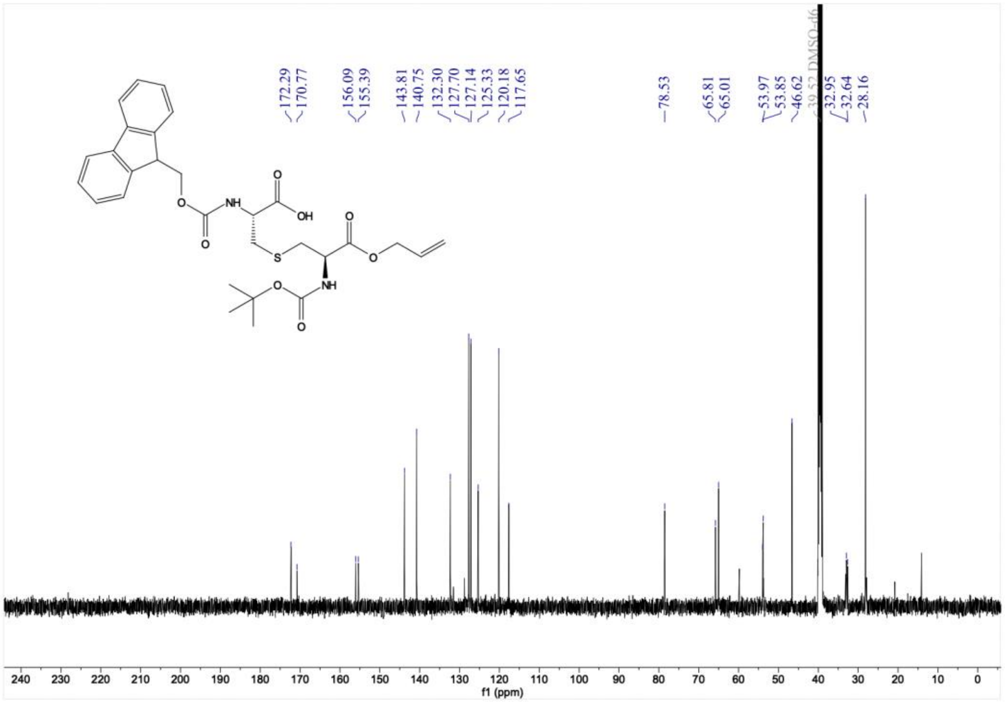

8. Reference

(1) Chalker, J. M.; Gunnoo, S. B.; Boutureira, O.; Gerstberger, S. C.; Fernández-González, M.; Bernardes, G. J. L.; Griffin, L.; Hailu, H.; Schofield, C. J.; Davis, B. G. Methods for Converting Cysteine to Dehydroalanine on Peptides and Proteins. Chem. Sci. 2011, 2 (9), 1666–1676. https://doi.org/10.1039/C1SC00185J.

(2) Manzor, K.; Proinsias, K. ó; Kelleher, F. Solid-Phase Peptide Synthesis of Analogues of the N-Terminus A-Ring Fragment of the Lantibiotic Nisin: Replacements for the Dehydroalanine (Dha) Residue at Position 5 and the First Incorporation of a Thioamide Residue. Tetrahedron Letters 2017, 58 (30), 2959–2963. https://doi.org/10.1016/j.tetlet.2017.06.052.

(3) Ross, A. C.; Liu, H.; Pattabiraman, V. R.; Vederas, J. C. Synthesis of the Lantibiotic Lactocin S Using Peptide Cyclizations on Solid Phase. J. Am. Chem. Soc. 2010, 132 (2), 462–463. https://doi.org/10.1021/ja9095945.

(4) Zheng, M.; Haeffner, F.; Gao, J. N-Terminal Cysteine Mediated Backbone-Side Chain Cyclization for Chemically Enhanced Phage Display. Chem. Sci. 2022, 13 (28), 8349–8354. https://doi.org/10.1039/D2SC03241D.